Turun yliopisto
University of Turku

FUNCTIONAL IMAGING OF INSULITIS IN TYPE 1 DIABETES

Teemu Kalliokoski

TURUN YLIOPISTON JULKAISUJA – ANNALES UNIVERSITATIS TURKUENSIS
Sarja - ser. D osa - tom. 1135 | Medica - Odontologica | Turku 2014

University of Turku

Faculty of Medicine
Department of Clinical Medicine
Pediatrics and Turku PET Centre
Doctoral Programme of Clinical Investigation

Supervised by

Professor emeritus Olli Simell (MD, PhD)
University of Turku, Faculty of Medicine
Department of Pediatrics

Adjunct professor Merja Haaparanta-Solin (MSc, PhD)
University of Turku, Faculty of Medicine
Turku PET Centre

Reviewed by

Professor Timo Otonkoski (MD, PhD)
University of Helsinki
Children's Hospital

Docent Olof Eriksson (MSc, PhD)
Uppsala University
Department of Medicinal Chemistry

Opponent

Professor Alberto Signore (MD, PhD)
Sapienza University
Nuclear Medicine Unit
Rome, Italy

The originality of this thesis has been checked in accordance with the University of Turku quality assurance system using the Turnitin OriginalityCheck service.

ISBN 978-951-29-5859-7 (PRINT)
ISBN 978-951-29-5860-3 (PDF)
ISSN 0355-9483
Painosalama Oy - Turku, Finland 2014

To Mervi,
and our children Elias and Iiris

ABSTRACT

Teemu Kalliokoski

FUNCTIONAL IMAGING OF INSULITIS IN TYPE 1 DIABETES

Department of Pediatrics and Turku PET Centre, Faculty of Medicine, University of Turku

Annales Universitatis Turkuensis, 2014, Turku, Finland

Type 1 diabetes (T1D) is an immune-mediated disease characterized by autoimmune inflammation (insulitis), leading to destruction of insulin-producing pancreatic β-cells and consequent dependence on exogenous insulin. Current evidence suggests that T1D arises in genetically susceptible children who are exposed to poorly characterized environmental triggers. Investigations largely focus on identifying patients at risk for T1D and slowing the β-cell destruction. Advances in positron emission tomography (PET) imaging have enabled the development of radiotracers for imaging insulitis, and assessing pancreatic β-cells. Here the use of 2-[^{18}F]fluoro-2-deoxy-D-glucose ([^{18}F]FDG) was evaluated for *in vivo* imaging of insulitis in both mice and T1D patients. Radioactivity uptake was up to 2.3 times higher in insulitis-affected islets of NOD mice compared to unaffected islets within the same pancreas or islets of healthy control mice. The findings of this thesis also demonstrated that the glucose uptake in the human pancreas measured by [^{18}F]FDG PET was inversely associated with the duration of diabetes. Patients with newly diagnosed T1D showed higher uptake than healthy controls or patients with a long duration of diabetes. We further evaluated 6-[^{18}F]fluoro-L-3,4-dihydroxyphenylalanine ([^{18}F]FDOPA) uptake in the healthy rat pancreas for visualization of β-cells after treatment with several enzymatic inhibitors. The pancreas exhibited increased radioactivity uptake and changes in the radiometabolic profile, allowing better discrimination between the pancreas and surrounding tissues of the rat. However, these manipulations were insufficient to separate islets from the exocrine pancreas.

Keywords: autoradiografia, [^{18}F]FDG, [^{18}F]FDOPA, imaging, insulitis, NOD mouse, PET, type 1 diabetes

TIIVISTELMÄ

Teemu Kalliokoski

FUNCTIONAL IMAGING OF INSULITIS IN TYPE 1 DIABETES

Lastentautioppi ja Turun PET Keskus, kliininen laitos, lääketieteellinen tiedekunta, Turun yliopisto.

Annales Universitatis Turkuensis, 2014, Turku, Finland

Nuoruustyypin eli tyypin 1 diabetes (T1D) on autoimmuunisairaus, jossa tuntemattomasta syystä haiman Langerhansin saarekkeisiin kertyy runsaasti immunologisesti aktivoituneita lymfosyyttejä (insuliitti) samalla kun yhä suurempi osa insuliinia tuottavista β-soluista tuhoutuu. T1D:n syntyä säätelevät voimakkaasti geneettiset tekijät, mutta toistaiseksi huonosti tunnetuilla ympäristötekijöillä on taudin synnyssä myös merkittävä rooli. Tässä tutkimuksessa tarkoituksena on löytää ne potilaat joilla on lisääntynyt riski sairastua T1D:een ja pyrkiä ennaltaehkäisemään tautiin sairastuminen.

Positroniemissiotomografia (PET) on lyhytikäisiä radioaktiivisia isotooppeja käyttävä leikekuvausmenetelmä. Väitöskirjassani selvitetään voidaanko ^{18}F-leimattua deoksiglukoosia ([^{18}F]FDG) käyttää tulehdusmerkkiaineena PET-kuvantamisessa. Tulokset osoittivat, että glukoosimetabolia on lisääntynyt jopa kaksinkertaiseksi sellaisissa NOD-hiirien haiman saarekkeissa, joissa on insuliitti, verrattuna terveisiin saarekkeisiin tai saarekkeita ympäröivään eksokriiniseen haimaan. Tulokseen perustuen tehtiin PET-kuvantamistutkimus aikuisille potilaille, jotka olivat juuri sairastuneet T1D:een. Heillä haiman glukoosinkäyttö oli merkitsevästi lisääntynyt heti sairastumisen jälkeen vähentyen sen jälkeen niin, että 6 kuukauden kuluttua haiman glukoosinkäyttö oli verrattavissa terveisiin verrokkeihin. Kolmannessa osatyössä selvitettiin miten ^{18}F-leimattu dihydroksifenyylialaniini ([^{18}F]FDOPA) kertyy terveen rotan haimaan kun dopamiinimetaboliaa muutetaan eri entsyymi-inhibiittoreiden avulla. Havaitsimme, että [^{18}F]FDOPA kertymää saadaan lisättyä jopa 7 kertaiseksi, jos rotalle annetaan edeltävästi esilääkkeenä katekoli-O-metyylitransferaasientsyymin (COMT) ja monoamiinioksidaasientsyymin A-tyypin (MAO-A) estäjien yhdistelmä. Kuitenkaan tällä esilääkeyhdistelmällä tai muilla testaamillamme esilääkkeillä Langerhansin saarekkeet tai β-solut eivät korostuneet eksokriinista taustaa vasten.

Tässä tutkimuksessa on ensimmäistä kertaa voitu osoittaa, että [^{18}F]FDG:n haimakertymä on merkittävästi lisääntynyt prediabeettisilla NOD-hiirillä. [^{18}F]FDG:n lisääntynyt käyttö haimassa voitiin osoittaa myös juuri diabetekseen sairastuneilla aikuisilla miehillä. Lisätutkimuksia tarvitaan kun halutaan selvittää lisääntyykö glukoosinkäyttö haimassa ennen diabetekseen sairastumista ja voidaanko tällä tavoin ennakoida sairauden puhkeaminen. Työssä voitiin osoittaa myös, että [^{18}F]FDOPA-injektion jälkeistä aktiivisuuskertymän määrää haimassa voidaan muuttaa käyttämällä eri esilääkkeitä tai niiden yhdistelmiä vaikkakaan [^{18}F]FDOPA PET ei toimi β-solukuvantamisessa.

Avainsanat: autoradiografia, [^{18}F]FDG, [^{18}F]FDOPA, insuliitti, kuvantaminen, NOD hiiri, PET, tyypin 1 diabetes

CONTENTS

ABBREVIATIONS

AADC	aromatic L-amino acid decarboxylase
AD	aldehyde dehydrogenase
ADP	adenosine diphosphate
ANOVA	one-way analysis of variance
ATP	adenosine triphosphate
BMI	body mass index
CM	human insulinoma cell line
CMFN	long-circulating magnetofluorescent nanoparticles
COMT	catechol-*O*-methyltransferase
DTBZ	dihydrotetrabenazine
FDA	6-[^{18}F]fluorodopamine
[^{18}F]FDG	2-[^{18}F]fluoro -2-Deoxy-D-glucose
[^{18}F]FDOPA	6-[^{18}F]fluoro-L-DOPA
FDOPAC	1,3,4-dihydroxy-6-[^{18}F]fluorophenylacetic acid
FHVA	6-[^{18}F]fluorohomovanillic acid
FITC	fluorescent isothiocyanate
fMRI	functional magnetic resonance imaging
GADA	glutamate decarboxylase autoantibody
Gd-DTPA	gadolinium-diethylenetriaminepentaacetic acid
GK	glucokinase
GLP-1R	glucagon-like peptide 1 receptor
GLUT	glucose transporter molecules
HbA_{1c}	glycolysated haemoglobin
5-HIAA	5-hydroxyindolacetic acid
HIG	human immunoglobulin
HK	hexokinase
HLA	human leukocyte antigen
HPLC	high performance liquid chromatography
5-HTP	5-hydroxytryptophan
IA-2A	insulinoma-associated protein 2 tyrosine phosphatase autoantibody
IAA	insulin autoantibody
ICA	islet cell autoantibody
IgG	immunoglobulin G
IL-2	interleukin 2
IL-2R	interleukin 2 receptor
INS-1	rat insulinoma cell line
ISPAD	International Society for Pediatric and Adolescent Diabetes

IU	international unit
IVGTT	intravenous glucose tolerance test
JDFU	Juvenile Diabetes Foundation units
LADA	latent autoimmune diabetes of adults
LC	lumped constant
MNP	magnetic nanoparticles
MRI	magnetic resonance imaging
NOD	non-obese diabetic
OGTT	oral glucose tolerance test
3-OMFD	3-O-methyl-fluorodopa
PET	positron emission tomography
PGC	protected graft copolymer
PST	phenolsulfotransferase
PVI	pancreatic volume index
ROI	region of interest
STZ	streptozotocin
T1D	type 1 diabetes
TCA	tricarboxylic acid cycle
VMAT2	vesicular monoamine transporter type 2
ZnT8	zinc transporter 8

LIST OF ORIGINAL PUBLICATIONS

This thesis is based on the following original publications, which are referred to in the text by their Roman numerals.

I. Kalliokoski T., Simell O., Haaparanta M., Viljanen T., Solin O., Knuuti J. & Nuutila P. (2005) An autoradiographic study of [^{18}F]FDG uptake to islets of Langerhans in NOD mouse. Diabetes Research and Clinical Practice. 70: 217-224

II. Kalliokoski T., Nuutila P., Virtanen K.A., Iozzo P., Bucci M., Svedström E., Roivainen A., Någren K., Viljanen T., Minn H., Knuuti J., Rönnemaa T. & Simell O. (2008) Pancreatic glucose uptake *in vivo* in men with newly diagnosed type 1 diabetes. The Journal of Clinical Endocrinology & Metabolism. 93: 1909-1914

III. Kalliokoski T., Tuomela J., Haavisto L., Forsback S., Snellman A., Helin S., Grönroos T., Solin O. & Haaparanta-Solin M. (2014) 6-[^{18}F]fluoro-L-DOPA PET uptake in the rat pancreas is dependent on the tracer metabolism. Molecular Imaging and Biology. 16: 403-411

1. INTRODUCTION

Type 1 diabetes (T1D) is a disease characterized by the destruction of pancreatic β-cells, which results complete dependence on exogenous insulin. The majority of cases of T1D have an immune-mediated nature, in which β-cells loss is caused by T-cell-mediated autoimmune inflammation (insulitis). The cause of T1D is multifactorial and still incompletely understood. The current evidence is that T1D arises in genetically susceptible children exposed to poorly characterized environmental triggers.

Diabetes, whether it is type 1 or type 2, is the leading cause of nephropathy, neuropathy, retinopathy, and coronary and peripheral vascular diseases. Diabetes with all its complications represents an enormous public health burden. It has been postulated that the care for T1D has improved in the past decades as judged by the reduced rates of microvascular diseases. However, data on cardiovascular diseases suggest that substantially less progress has been made in reducing the rates of macrovascular disease. All guidelines emphasize the importance of improved glycemic control to optimize cardiovascular health in young people with T1D (Maahs *et al.*, 2010).

Since T1D is the major type of diabetes in the young and adolescents, accounting for 85% or more of all diabetes cases in subjects less than 20 years of age worldwide, it is a major goal of future research to identify the factors behind the increasing rate of T1D and thus to reverse the current trends. Identification of patients at risk for T1D and slowing down the β-cell destruction are two of the main focuses of investigation. In Finland the incidence of developing T1D in childhood is the highest in the world.

Positron emission tomography (PET) is a nuclear imaging method which provides four-dimensional (4D) information of functional processes in the body. In addition to 3D visual information it offers tracer biodistribution data in the body over time. Magnetic resonance imaging (MRI) and computed tomography (CT) can offer high spatial resolution but PET on the other hand has high sensitivity. Under clinical conditions the resolution of CT, MRI, SPECT or PET does not allow the detection of single islets of Langerhans. None of these techniques combine both advantages in one imaging method which makes it challenging to choose the right imaging modality. PET-MRI and PET-CT are hybrid imaging methods that incorporate MRI or CT for anatomy and PET for functional imaging.

The possibility of non-invasive imaging of T1D associated changes in the pancreas would expand the horizon of disease pathophysiology. The advances in PET imaging have been partly due to the introduction of new specific radiotracers. Identification of tracers specific for the inflammatory cells and insulin-producing pancreatic β-cells would greatly improve the identification of disease development and progression in addition to aiding in therapy evaluation.

2. REVIEW OF THE LITERATURE

2.1. The pancreas

2.1.1. Anatomy of pancreas

The human pancreas is located in the loop of the duodenum in front of the inferior vena cava and left renal vein with its tail reaching the splenic hilum. The pancreas comprises a head, uncinate process, neck, body, and tail (Ellis, 2013). The pancreas possesses both endocrine and exocrine functions. The endocrine pancreas consists of clusters of cells located in the islets of Langerhans scattered throughout the pancreas producing several important hormones such as glucagon, insulin, somatostatin, and pancreatic polypeptides. There are differences between humans and rodents in the anatomy of their pancreases, especially in the ductal anatomy. In humans, the pancreas is distinct and well defined, whereas in rat and mouse, it is a rather diffuse organ enclosed in the dorsal mesentery (Case, 2006). In the rat, the pancreas lies between duodenum and spleen. The rat pancreas is made up of four regions; lower duodenal, upper duodenal, gastric, and splenic. The size-frequency distribution of the diameters of the islets of Langerhans in the rat has shown an overall shift towards smaller sizes in the upper duodenal region, and towards larger sizes in the splenic region (Elayat *et al*., 1995). The islets are highly vascularised with fenestrated capillaries; of the inflowing arterial blood in rat, 6% goes to the islets which makes up 0.3% of the organ mass and 94% goes to the acini (non-islet tissue) (Lifson *et al*., 1985). The rest of the pancreas is constituted of exocrine cells secreting pancreatic juice, which contains digestive enzymes such as lipases, trypsin and amylase. The enzymes are secreted in an inactive form; they are activated in the duodenum by enterokinase enzymes.

The arterial circulation in humans in the head of the pancreas is supplied by the anterior and posterior pancreaticoduodenal arteries forming arcades in the pancreaticoduodenal sulcus with the tissue drained by the pancreaticoduodenal veins (Fig. 1). The body and tail of the pancreas are supplied by dorsal, inferior, and caudate pancreatic arteries, and they are drained by inferior and left pancreatic veins (Ibukuro, 2001).

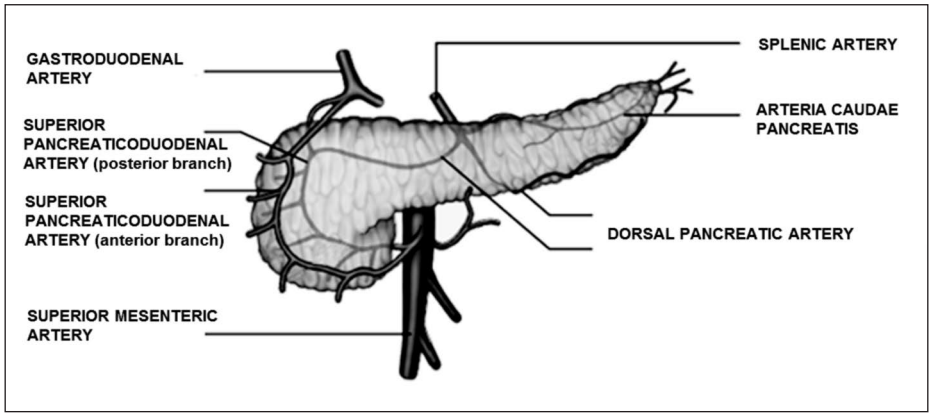

Figure 1. Vasculature of the human pancreas (modified from Ellis, 2013).

2.1.2. Endocrine pancreas

Scientists estimate that there are at least 1 million islets of Langerhans in a healthy, adult human pancreas. The pancreatic islets are clusters of functionally related endocrine cells, with each islet containing approximately 3,000 to 4,000 cells dispersed throughout the exocrine parenchyma of the pancreas (Fig. 2). They make up only 1 to 2 percent of the entire organ (Bonner-Weir, 1994). The size of individual islets is 50–300 μm (Sweet *et al*., 2004). Histochemical stainings, transmission electron microscopy, and immunohistochemistry have shown different cell types in the islets. Glucagon-producing α-cells, insulin-producing β-cells, somatostatin-producing δ-cells, pancreatic polypeptide-producing PP-cells, serotonin-producing enterochromaffin-cells, and ghrelin-producing ε–cells have all been found in the human islets. Ghrelin was given the name ghrelin, for its ability to stimulate growth hormone (GH) secretion (GH-relin) (Wierup *et al*., 2014). The islets of the rat consist of a central core of β-cells surrounded by a rim of α-, δ- and PP-cells. In rats, the tail (or splenic part) of the pancreas contains the highest number of islets (Elayat *et al*., 1995). In a small human islet (40–60 μm in diameter), β-cells occupy a core position, α-cells have a mantle position, and the vessels are located at their periphery. In islets bigger than that, the α-cells have a similar mantle position but are found also along vessels that penetrate and branch inside the islets (Bosco *et al*., 2010). Human islets contain proportionally fewer β-cells (about 60%) than mouse islets (Cabrera *et al*., 2006).

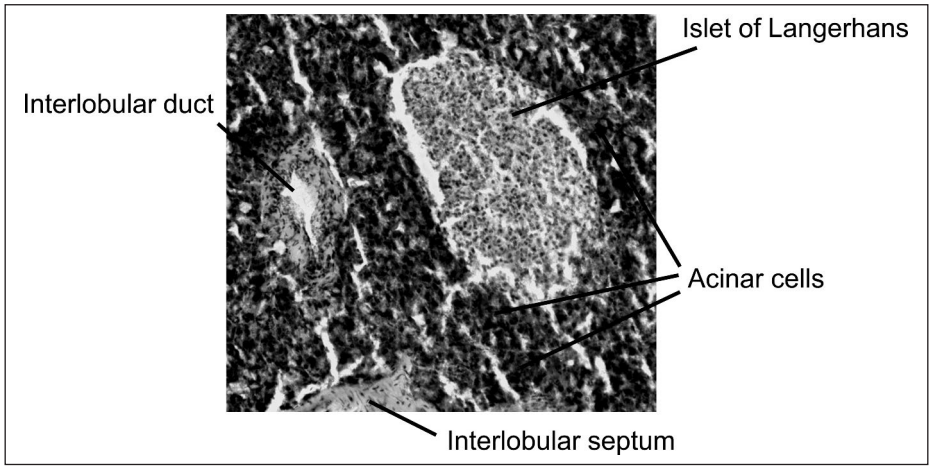

Figure 2. Islet of Langerhans are scattered throughout the exocrine pancreas (acini). Figure shows the histology of a mouse pancreas.

It has been postulated that both the arrangement of the cells within the islets, and the distribution of the islets throughout the pancreas are important for their function. Islet blood flow is regulated by signals, such as hormones and nutrients that reach the islet vasculature from distant tissues via the bloodstream. In addition, islet perfusion determines communication between endocrine and exocrine cells and between different types of endocrine cells within islets (Ballian & Brunicardi, 2007). In humans, islets have an intralobular location and they are drained by numerous portal vessels that lead the blood from the islets to the lobular capillary network. In rats and mice a considerable number of islets are located interlobularly from whence they drain directly into veins (Murakami *et al.*, 1993). In rats, the arterial blood circulates first to the cortical capillaries of the islets only later filling the deep capillaries. Therefore, the blood mainly flows from the α-δ -cell mantle towards the β-cell core. This intra-insular microcirculatory design from the superficial to deep layers has thought to enable insulin regulation by glucagon and somatostatin (Murakami, 1997). However, the complete understanding of the microcirculation in the islets of Langerhans is still lacking.

Nerve fibers enter the pancreas in association with blood vessels to acinar tissue and islets (Ushiki & Watanabe, 1997). Adrenergic fibers innervate vessels, acinar cells and islets. Cholinergic nerves are found mainly in islets (Miller, 1981). The nerves accompanying the arteries transmit branches toward the islets of Langerhans and form a dense plexus around the islets (Ushiki & Watanabe, 1997). The secretions from both acinar and islet cells are modulated by nerves. Nerve fibers extending from intrinsic ganglia which are activated by preganglionic vagal fibers, release acetylcholine into the islets causing the release of insulin from β-cells through the stimulation of muscarinic receptors. The stimulation of insulin secretion by parasympathetic neurotransmitters is balanced by inhibition of sympathetic neurotransmitters (Bockman, 2007).

The blood flow in the pancreas is affected by nerves. Parasympathetic and sympathetic nerve activation changes the blood flow, which in turn modifies exocrine and endocrine secretion. Blood flow through the islets may change independently in relation to the flow through the exocrine pancreas. Infusion of glucose directly into the duodenum triggers increased blood flow in the islets. Thus, peripheral sensory function, afferent transmission, and efferent activity are all involved in controlling a specific part of pancreatic blood flow (Bockman, 2007).

2.1.3. Glucose metabolism in the pancreas

Glucose is taken up in the tissue by either a mechanism based on mass action or more importantly in an active manner by specific glucose transporter molecules (GLUT) situated on the cell membrane (Thorens, 1996). The specificity and affinity for different glucose and related hexoses have been characterized for more than ten GLUTs. GLUT molecules are located in the cytosol as vacuoles in the resting phase. They are transported to the cell membrane in order to meet the cell's enhanced glucose needs (Bell *et al*., 1990). GLUT1, GLUT3, and GLUT4 are high-affinity transporters; the number of transporters on the plasma membrane controls the flux of glucose into the cells. The amount of transporters on the cell surface determines the rate of glucose metabolism. These transporters are usually expressed at high levels in tissues highly dependent on glucose as an energy source. The low affinity, high capacity transporter GLUT2 is present in specific tissues to allow a high glucose flux into the cell. The GLUT2 transporter is bidirectional and therefore it allows glucose both to enter and exit the cell (Leturque *et al*., 2005). In low blood glucose states, GLUT2 is expressed in large amounts on the rat hepatocyte plasma membranes facilitating the net hepatic efflux of glucose. If the liver is perfused with insulin, a marked decrease in the presence of GLUT2 is observed in the hepatic cell membrane which parallels the insulin-mediated reduction in hepatic glucose production (Eisenberg *et al*., 2005).

Immunostaining has revealed that GLUT2 is located on the lateral membranes of rat pancreatic β-cells where it allows a rapid equilibration of glucose inside the cells (Fig. 3), which is then a prerequisite for insulin secretion from β-cells. GLUT3 immunoreaction has predominantly been localized in the cytoplasm of β-cells. GLUT3 is considered to relate primarily to the basal uptake of glucose (Sato *et al.,* 1996). In humans all three (GLUT1-3) glucose transporters are expressed in islets and β-cells. Although GLUT2 is well established as the principal glucose transporter in rodent β-cells, in human β-cells GLUT2 expression seems to have a lower implication compared to GLUT1 and GLUT3 transporters (McCulloch *et al.*, 2011). GLUT1 and GLUT3 have equivocally important role in the regulation of insulin secretion in humans (McCulloch *et al.*, 2011). One example is patients with Fanconi–Bickel syndrome, a rare disorder of carbohydrate metabolism caused by GLUT2 mutations. In them GLUT2 mutation display marked

disturbances of hepatic and renal glucose metabolism, rather than defective insulin secretion (Santer *et al.*, 1998). In human and rodents, GLUT4 accounts for the most part of the stimulatory effect of insulin on glucose uptake into skeletal muscle and fat cells. In the basal state GLUT4 transporters are stored in intracellular vesicles. They are translocated to the plasma membrane in response to insulin which thus regulates the rate of glucose uptake to the cell (Thorens 1996, Czech *et al*., 1992, Czech *et al.*, 1999). In both humans and rats, GLUT4 has also been demonstrated to be located in the pancreatic islets (Kobayashi, 2004). GLUT5 is primarily a fructose carrier (Blakemore *et al*., 1995).

After entering the cell, glucose is rapidly phosphorylated by tissue-specific isoenzymes known as hexokinases (HK) (Katzen, 1970, Wilson, 2003); this is an ATP-dependent process, leading to the formation of glucose-6-phosphate. Glucose is capable of leaving the cell via the same carrier through which it entered, but glucose-6-phosphate cannot be transported across the plasma membrane. Glucose metabolism in the β-cell is mainly controlled by hexokinase-IV, also named glucokinase (GK) which is present in human endocrine pancreas but is not found in the exocrine pancreas (Bedoya *et al.*, 1986). Other hexokinases are located in the pancreatic exocrine cells (Trus, 1981, Schuit *et al.*, 1999). GK occupies an important role in controlling glucose phosphorylation and metabolism in pancreatic β-cells, it can be considered to function as a pacemaker of glycolysis at physiological glucose levels. It determines the rate, affinity, cooperativity, and anomeric discrimination of glucose metabolism (Meglasson & Matschinsky, 1984) in the endocrine tissue.

In general, glucose-6-phosphate is stored as glycogen or converted to pyruvate (glycolysis). Pyruvate is oxidized in the mitochondria into acetyl coenzyme A and further oxidized to produce CO_2 and water as the end products (Meisenberg & Simmons, 1998). Activity in the pentose phosphate pathway accounts for a significant portion of the total glucose oxidation in tissues such as liver, which possess active fatty acid or cholesterol synthesis. The pentose phosphate pathway does not normally contribute significantly to the metabolism of glucose in the endocrine pancreas (Macdonald, 1993). β-cells have unique features in glucose utilization. β-cells express low levels of lactate dehydrogenase (LDH) and plasma membrane monocarboxylate (lactate) transporter-1 (MCT-1) (Sekine *et al*., 1994, Zhao *et al*., 2001). These specializations ensure that almost all of the glucose-derived pyruvate enters the tricarboxylate/citrate (TCA) cycle (Fig 3.) and is either broken down to H_2O and CO_2 yielding ATP, or assimilated into newly synthesised proteins (Rutter, 2004).

2.1.4. Regulation and measurement of insulin secretion

The main function of pancreatic β-cells is to synthesize and secrete insulin at appropriate rates to limit blood glucose fluctuations within a narrow range. Excessive secretion of

insulin causes hypoglycemia, and insufficient secretion leads to hyperglycemia (Rutter, 2004). Blood glucose homeostasis is mainly regulated by the balanced secretion of insulin and glucagon. Pancreatic β-cells secrete insulin which in turn reduces the blood glucose concentration by promoting glucose storage into the liver and by stimulating glucose metabolism in adipose and muscle cells (Czech, 1992). Pancreatic α-cells secrete glucagon which increases the blood glucose level by promoting glycogenolysis and gluconeogenesis.

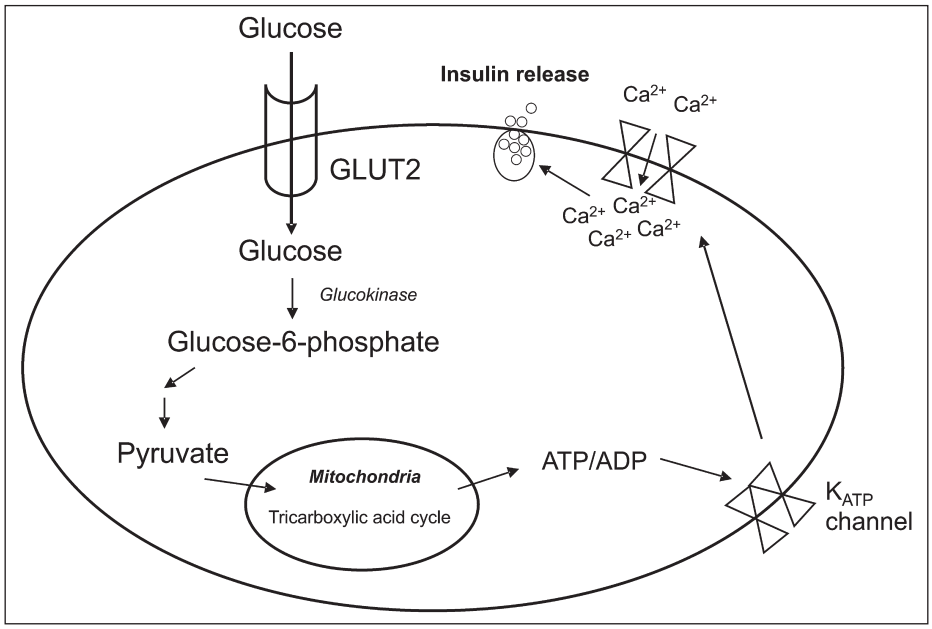

Figure 3. Glucose equilibrates in β-cells via GLUT2-mediated facilitated diffusion. Mobilization of GLUT2 to the plasma membrane is insulin-independent. Since it is a low affinity transporter protein, it enables a high glucose influx. After entering β-cells, glucose is phosphorylated by glucokinase. The endpoint of glycolysis is the metabolic substrate pyruvate which is oxidized through the tricarboxylic acid cycle (TCA) by mitochondria to produce ATP. This increases the intracellular ATP/ADP ratio, sequentially leading to closure of K_{ATP} channels, depolarization of the plasma membrane and opening of voltage dependent Ca^{2+} channels increasing Ca^{2+} level in the cell, ultimately triggering the exocytosis of insulin-containing granules (Modified from Fu *et al*., 2013).

Insulin secretion is under very tight control which is primarily regulated by glucose itself (Fig. 3) but it also involves metabolic, neural and hormonal factors (Fu *et al*., 2013). Glucose stimulates insulin secretion by generating triggering and amplifying signals in β-cells. The triggering pathway is illustrated in figure 3. The triggering pathway predominates over the amplifying pathway, which remains functionally silent as long as Ca^{2+} concentration in the cell remains low by the triggering pathway; i.e., as

long as glucose has not reached its threshold concentration. The amplifying pathway serves to optimize the secretory response not only to glucose but also to nonglucose stimuli (Henquin *et al.*, 2003). The amplifying pathway has been studied by elevating and clamping the Ca^{2+} concentration in β-cells by a depolarization with either a high concentration of sulfonylurea or a high concentration of K^+ in the presence of diazoxide (K_{ATP} channels are then respectively blocked or held open). Under these conditions, glucose increases insulin secretion in a concentration-dependent manner (Henquin *et al*., 1982). This increase in secretion is highly sensitive to glucose, requires glucose metabolism, is independent of activation of protein kinases A and C, and does not seem to implicate long-chain acyl-CoAs. Acyl-CoA is a group of coenzymes involved in the metabolism of fatty acids. Whether insulin is secreted or not, is determined by the triggering pathway (the increase in Ca^{2+}). The amplifying pathway serves to optimize the secretory response induced by the triggering signal (Henquin *et al.*, 2003).

Glucagon-like peptide 1 (GLP-1) is an incretin hormone, which belongs to the group of gastrointestinal hormones that stimulate a decrease in blood glucose level. It is secreted from the L-cells of the small intestine in response to the ingestion of a meal (Ørskov, 1992). Together with the related hormone glucose-dependent insulinotropic polypeptide (GIP), GLP-1 is responsible for the augmentation of insulin secretion that results from oral stimulation of insulin secretion with nutrients (Nauck *et al*., 1993).

The autonomic nervous system influences insulin secretion (Taborsky, 2011). Parasympathetic nerves stimulate insulin secretion via their neurotransmitters (Woods & Porte, 1974). Sympathetic nerves and their neurotransmitters on the contrary inhibit the insulin secretion (Smith & Davis, 1983). The postganglionic nerve fibres innervating the islets release acetylcholine, which directly stimulates insulin secretion from the β-cells via the activation of muscarinic receptors (Ahrèn, 2000). Recently Rodriguez-Diaz and co-workers have shown that the innervation of the human islet is qualitatively different from that of the mouse islet. They were able to establish that in the mouse islets the sympathetic axons primarily innervate α-cells, whereas both β and α-cells receive parasympathetic input. By contrast, the innervation in human islets is sparse and most human endocrine cells lack conventional autonomic innervation. Cholinergic innervation seems to be minor in human islets, and the sympathetic axons penetrating the islet contact smooth muscle cells of the blood vessels (Rodriguez-Diaz *et al*., 2011).

Insulin and C-peptide are released together into the blood, since they are formed in the same secretory vesicle (Fu *et al*., 2013). C-peptide levels determined within the first few years after the diagnosis may help in confirming T1D if the levels are low (e.g. non-fasting blood C-peptide < 0.2 nmol/l with hyperglycaemia confirms severe insulin deficiency). However, higher levels should be interpreted with caution (particularly in obese patients or in patients with features of insulin resistance) and may simply reflect

continued insulin secretion seen in the early T1D period (Jones & Hattersley, 2013). Thus the C-peptide level in blood can be used as an indirect estimation of functional β-cell mass (Van Cauter *et al*., 1992).

2.1.5. Dopamine metabolism in the pancreas

The catecholamines, dopamine, norepinephrine, and epinephrine, constitute a class of chemical neurotransmitters and hormones that occupy key positions in the regulation of many physiological processes and they are important in the development of neurological, psychiatric, endocrine, and cardiovascular diseases (Eisenhofer *et al.*, 2004). Dopamine is a monoamine which functions as a neurotransmitter in the brain. It is also a precursor for norepinephrine and epinephrine. Dopamine is produced in several areas of the brain, including the substantia nigra and the ventral tegmental area. In addition, dopamine is a neurohormone released by the hypothalamus, and it plays a role to regulate its own peripheral neurotransmission (Lackovic *et al.*, 1983).

Dopamine has also other functions than neurotransmission. Pancreas has been shown to be an important source of nonneuronal dopamine in the body. In rats, dopamine has been detected in the exocrine cells which produce digestive enzymes. Duodenal juice contains high levels of dopamine which in turn protects the intestinal mucosa against injury (Mezey *et al.*, 1996). In the endocrine pancreas, dopamine has been detected in mouse β-cell secretory granules after the injection of radiolabeled L-DOPA (Ericson *et al*., 1977). L-DOPA administration changes the glucose metabolism in the pancreas; the glucose-induced insulin response was diminished when L-DOPA was given together with glucose. This inhibition was eliminated by pretreatment with a peripheral AADC inhibitor (Lundquist *et al*., 1991). Nonetheless, pancreatic islets do not have the dopaminergic neurons and the molecular mechanisms responsible for the inhibition of insulin secretion remain unknown (Ustione *et al*., 2013).

2.2. Diabetes

2.2.1. Genetic predisposition and incidence of T1D

In the 1970s, T1D was recognized as being associated with genetic variants in the human leukocyte antigen (HLA) on chromosome 6p21.3 (Todd *et al.*, 1987). In fact two genes, HLA class II DR3 and DR4, are most closely associated with T1D. These genes were originally investigated as candidate genes for T1D because their products are associated with the presentation of antigens to the cellular immune system. HLA variants have been shown to account for approximately 50% of the T1D genetic susceptibility. More than 40 genes account for the remaining 50% of the genetic risk (Todd *et al.*, 1987). Those children who carry both of the high risk HLA haplotypes (DR3–DQ2 and DR4–DQ8) have a risk of approximately 1 in 20 to receive a diagnosis of T1D by the age of 15 years.

If the child has a sibling who has T1D and he/she has the same haplotypes, the risk is even higher (approximately 55%) (Concannon *et al.*, 2009).

In the early 1990s, the World Health Organization (WHO) began its Multinational Project for Childhood Diabetes (DIAMOND Study). The overall incidence was found to vary by more than 350-fold among countries in the same region and between regions the variation was even more startling from 0.1/100,000 per year in China and Venezuela to 37.8/100,000 per year in Sardinia and up to 40.9/100,000 per year in Finland (DIAMOND Project Group, 2006). EURODIAB Study collected data from 17 countries of children younger than 15 years of age between 1989 and 2003. The highest incidence was reported in Finland at 52.6/100,000 and lowest in Lithuania 10.3/100,000 (Patterson *et al.*, 2009).

Harjutsalo and coworkers have shown that the incidence of T1D in Finland has increased from 31.4/100,000 in 1980 to 64.2/100,000 in 2005 (Fig. 4). The relative annual increase 4.7% was highest among children under 5 years of age, while it was 2.7% among 5–9-year-old children, and only 1.7% in the oldest age group (age from 9 to 14 years). From 1980 to 2005, the overall incidence rate of T1D in Finnish children has doubled (Harjutsalo *et al.*, 2008). It has been stated that these kinds of increases in incidence cannot be attributed to genetic shifts in such a short period of time. Therefore causative agents in the environment are being investigated.

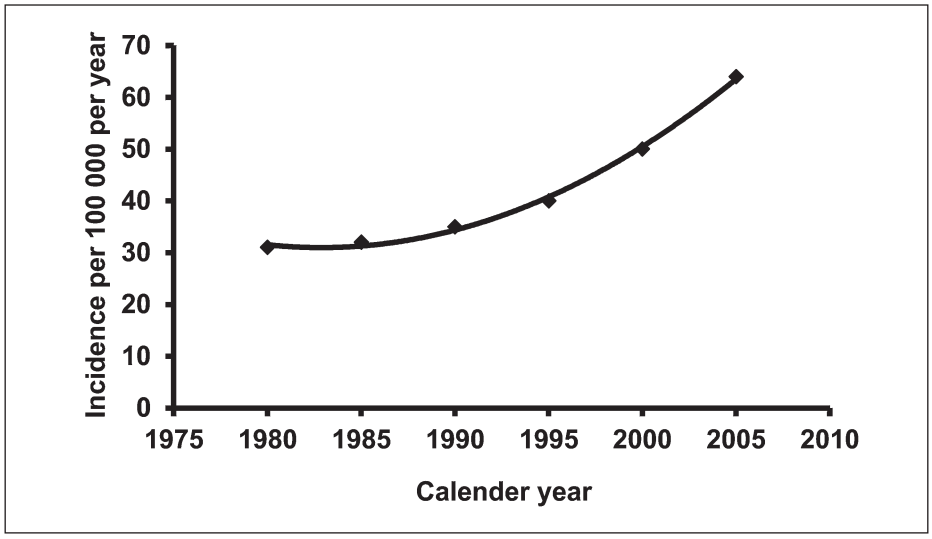

Figure 4. Incidence rate of T1D diagnosed at or before 14 years of age in Finland (modified from Harjutsalo *et al.*, 2008)

2.2.2. Etiology and pathogenesis of type 1 diabetes

Type 1 diabetes mellitus is characterized by loss of the insulin-producing β-cells in the pancreas, leading to insulin deficiency (Eisenbarth, 1986). In the majority of cases, T1D has an immune-mediated nature, in which β-cell loss is attributable to T-cell-mediated autoimmune attack (Bach, 1994). At the same time, 5.8% of the children who developed T1D did not express T1D specific autoantibodies at the time of diagnosis (Ziegler *et al*., 2013). The American Diabetes Association and the World Health Organization have proposed that T1D should be subdivided into autoimmune (immune-mediated) diabetes (type 1A) and idiopathic diabetes with β-cell destruction (type 1B) (Report of the Expert Committee on the Diagnosis and Classification of Diabetes Mellitus). The insulin deficiency associated with T1D is believed to require an environmental agent or agents to trigger autoimmunity in genetically susceptible subjects. The disease may present at any age, but the majority of patients are diagnosed before the age of 30 years.

Little is known about the etiological foundations for pathogenesis of T1D in humans, but a number of theories, based on data from humans and animal models, have been proposed to explain how β-cell autoimmunity is initiated and eventually progresses to a state of insulin deficiency, which then leads to hyperglycemia (Rowe, 2011). Some of the theories include molecular mimicry resulting from crossreactivity of viral (Roep *et al*., 2002) or dietary antigens (Virtanen *et al.*, 1993) with β-cell antigens, gut microflora that drive deleterious immune responsiveness (Brugman *et al*., 2006), dysfunctional β-cell antigen expression in the thymus (Fan *et al*., 2009) and pancreatic lymph nodes (Yip *et al*., 2009).

Enviromental triggers such as dietary factors have been extensively studied but without any conclusive and consistent findings (Stanescu *et al.*, 2012). Some cow's milk proteins share structurally homologous sequences with an islet cell antigen, leading to the possibility of molecular mimicry as the trigger for β-cell destruction. In one study, early exposure to cow's milk proteins has been linked with an increased risk towards T1D (Virtanen *et al.*, 1993). However, another study, the Diabetes Autoimmunity Study in the Young (DAISY), could detect no association between early exposure to cow's milk and β-cell autoimmunity (Norris *et al.*, 1996). In a multinational TRIGR (Trial to Reduce IDDM in the Genetically at Risk) study the use of a hydrolyzed infant milk formula, when compared with a conventional infant milk formula, did not reduce the incidence of diabetes-associated autoantibodies after 7 years of age. The absolute risk of positivity for 2 or more islet autoantibodies was 13.4% among those randomized to the extensively hydrolyzed casein formula compared to 11.4% among those randomized to the conventional cows' milk–based formula (Knip *et al*., 2014). Furthermore, the DAISY study found no association between D vitamin intakes in relation to the progression over T1D even though low level of vitamin D has been considered as an environmental susceptibility factor (Norris *et al.*, 1996).

Since there is a seasonal variation in T1D occurrence, a viral trigger has also been proposed with enteroviruses being postulated as the culprits since children who developed diabetes-associated autoantibodies had higher levels of enterovirus antibodies than the control subjects (Sadeharju *et al.*, 2001, Laitinen *et al*., 2014). Another finding has been that signs of an enterovirus infection at 12 months of age were associated with the appearance of autoimmunity among the children who had been exposed to conventional cows' milk–based infant formula before 3 months of age, which could provide an explanation for the controversial findings obtained when analyzing the effect of any single factors on the appearance of T1D-associated autoimmunity (Lempäinen *et al*., 2012).

2.2.3. Insulitis in Non-Obese Diabetic mouse

The histopathology of T1D is defined by a reduced β-cell mass in association with insulitis, a lymphocytic infiltration affecting the islets of Langerhans (Bottazzo *et al*., 1985). There are animal models for T1D, but unfortunately they are known to differ from the human disease in many respects (Table 1.). Nonetheless, the use of animal models to study T1D is fundamental to advancements in the understanding of basic biologic mechanisms and disease-specific dysfunctions. In particular, the non-obese diabetic (NOD) mouse has played an important role in the clarification of disease mechanisms, identification of autoantigens, and the development of a better understanding of the genetic pathogenesis of T1D (Thayer, 2010).

Table 1. Comparison of differences in autoimmune diabetes in NOD mice and in humans (Modified from Roep *et al*., 2004)

	HUMANS	MICE
T-cell-driven insulitis	Mild	Severe
Humoral reactivity to β-cells	GAD65, IA2, and insulin	Insulin
Insulin gene	One	Two
GAD65 expression by β-cells	Yes	No
Incidence	0.25-0.40%	>80%
Incidence in genetically susceptible subjects	5-30%	>80%
Gender bias	No	Females
Peri-insulitis	No	Yes
Lymphocytic infiltrates in other tissues	Minority of individuals	All
Maternal autoantibodies	Potentially reduced risk of T1D	Diabetogenic
B cells required	No	Yes
Succesful intervention therapies	Pending	>195

The earliest evidence of insulitis in the histology in the NOD mouse is identified by a swelling of the blood vessels adjacent to islets that occurs at about 3 weeks of age in female mice. At approximately 7 weeks, increasing numbers of dendritic-like cells

and macrophages begin to appear at the islet periphery near to the blood vessels (Fig. 5). At this stage, some islets already display the presence of infiltrating macrophages. Thereafter CD4+ and CD8+ T cells move out of blood vessels near to the islets. In the next stage, the lesions are characterized by a massive infiltration of macrophages, T cells, and B cells. At the same time, there are reductions in the number of functioning insulin positive β-cells. As insulitis proceeds to its final stage in NOD mice, no β-cells are detectable, and only a few glucagon-positive α-cells are seen, similar to the insulitis observed in fulminant T1D. Finally immune cells are present in varying numbers in some islets and other large islets can be found without any β-cells or immune cells (Rowe, 2011).

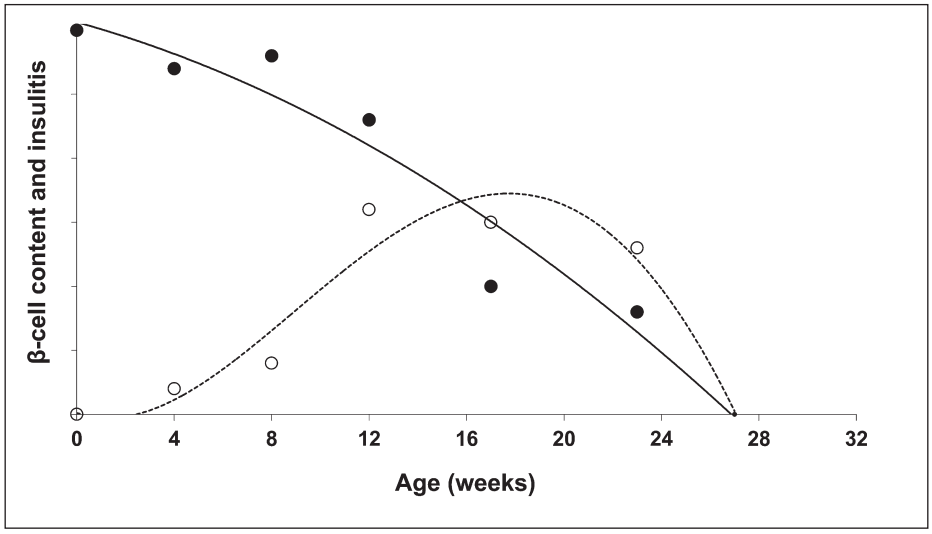

Figure 5. An illustration of pancreatic β-cell mass destruction (filled symbols) relative to the extent of insulitis (open symbols) in female NOD mice. Hyperglycemia occurs usually at 15-22 weeks of life (modified from Signore *et al.* 1994)

2.2.4. Insulitis and T1D specific autoantibodies in human

The autoimmune etiology of T1D has primarily been based on the identification of islet cell reactive autoantibodies in the serum of patients with or at a genetic risk for T1D (Kupila *et al.*, 2002), as well as the presence of lymphocytic infiltrates in the pancreatic islets of patients who died shortly after disease onset (Foulis *et al.*, 1984). The cytotoxic T-cell mediated destruction of insulin-producing β-cells is thought to be initiated by some unknown antigen, leading to the destruction of more than 75% of β-cells mass at clinical diagnosis of T1D (In't Veld, 2011). Definition criteria for insulitis have varied from 2 to 15 infiltrating cells per islet of Langerhans (in tissue sections) (In't Veld, 2011). The infiltrate consists predominantly of T-cells, in which CD8+ lymphocytes dominate, but it may also contain CD4+ lymphocytes, B-lymphocytes and macrophages (Foulis *et*

al., 1986). The cellular response is accompanied by a humoral response that includes the production of autoantibodies against a wide array of β-cells antigens (Eizirik, 2009). The presence of an islet cell autoantibody signifies that an autoimmune reaction has taken place (Schranz & Lernmark, 1998).

In first degree relatives of T1D patients, the risk for developing the disease has been observed to be higher when multiple positivity is present for autoantibodies against the islet cell cytoplasm (ICA), insulin (IAA), glutamate decarboxylase (GADA) or insulinoma-associated protein 2 tyrosine phosphatase (IA-2A) (Kulmala *et al.*, 1998). ICAs are IgG class molecules which react against structures of islet cells and in that respect they are not β-cell specific. Individuals may have relatively low levels (<10 JDFU) of ICA without developing T1D. However, at the time of diagnosis higher levels of ICA autoantibodies are most often present in the serum. One finds that IAA is positive in up to 81% of the very young children who have developed T1D, and this may be the first manifestation (Elding Larsson *et al*., 2014). High levels of IAA correlate with fast β-cell destruction and a rapid progression towards T1D. Autoantibodies against GAD65, IA-2A and zinc transporter 8 (ZnT8) have also associated with T1D (Merger *et al.*, 2013).

About 90% of Caucasian children will have at least one of these autoantibodies at the time of diagnosis of T1D (Atkinson & Eisenbarth, 2001, Ziegler *et al*., 2013). The risk of T1D in children who have no islet autoantibodies has been shown to be 0.4% by the age of 15 years. Progression to T1D during a 10-year follow-up after islet autoantibody seroconversion with a single islet autoantibody has been documented to be 14.5% in comparison to multiple islet autoantibodies when the majority of subjects (69.7%) will develop T1D. Progression to T1D in the children with multiple islet autoantibodies was found to be rapid in those children who had islet autoantibody seroconversion at age younger than 3 years (Ziegler *et al*., 2013).

The presence of insulitis appears to be more dependent on earlier onset age than the variability of disease duration. For example, in one study, onset age among the cases without insulitis was 17.1 years, while among those with insulitis it was much younger 7.9 years (Gepts, 1965). In the review article of In't Veld, insulitis was observed in 73% of young (≤ 14 years) T1D patients with a short (≤ 1 month) duration of the disease, in 60% of young patients with a disease duration between one month and one year, and only in 4% of young patients with a duration of disease longer than one year (In't Veld, 2011). In the Finnish-population based DIPP (Diabetes Prediction and Prevention) study children with HLA-conferred susceptibility to T1D, and who progressed to clinical T1D before puberty, developed diabetes associated autoantibodies predominantly before 4 years of age, peaked in seroconversion rate during the second year of life (Parikka *et al*., 2012).

It is worthwhile remarking that histopathological lesions, which have been observed in cases with recent onset disease and particularly in NOD mice, will only reflect the final stages of a process that have been going on for a long period of time. There is less material available of earlier stages of the disease in human. It is challenging to study this topic since the islets are scattered throughout the pancreas and inflammatory lesions affect concurrently only a small part of the islets which are not homogeneously distributed throughout the gland. In young patients with recent onset disease (<1 month) an average of 34% of the islets contains β-cells, but only 33% of these islets also show insulitis. In older patients with recent onset disease an average of 63% of the islets contain β-cells, but with only 18% of the insulin-containing islets showing insulitis (In't Veld, 2011). At the same time, some islets in other parts of the pancreas may remain intact (Foulis & Stewart, 1984).

In humans not all individuals who are autoantibody-positive progress to overt disease. There are some reports that it is a process which may involve periods of fulminant destruction followed by episodes of repair and regeneration. It has been speculated whether in the two autoantibody-positive organ donors who did not become diabetic, that the insulitis-induced β-cell loss had been fully compensated by the formation of new β-cells (In't Veld, 2007). In adults, there is also a rare, nonautoimmune, fulminant T1D which is a novel subtype of T1D characterized by the absence of both insulitis and diabetes-related antibodies, an abrupt onset, and with high serum pancreatic enzyme concentrations. Pancreatic biopsies reveal neither insulitis nor hyperexpression of MHC class I molecules in islets (Imagawa, 2000). As many as 10% of adults initially believed to have type 2 diabetes in fact are found to have antibodies associated with T1D. β-cell destruction among these subjects seems to occur more slowly than in young T1D patients (Naik & Palmer, 2003). Approximately 2–12% of adult patients with diabetes suffer from this form of immune-mediated diabetes mellitus, which is called latent autoimmune diabetes of adults (LADA) (Merger *et al.*, 2013).

2.2.5. Natural course of type 1 diabetes

The most common visible symptoms of T1D are polyuria, polydipsia, weight loss, fatigue, malaise and features of ketoacidosis measurements (Elding Larsson *et al*., 2014). These symptoms usually develop over weeks or a few months, though occasionally the patient may be aware of them for only a few days before diagnosis. The diagnosis of T1D is made on the basis of hyperglycemia and the determination of anti-islet antibodies (Atkinson & Eisenbarth, 2001). The rate of β-cell loss after the diagnosis of T1D is highly variable and may depend in part on the aggressiveness of the T1D disease pathology. This aggressiveness may be determined by several factors including the underlying genetic predisposition, age of the patient, metabolic control, and may vary within individuals over the course of their diabetes (Palmer, 2009).

Insulin treatment replaces or supplements the body's own insulin secretion, restoring normal or near-normal blood glucose levels. Good metabolic control has been shown to be important for delaying and hopefully preventing the chronic complications of diabetes (Diabetes control and complications trial research group, 1993). Nonetheless, achieving this level of control is a major undertaking for the patient and his/her family. A major improvement in the prognosis of T1D would be prevention of the disease. Although there are promising results in experimental preventative set-ups, human prevention trials have been less promising so far (Gale *et al*., 2004, Näntö-Salonen *et al*., 2008)

2.2.6. Predicting type 1 diabetes

At present, the onset and progression of T1D can be assessed through indirect means, i.e. islet cell autoantibodies, oral glucose tolerance test (OGTT), intravenous glucose tolerance test (IVGTT), or plasma glucose, insulin, and C-peptide measurements (Elding Larsson *et al*., 2014). There is a considerable clinical and research need for non-invasive and reliable method for quantifying islet mass, β-cell mass or the immunological process within the pancreas as a means of monitoring the onset and progression of T1D. The ability to detect lymphocytic infiltration and associated changes in pancreas would help in identifying those individuals with subclinical T1D as early as possible, ensuring an early initiation of interventions to prevent or reverse overt diabetes. At the moment, the only accepted endpoint for trials in these areas is the clinical diagnosis of diabetes.

2.3. Positron emission tomography (PET)

Positron emission tomography (PET) is a non-invasive nuclear imaging method, based on the use of short-lived isotopes such as ^{18}F, ^{11}C, and ^{15}O, which can be used as labels in natural substrates or in pharmaceuticals. These isotopes decay by emitting a positron, which annihilates with an electron, producing two photons emitted simultaneously in opposite 180 degree directions. The PET scanner recognizes these coincident photons in a ring of detectors and forms cross-sectional images of the tracer after several corrections using mathematical models (i.e. tissue attenuation). Before the introduction of hybrid PET/CT scanners in the late 1990s, a transmission scan for the correction of photon attenuation was performed with a removable ring source containing germanium (^{68}Ge). If a more specific anatomical reference was needed, then an additional CT or MRI was performed prior to or after the PET scan. Hybrid PET/CT added a major new dimension to the utility of PET. With PET/CT, areas of abnormal uptake can be localized to specific morphological structures. Recent development in hybrid scanners has seen the introduction of combined PET and MRI. PET offers the acquisition of functional data at the molecular level, MRI provides superior soft-tissue resolution and anatomy along with semiquantitative macromolecular information (Glaudemans *et al*., 2012).

2.4. *In vivo* imaging of insulitis and β-cell mass

2.4.1. Scintigraphy and SPECT in imaging insulitis

Scintigraphy is a diagnostic technique in which the radiation emitted by a radioactive substance administered into the subject is visualized in a two-dimensional picture. SPECT imaging is performed by using a camera to acquire multiple 2-D projections and then the 3-D dataset is applied by computer. Scintigraphy with radiolabelled polyclonal human immunoglobulin (HIG) has been used for diagnosis and follow-up of acute and chronic inflammatory diseases, such as osteomyelitis and rheumatoid arthritis (Stoeger *et al.*, 1994). Seven out of 15 newly diagnosed T1D patients showed a significant accumulation of radiolabelled HIG in the inflamed pancreas. Six out of seven patients with positive scintigraphy had residual β-cell function and contemporaneous partial clinical remission (Barone *et al.*, 1998). In another study by the same group, two out of five ICA positive individuals showed a significant accumulation of HIG in the pancreas. Subsequently, they all developed clinical T1D later on (Signore *et al.*, 1996).

Interleukin 2 (IL-2) is produced by antigen- or mitogen-activated T lymphocytes and plays a central role in the development of the immune response. IL-2 is thought to act on T cells through its receptor. IL-2 and its surface receptor (IL-2R) are essential components in the growth and proliferation of the effector cells of immunity (Hatamori *et al.*, 1989). As approximately 15% of islet-infiltrating lymphocytes express IL-2R, recombinant IL-2 has been labelled with Iodine-123 (^{123}I) to detect insulitis with scintigraphy (Signore *et al.*, 1992 & 1994, Rolandsson *et al.*, 2001). These studies demonstrated that ^{123}I-labelled IL-2 (^{123}I-IL-2) administered i.v. accumulated specifically in the inflamed pancreas of NOD mice. In humans, ^{123}I-IL-2 scintigraphy was positive in 5 out of 10 patients with newly diagnosed T1D, likely as evidence of ongoing insulitis. Five ICA positive first-degree relatives who were imaged in this study developed diabetes later on. They all showed significant accumulation of ^{123}I-IL-2 in the pancreas (Signore *et al.*, 2003). In another study, 31% of the patients with T1D showed positive scintigraphy of ^{99m}Tc-interleukin-2 at the time of diagnosis. Positive or negative accumulation of tracer in the pancreas did not correlate to any metabolic or immunological parameters at diagnosis. However, patients with positive accumulation showed higher C-peptide values at 3 months and lower insulin requirements at 1 year when compared to tracer negative patients (Chianelli *et al.*, 2008).

2.4.2. SPECT and PET in β-cell imaging

At clinical diagnosis of T1D, it is estimated that less than 25% of functional β-cells are remaining (In't Veld, 2011). In addition in T2D, the reduction of β-cell mass is one key element of the pathology. Therefore, non-invasive β-cell imaging, which would allow an evaluation of the reduction and of the remaining β-cell mass, is considered to be a high-priority field of investigation.

A potential target for measurement of the β-cell mass is the glucagon-like peptide 1 receptor (GLP-1R) as it is abundantly expressed in rat, mouse and human pancreatic β-cells but not in other cells of endocrine pancreas (Mann *et al.*, 2007). GLP-1 induces the release of insulin via binding to its specific pancreatic β-cell receptor. Exendin is a stable agonist of the GLP-1R. Brom and co-workers observed a correlation between ^{111}In-labelled exendin uptake by SPECT in relation to the remaining β-cell mass of rats with alloxan-induced β-cell loss (Brom *et al*., 2014). In human studies, the pancreas was visible in SPECT images while the pancreatic uptake showed high inter individual variation with lower uptake in patients with T1D (Brom *et al*., 2014).

The same receptor has been studied with PET imaging. The GLP-1R agonist ^{64}Cu-(Lys40(DOTA)NH2)exendin-4 accumulated specifically in pancreatic islets but the overall activity difference in the pancreas between healthy and diabetic rats remained low (Connolly *et al.*, 2012). In the study by Selvaraju and co-workers the pancreatic uptake in rats with STZ-induced diabetes was decreased by more than 80% compared with that in healthy controls, as measured by organ distribution of ^{68}Ga-DO3A-exendin-4. Despite the GLP-1R–specific uptake the proximity to the kidney with high uptake limited the visualization of rodent pancreas with ^{68}Ga-DO3A-exendin-4. For that reason the *in vivo* imaging of rodent pancreatic islets with ^{68}Ga-DO3A-exendin-4 is difficult or impossible (Selvaraju *et al*., 2013). Similar results were obtained with [^{64}Cu]NODAGA-exendin-4 in *ex vivo* and *in vivo* studies with rodents which showed GLP-1R-specific labelling of pancreatic islets but the radiation dose in the kidneys limit its use as a clinical tracer (Mikkola *et al*., 2014). Different species might have differences in GLP-1R expression since pancreatic uptake of [^{68}Ga]Ga-DO3A-VS-Cys40-Exendin-4 was not reduced by destruction of β-cells in STZ-induced diabetic pigs (Nalin *et al*., 2014).

Vesicular monoamine transporter type 2 (VMAT2) has been shown to express in dopamine nerve terminals in the pancreatic β-cells but it is absent in the exocrine cells (Weihe *et al.*, 1994, Maffei *et al.,* 2004). It is an integral membrane protein that transports dopamine, norepinephrine, and serotonin into the transport vesicles of synaptic terminals of monoaminergic neurons (Weihe *et al*., 2000). Dihydrotetrabenazine (DTBZ) is a specific ligand for VMAT2. Determination of [^{11}C]DTBZ uptake with PET in the pancreas of diabetes prone BB rats appeared to correlate to the loss of β-cell mass and glycemic control (Souza *et al.*, 2006). Binding to the pancreas was reduced after the development of diabetes but there was no evidence of islet-specific accumulation of radioactivity in the rat pancreas (Fagerholm *et al.*, 2010). The presence of VMAT2 binding potential in the pancreas using [^{11}C]DTBZ PET was compared in patients with long-standing T1D and healthy controls. The signal was reduced in T1D patients but it correlated poorly with β-cell mass and at the same time, nonspecific binding within the pancreas overestimated β-cell mass similarly as earlier with rats (Goland *et al.*, 2009). ^{18}F-fluoropropyl-dihydrotetrabenazine (^{18}F-FP-(+)-DTBZ) has an eight-fold higher binding affinity for

VMAT2 molecule than [^{11}C]DTBZ. The dynamic range for quantitative PET of β-cell mass was determined using ^{18}F-FP-(+)-DTBZ; significant correlations of tracer binding in the pancreas with C-peptide release was found indicating that ^{18}F-FP-(+)-DTBZ PET could be used to discriminate between healthy controls and T1D subjects (Normandin *et al*., 2012). However, PET imaging does not differentiate between the cellular localization of VMAT2 in the endocrine (islets) and exocrine regions of the pancreas. Hong and co-workers have demonstrated recently that the predominant presence of VMAT2 binding sites are associated with α-cells and PP-cells but not with β-cells in primate pancreatic islets, which was also consistent with the expression pattern of VMAT2 in rodent islets (Hong *et al*., 2014).

The accumulation of various PET tracers into rat insulinoma INS-1 cells was compared to isolated rat islets and a human pancreatic ductal cell line (PANC-1) (Sweet *et al.*, 2004). Glibenclamide and fluorodithizone showed the highest specificity for islets and INS-1 cells relative to PANC-1. Dopamine was taken up more by islets than by PANC-1 cells, although not by INS-1 cells. [^{18}F]FDG specificity to the INS-1 and islets was very low. Glibenclamide was the most promising molecule in this report based upon the criteria of specificity.

Some other promising molecules which have been used to image β-cell mass, or which are physiologically associated with high cellular specificity are summarized in the review articles of Wu & Kandeel (2010), Malaisse & Maedler (2012), and Andralojc and co-workers (2012).

2.4.3. Magnetic Resonance Imaging (MRI) of insulitis

Insulitis is accompanied by a range of microvascular alterations, including modifications of endothelial cells, vascular swelling and leakage, enhanced islet blood flow and influxes of inflammatory-cell populations as described earlier. MRI of magnetic nanoparticles (MNP) has been reported to be sensitive to such changes. In the BDC2.5/NOD model, the microvascular changes developed dramatically 3 days after cyclophosphamide injection, just two days prior to the onset of overt diabetes. Turvey and co-workers were able to differentiate between new-onset diabetics, nondiabetic NOD littermates at the risk of developing diabetes, and noninsulitic Eα16/NOD mice by using MRI-MNP (Turvey *et al*., 2005). Microvascular alterations were observed by long-circulating magnetofluorescent nanoparticles (CMFN) extravasating from vessels into the surrounding tissue and they were engulfed by the activated macrophages that had invaded the tissue. The nanoparticle-induced signal changes were less striking in the standard NOD model than in the more homogeneous and synchronous BDC2.5/NOD mice. This divergence was explained by the kinetic difference in the insulitis lesions present in these two types of mice, the lower frequency of autoreactive T cells

in the former promoting a more progressive onset of insulitis (Denis *et al.*, 2004). In another study, MRI was able to distinguish between NOD mice that would or would not develop clinical diabetes and it permitted an estimation of time to the onset of diabetes. The MRI-MNPs of 6- and 10-week-old mice were the most predictive (Fu *et al*., 2012).

MNP ferumoxtran-10 has a dextran coating and size characteristics similar to those of the MNPs used in the animal experiments. It is taken up by macrophages, while not provoking activation or inducing proinflammatory cytokines or superoxide anions. It is not chemotactic, and it does not interfere with Fc-receptor–mediated phagocytosis. When the difference of T2 relaxation time (ΔT2) before and after the injection of MNP ferumoxtran-10 was compared in 10 diabetic patients with less than 6 months from diagnosis, and 12 non-diabetic controls, there was a significant difference in the ΔT2 measured from pancreas. There was no correlation between the ΔT2 of pancreas and the daily insulin requirement, the time since diagnosis, the age, HbA_{1c} level, or autoantibody titers (Gaglia *et al*., 2011). They reported a pancreatic volume index (PVI) by dividing the pancreatic volume by body-surface area in diabetic patients to be about two-thirds of the controls. The pancreatic volume has earlier been shown to be reduced by 48% in long-standing T1D as compared with age matched normal subjects (Williams *et al.*, 2007).

Vascular swelling and increased blood flow precede insulitis in streptozotocin (STZ)-induced mouse model of T1D and it resembles insulitis in NOD mouse. A long circulating paramagnetic contrast agent, protected graft copolymer (PGC) covalently linked to gadolinium-diethylenetriaminepentaacetic acid residues (GdDTPAs) labeled with fluorescein isothiocyanate (PGC-GdDTPA-F), was used for the noninvasive semiquantitative evaluation of vascular changes in the STZ mouse model. Significantly greater accumulation of PGC-GdDTPA-F in the pancreata of diabetic animals was demonstrated compared with controls. *Ex vivo* histology revealed extensive distribution of PGC-GdDTPA-F within the vascular compartment of the pancreas, as well as considerable leakage of the probe into the islet interstitium. In contrast, in nondiabetic controls, PGC-GdDTPA-F was largely restricted to the pancreatic vasculature at the islet periphery (Medarova *et al*., 2007).

Few MRI studies have focused on following the homing of diabetogenic immune cells to the pancreas. Lymphocytes derived from diabetic NOD mouse and labelled with novel crosslinked iron oxide nanoparticles derivatized with membrane translocation signal (CLIO-tat) were visualized within the islets. The same label was not detected in the pancreas of control animals (Moore *et al.*, 2002). ^{19}F MRI has been used to show the early homing of diabetogenic T cells to the pancreas. Approximately 2% of the T cells labelled *ex vivo* with the perfluoropolyether nanoparticles reached the pancreas; MHC-mismatched nonspecific T cells were not detected in the pancreas (Srinivas *et al.*,

2007). Moore and co-workers reported an antigen-specific magnetic label to selectively target a prevalent population of diabetogenic $CD8^+$ T-cells that contribute to the progression of insulitis in NOD mice (Moore *et al*., 2004). Superparamagnetic nanoparticles coated with multiple copies of a high-avidity peptide/major histocompatibility complex ligand of T-cells (NRP-V7/Kd) were used to detect inflammation of pancreatic islets by autoreactive T-cells in real time by MRI. The goal of the study was to engineer MRI probes that were capable of labelling specific populations of autoreactive lymphocytes within the total lymphocyte pool of a given individual (Moore *et al*., 2004).

Inspired by an earlier result with ^{123}I-IL-2 with scintigraphy, the uptake of IL-2 labelled Gd-DTPA in the pancreas of prediabetic NOD mice was determined *ex vivo* with 1.5T MRI. The pancreas-to-background ratio was 1.5-times higher in the non-diabetic 12 week old female NOD mice 24h after receiving IL-2-Gd-DTPA instead of plain Gd-DTPA (271 ± 37 vs. 183 ± 0.1, $p = 0.04$). At the same time, the pancreas-to-plasma ratio of gadolinium was 25-fold for IL-2-Gd-DTPA (Kalliokoski *et al.*, 2011).

2.4.4. MRI in β-cell imaging

A few MRI markers have been investigated for their potential to image β-cell mass in the pancreas. Manganese (Mn^{2+}) has been used as a MRI contrast agent as it shortens the longitudinal relaxation time (T1). In pancreas, it enters the β-cells through voltage-gated calcium (Ca^{2+}) channels (Fig. 3.). Glucose-stimulated Mn^{2+} enhancement in the MRI signal increased by 50% within the pancreas of healthy mice but only by 9% in streptozotocin induced diabetic mice. However, this difference was not statistically significant (Antkowiak *et al.*, 2009). One limitation to the use of Mn^{2+} as a β-cell imaging agent is its lack of specificity and its potential cytotoxicity.

Wang and co-workers have synthesized an exendin-4 conjugated magnetic iron oxide based nanoparticle (MNEx10-Cy5.5) probe targeting glucagon-like peptide-1 receptor (GLP-1R), a receptor which is highly expressed on the surface of pancreatic β-cells. When MNEx10-Cy5.5 probe was injected to mice the *in vivo* MR imaging showed a significant T2 relaxation time shortening in the pancreas compared to the control animals injected with the non-targeted probe. The mechanism of nanoparticle accumulation in the pancreas reflected both target specific and passive (vascular) uptake leading to the detectable MRI signal change in the pancreas (Wang *et al*., 2014).

GdDOTA-diBPEN–$(Zn)_2$ has been investigated as a MR contrast agent for β-cell imaging. The affinity of MRI marker GdDOTA-diBPEN to albumin increased when Zn^{2+} ions were present with GdDOTA-diBPEN (Esqueda *et al*., 2009). The resulting GdDOTA-diBPEN–$(Zn)_2$ complex enhances water proton relaxivity when it is bound to albumin. If Zn^{2+} is absent, the proton relaxivity of GdDOTA-diBPEN is below the MRI detection limit. If the MRI was performed after the administration of

GdDOTA-diBPEN, the MRI signal of the pancreas was not enhanced by the agent. However, signal enhancement was observed after glucose had been elevated to a level that stimulated insulin secretion. Insulin is packaged into a Zn^{2+}/insulin complex in the β-cells, and the insulin release enhances Zn^{2+} ion concentration in the pancreas (Li, 2014). The MR images of control mice displayed a higher signal in the pancreas after injection of a bolus of glucose followed by a low dose of the Zn^{2+} sensor GdDOTA-diBPEN. The same enhancement was not observed in mice pretreated with STZ.

2.5. PET tracers for imaging of healthy and prediabetic pancreas (study I-III)

2.5.1. Tracers for imaging of pancreatic glucose metabolism; 2-Deoxy-2-[^{18}F]fluoro-D-glucose ([^{18}F]FDG)

2-Deoxy-2-[^{18}F]fluoro-D-glucose ([^{18}F]FDG) is a labelled glucose analogue in which the hydrogen in the 2-position has been replaced by fluorine-18 ($T_{½}$=109.8 min). Intravenously injected [^{18}F]FDG is transported into the tissue by the same carriers as glucose. Inside the cell, [^{18}F]FDG is phosphorylated to [^{18}F]FDG-6-phosphate by hexokinase II. After phosphorylation [^{18}F]FDG-6-phosphate enters the glycolytic pathway but it cannot undergo glycolysis and is trapped into the cell (Horton *et al.*, 1973). Therefore, higher glucose consumption in the cells leads to a higher intracellular [^{18}F]FDG concentration in the tissue.

[^{18}F]FDG uptake has been related to GLUT1 expression in the tissue (El-Chemaly *et al*., 2013). Alterations in [^{18}F]FDG uptake have been explained to rely on differences in GLUT activity rather than by differences in number of transporters present (Higashi *et al*., 2000). Activation of aerobic glycolysis in pheochromocytomas and paragangliomas has been shown to associate with increased [^{18}F]FDG accumulation due to increased glucose phosphorylation by hexokinases rather than increased expression of GLUTs (Van Berkel *et al*., 2014).

The fractional rate of tracer uptake and phosphorylation (K_i) in the tissue can be calculated by using a graphical analysis technique (Patlak *et al*., 1985). Graphical analysis is valid under steady-state conditions. The quantification of glucose uptake via [^{18}F]FDG is possible when the rate of [^{18}F]FDG uptake relative to glucose from plasma into tissue is known.

2.5.2. Tracers for imaging of pancreatic amino acid metabolism; [^{11}C]methionine

Methionine is an essential amino acid needed for protein synthesis, transmethylation reactions, polyamine synthesis, and as a precursor for transsulfuration pathways. The natural amino acid, methionine, labelled with ^{11}C ($T_{½}$ = 20.3 min) has the same chemical properties as the unlabelled precursor. Transport of methionine into the cell is for the

most part mediated by sodium-independent system-L which is also a transport system for amino acids such as valine, leucine and phenylalanine (Kobayashi *et al.*, 2012).

Radiolabeled amino acids such as [^{11}C]methionine have been widely used as tracers for detection of malignancies with PET. The uptake of [^{18}F]FDG into normal human pancreas is modest, but [^{11}C]methionine accumulates in the pancreas much more intensely than in the surrounding tissues (Syrota *et al.*, 1981), which is ideal for delineating tissue margins. In rats, [^{11}C]methionine accumulates in the pancreas, liver, kidney, and spleen quantitatively in this order (Kubota *et al.*, 1984).

2.5.3. Tracers for imaging of dopamine synthesis in pancreas; [^{18}F]FDOPA

The PET tracer fluorine-18 labeled L-dihydroxyphenylalanine ([^{18}F]FDOPA) was one of the earliest ^{18}F-labeled compounds to be used to investigate the activity of the dopaminergic system (Firnau *et al.*, 1973). The radiolabelled FDOPA is transported across the membrane by an amino acid transporter, after which it is decarboxylated into fluoro-dopamine (FDA) and stored in vesicles. The retention of neurotransmitters is considered to be the result of tissue uptake, decarboxylation, and granular storage by vesicular monoamine transporters.

The uptake of FDOPA in the tissues can be enhanced if enzyme inhibitors are used to manipulate the metabolic pathway (Fig. 6). If enzyme inhibitors are not used, the majority of FDOPA is metabolized to 3-O-methyl-fluorodopa (3-OMFD). FDOPA is metabolized to 3-OMFD by catechol-*O*-methyltransferase (COMT) and to 6-fluorodopamine (FDA) by aromatic amino acid decarboxylase (AADC). The two isoforms of MAO, MAO-A and MAO-B, deaminate FDA to produce 1,3,4-dihydroxy-6-fluorophenylacetic acid (FDOPAC) before it is converted into 6-fluorohomovanillic acid (FHVA) by COMT (Melega *et al.,* 1990, Wang *et al.,* 1997).

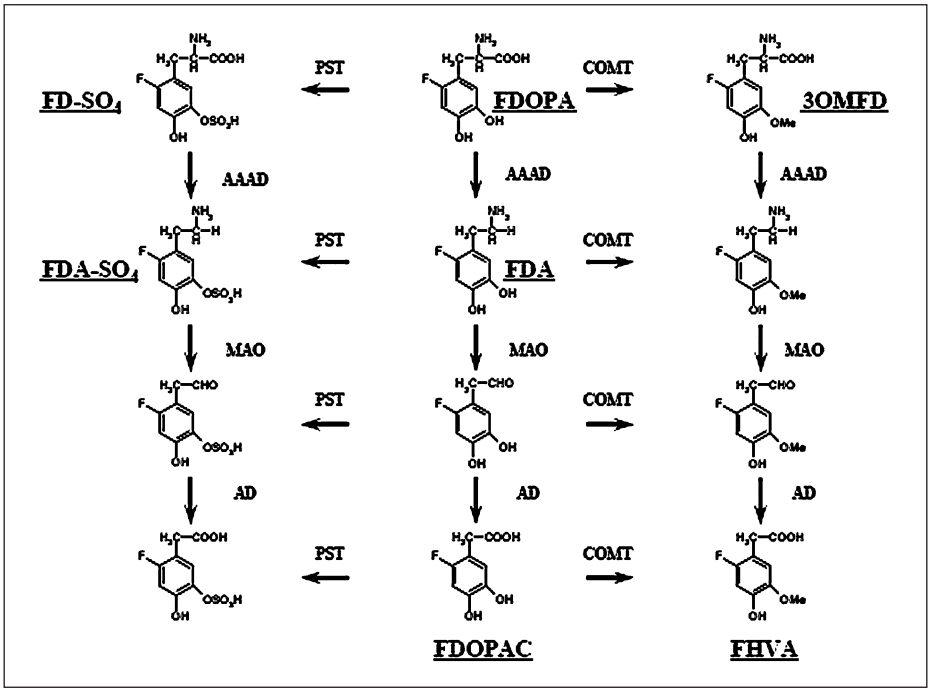

Figure 6. Schematic model of FDOPA metabolites and enzymes. FDOPA, 6-fluoro-L-DOPA; FDA, 6-fluorodopamine; 3-OMFD, 3-O-methyl-fluorodopa; FDOPAC, 1,3,4-dihydroxy-6-fluorophenylacetic acid; FHVA, 6-fluorohomovanillic acid; AAAD, aromatic amino acid decarboxylase; COMT, catechol-*O*-methyltransferase; MAO, monoamine oxidase; PST, phenolsulfotransferase; AD, aldehyde dehydrogenase. Sulfatated metabolites (SO_4) have been presented only in the plasma, not in the tissue (Reproduced with permission from Ruottinen *et al.*, 2001).

Increased activity of L-DOPA decarboxylase was found to be a characteristic of a neuroendocrine tumor (Gazdar *et al.*, 1988). Later on [^{18}F]FDOPA has proven to be a useful tool for localization of gastrointestinal malignancies (Nanni *et al.*, 2006) and neuroendocrine tumors in adult patients (Kauhanen *et al.,* 2007, Kauhanen *et al*., 2009), and it has become the golden standard in the detection and differentiation of pancreatic lesions such as focal β-cell hyperplasia and ectopic lesions in congenital hyperinsulinism of infancy (Otonkoski *et al*., 2006, De Lonlay *et al*., 2006, Blomberg *et al*., 2013). Although several studies have shown that normal pancreatic cells take up L-DOPA, the relatively low β-cell specificity has not precluded the use of this compound as a PET imaging agent with which to assess the β-cell mass in diabetic patients (Wu & Kandeel, 2010).

3. AIMS OF THE STUDY

The overall aim of this thesis was to evaluate the imaging potential of [^{18}F]FDG, [^{11}C]methionine, and [^{18}F]FDOPA PET to detect changes in the pancreas that are associated with the development of type 1 diabetes.

The specific aims of each study were as follows:

1. To study if [^{18}F]FDG combined with autoradiography could be useful in the visualization of insulitis in the pancreas of NOD mice (I).

2. To evaluate whether [^{11}C]methionine and/or [^{18}F]FDG PET could be of benefit in the visualization of the inflammatory process in the islets and their surrounding tissue in the pancreas of newly diagnosed T1D adult patients (II).

3. To investigate how enzyme inhibitors could change [^{18}F]FDOPA distribution and metabolism in the rat pancreas, and if they would enhance the possibility of β-cell imaging with [^{18}F]FDOPA PET (III).

4. SUBJECTS AND STUDY DESIGNS

4.1. Experimental protocols (I and III)

4.1.1. Animals

The Animal Experiment Board of the Province of Southern Finland and the University of Turku Ethics Committee for Animal Experiments approved the animal studies (I, III).

At the time of experiments, the animals were housed under standard conditions (21 °C, humidity 55 ± 5%, 12-hour light cycle). Before the experiment, the mice fasted for six hours but had free access to water. The rats had free access to standard laboratory chow and tap water.

Female BALB/c and NOD mice were purchased from the M&B Laboratories (Ry, Denmark). A total of 25 healthy female BALB/c mice (age 8, 9, 13 or 20 weeks, n=3-9 in each age group), of which 11 were used in a prestudy, and 21 female NOD mice (NOD/Bom; age 8, 12, 14, 15 and 16 weeks, n = 4, 5, 5, 2 and 5 in the age groups, respectively) participated in the actual study.

Male SD rats (Harlan Sprague-Dawley, Indianapolis, IN, USA; n = 68, weight 284 ± 36 g) were used in study III.

4.1.2. Study design for NOD mice (I)

In a prestudy, the optimal time point for the actual uptake experiments was determined based on the decline of [^{18}F]FDG activity in the blood and the enhancement in [^{18}F]FDG accumulation to the pancreas (see details in Methods). As the half-life of ^{18}F is 109.8 min, in this study a 90-min time point was chosen for the estimation of [^{18}F]FDG uptake in the pancreas (Fig. 7).

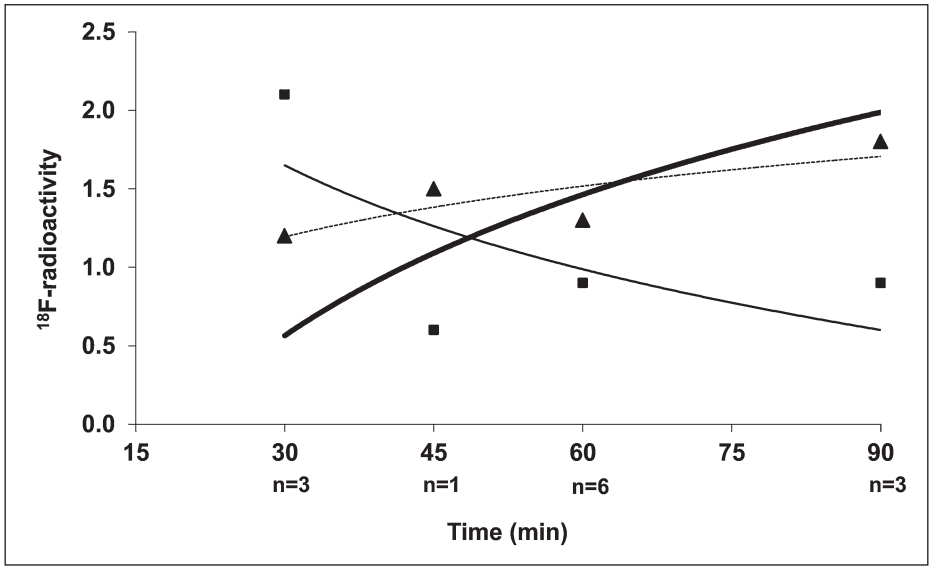

Figure 7. The optimal time point for the [^{18}F]FDG uptake studies was determined based on the decline in the blood ^{18}F-radioactivity (■) curve (thin line) and increase in ^{18}F accumulation to the pancreas (▲) (dashed line). The pancreas-to-blood uptake ratio (dark line) increased rather steadily for at least 90 min. The ratio at 60 min was 1.5 ± 1.2 and had reached 2.2 ± 0.6 at 90 min. At 90 min, the ^{18}F-radioactivity in the pancreas was most likely to be tissue specific. Figure has been modified from the publication I.

In the uptake study the mice received 3.7 ± 2.3 MBq of [^{18}F]FDG in physiological saline through the tail vein as a single bolus. The mice were decapitated 90 min after the tracer injection. The mice were weighed and tissue samples from blood, pancreas, liver, skeletal muscle, and cortical brain were collected for biodistribution and autoradiographic studies.

4.1.3. Study design for rats (III)

The characteristics of the Harlan Sprague-Dawley study groups are listed in Table 2.

Table 2. The premedications, characteristics and injected activity of [^{18}F]FDOPA in the experimental animals**.**

Group	Premedication	Number of animals	Animal weight (g)	Injected activity (MBq)
VEHICLE	0.9% NaCl	n = 7	279 ± 38	50 ± 10
AADC	Carbidopa	n = 6	261 ± 26	40 ± 13
MAO-A	Clorgyline	n = 3	283 ± 25	44 ± 3
MAO-B	Deprenyl	n = 7	278 ± 40	36 ± 10
COMT	Ro 41-0960	n = 8	286 ± 35	45 ± 11
AADC & COMT	Carbidopa and Ro 41-0960	n = 4	259 ± 16	45 ± 5
MAO-A & COMT	Clorgyline and Ro 41-0960	n = 5	264 ± 25	42 ± 15
MAO-B & COMT	Deprenyl and Ro 41-0960	n = 9	298 ± 41	47 ± 14

Pretreatments were first administered intraperitoneally 30 min before the injection of [^{18}F]FDOPA. Pretreatments carried out included vehicle (0.9% NaCl), as a control group. Carbidopa (S-[-]-carbidopa), a selective inhibitor of AADC, was used at a dose of 18 mg/kg. For the inhibition of MAO-A and MAO-B, 10 mg/kg of clorgyline (methyl-*N*-propargyl-3-[2,4-dichlorophenoxy]) and 10 mg/kg deprenyl (R-[-]-deprenyl hydrochloride), respectively, were used. The COMT inhibitor Ro 41-0960 was given at a dose of 30 mg/kg. Combinations of COMT + AADC, COMT + MAO-A, and COMT + MAO-B were administered with doses in line with the single dose pretreatments. All inhibitors were purchased from Sigma Aldrich Chemicals (Steinheim, Germany).

The design of the rat study is shown in Figure 8. [^{18}F]FDOPA (45.3 ± 14.0 MBq) was injected into the tail vein 30 min after the pretreatments. Thirty minutes after the injection of [^{18}F]FDOPA, animals (n=61) were sacrificed by CO_2 inhalation. Blood and tissue samples were rapidly dissected, weighed, and prepared for further analysis. 60 min dynamic [^{18}F]FDOPA PET/CT scans were performed in seven rats starting at 30 min after pretreatments with vehicle (n=1), AADC (n=3) inhibitor or with the combination of COMT and MAO-A (n=3) inhibitors.

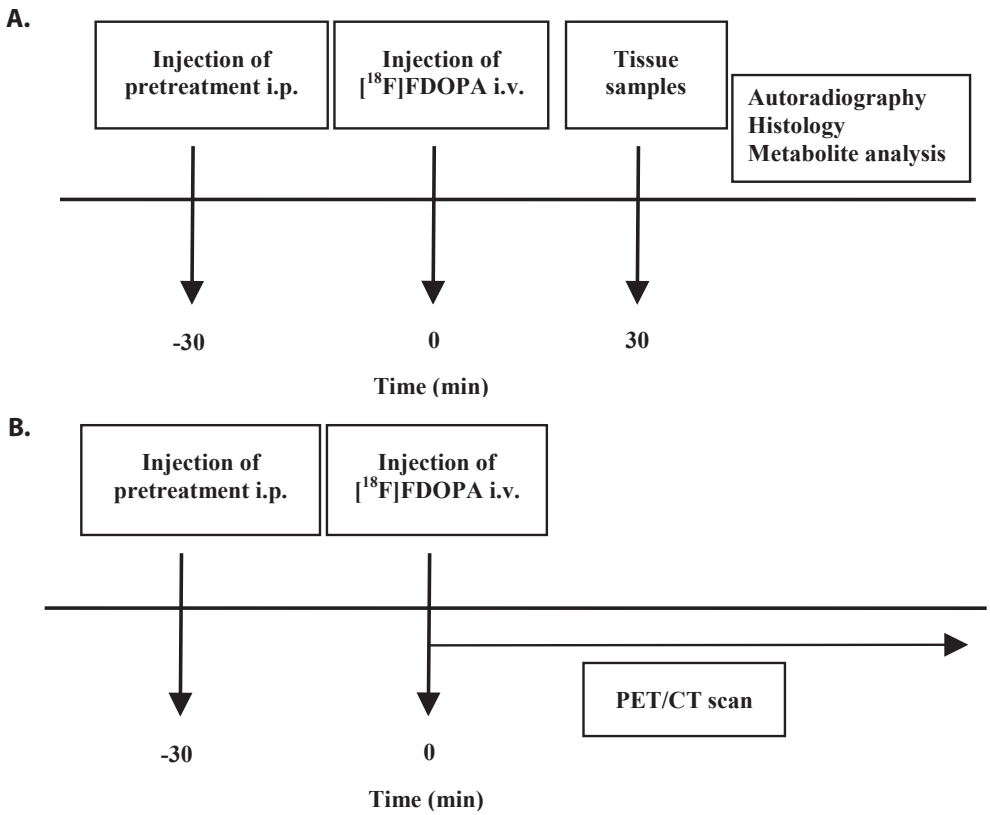

Figure 8. Study design III. Tissue distribution of [^{18}F]FDOPA (A.) and dynamic PET scan (B.).

4.2. Experimental protocol (II)

4.2.1. Study subjects (II)

The nature, purpose and potential risks of the study were explained to all subjects as part of the written informed consent procedure. The Ethics Committee of the Turku University Hospital approved the study (II).

The characteristics of the study subjects are shown in Table 3. A total of sixteen adult male patients with newly diagnosed multiple autoantibody positive T1D participated in the study. The patients had classical symptoms of T1D and fulfilled the WHO diagnostic criteria. The control group included nine age-matched healthy men without any medication. None of the subjects had clinical symptoms of pancreatitis.

Table 3. The clinical characteristics of the T1D patients and healthy controls included in the study.

	Age (yr)	BMI (kg/m^2)	Duration of diabetes (months)	Insulin dosage (IU/kg/day)	Fasting C-Peptide (nmol/L)	HbA_{1c}	ICA (JDFU)	Autoantibodies (RU) GADA	IA-2A	IAA
T1D	24	23.5	6	0.23	0.24	12.0 %	15.0	39.3	105.6	1.0
	32	25.6	5	0.52	0.14	15.2 %	8.0	4.7	23.2	103.9
	19	20.1	2	0.49	0.29	9.9 %	110.0	157.7	0.1	137.3
	35	28.1	3	0.22	0.15	14.1 %	219.0	155.5	44.3	46.9
	22	17.5	0.7	0.58	0.15	10.2 %	0.0	8.6	0.1	127.2
	40	21.9	0.4	0.29	0.16	10.5 %	8.0	117.8	7.0	28.5
	22	19.6	0.75	0.59	0.15	15.3 %	15.0	149.8	0.1	1.0
	33	23.2	0.25	0.73	0.26	10.3 %	28.0	-	1.3	5.1
	21	17.7	0.25	0.50	0.26	12.2 %	15.0	5.9	68.0	1.0
	21	20.0	2	0.69		15.3 %	96.0	5.2	80.2	3.0
	20	21.6	6.8	0.36	<0.13	13.5 %	49.0	47.0	100.4	264.5
	22	20.0	0.4	0.95	0.15	13.1 %	13.0	29.8	0.3	5.0
Healthy	32	25.1	no	no	-	5.7 %	0.0	0.1	0.1	2.9
	37	25.4	no	no	-	4.8 %	0.0	0.1	0.1	1.0
	25	18.8	no	no	-	5.5 %	0.0	0.1	0.1	1.0
	34	24.6	no	no	-	5.3 %	0.0	0.1	0.1	1.0
	26	24.9	no	no	-	5.7 %	0.0	0.1	0.1	1.0
	35	24.7	no	no	-	5.2 %	0.0	-	0.1	1.0
	32	27.8	no	no	-	5.0 %	0.0	0.2	0.1	1.0
	44	26.3	no	no	-	-	0.0	0.1	0.1	0.1
	24	26.6	no	no	-	-	3.0	2.6	0.1	0.2

BMI = body mass index, HbA_{1c} = glycolysated haemoglobin, ICA = islet cell autoantibody, GADA = glutamate decarboxylase autoantibody, IA-2A = insulinoma-associated protein 2 tyrosine phosphatase autoantibody, IAA = insulin autoantibody, T1D = type 1 diabetes. C-peptide and HbA_{1c} values were measured at the time of diagnosis of type 1 diabetes. In the healthy volunteers HbA_{1c}, and from all participants diabetes-associated autoantibodies and BMI were measured at the time of the PET scan. Insulin dosage included both long- and short acting insulin at the time of the PET study.

Volunteers were recruited using public announcements on student notice boards. Inclusion criteria for the volunteers were age range 18-45 years and BMI 18-30 kg/m^2. Volunteers were healthy as judged by history, physical examination, and routine laboratory tests including fasting blood leucocyte and erythrocyte counts, hemoglobin, and plasma glucose. The subjects were not taking any medication.

PET data were not obtained in one diabetic patient due to technical problems during the study. One patient was excluded from the final analysis since he was in clinical remission

requiring only 2 IU of short acting insulin before breakfast. Two additional patients were excluded from the study because normoglycemia was not achieved during the PET study. Twelve type 1 diabetic patients and nine healthy subjects were included in the final analysis. All subjects were non-smokers.

4.2.2. Study design (II)

All subjects were studied after an overnight fast, and with the subjects lying in the supine position on the PET scanner bed. Two venous catheters were inserted, one in the antecubital vein for infusion of saline, insulin, glucose, and [^{18}F]FDG, and another in contra-lateral heated vein for sampling of arterialized venous blood. The hand chosen for sampling was heated to "arterialize" venous blood since assays of insulin, glucagon, pyruvate and free fatty acids from the heated vein have proven to be very close to the arterial values (Green *et al.*, 1990, Ericson *et al.*, 1987).

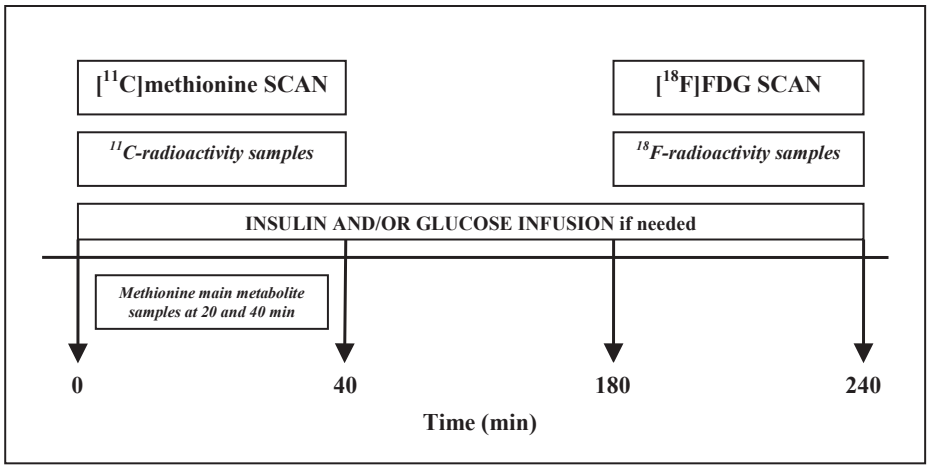

Figure 9. Study design II.

Prior to the [^{18}F]FDG PET study, MRI was performed on the day before the PET scan. In addition [^{11}C]methionine scanning was performed for anatomical localization of the pancreas to nine diabetic patients and seven healthy controls (Fig. 9). Subsequently, this procedure was replaced by hybrid PET/CT device. All patients underwent PET studies no later than 7 months after the diagnosis of T1D. Patients with diabetes were rendered normoglycemic before the start of the study. The regular dose of intermediate or long-acting insulin was reduced by one-half. Subjects fasted for 12 hours before the study. Therefore short-acting insulin was withdrawn on the morning of the study from the diabetic patients.

5. METHODS

5.1. PET imaging

5.1.1. Production of positron emitting tracers (I-III)

All tracers were synthesized in the Radiopharmaceutical Chemistry Laboratory of Turku PET Centre. [^{18}F]FDG ($T_{1/2}$ = 109.8 min) was synthesized with an automated apparatus, according to the modified method of Hamacher *et al.* (1986). The specific radiochemical purity exceeded 98% and the specific activity was 76 MBq/nmol. [^{11}C]Methionine ($T_{1/2}$ = 20.3 min) was prepared as described (Någren & Halldin, 1998). The radiochemical purity exceeded 92% and the specific activity exceeded 37 MBq/nmol (Någren 1993). [^{18}F]FDOPA was synthesized as described by Forsback *et al.* (2008). The specific activity of [^{18}F]FDOPA exceeded 5.8 GBq/µmol, and the radiochemical purity exceeded 98% in every production batch.

5.1.2. Tracer biodistrubution (I, III)

In study I, tissue samples were measured for ^{18}F-radioactivity and expressed as a percentage of injected dose per gram tissue (%ID/g). The uptake represents the total ^{18}F-activity in the tissue including [^{18}F]FDG, [^{18}F]FDG 6-phosphate and UDP-[^{18}F]FDG (UDP-2-deoxy-2-[^{18}F]fluoro-α-D-glucopyranose). In study III, tissue samples were measured for total ^{18}F-radioactivity in blood, pancreas, spleen, liver, skeletal muscle, myocardium, kidney, striatum, adrenal glands, and for the small and large intestine and expressed as %ID/g.

5.1.3. Radioactivity distribution in pancreas sections (I, III)

The distribution of ^{18}F-radioactivity in pancreas cryosection was measured by digital autoradiography. The pancreas slices were prepared immediately after the sacrifice of the animal. The pancreas was removed and chilled in isopentane/CO_2 slush. In study I, sections of 20 and 10 µm thicknesses were alternately cut from the pancreas with a cryomicrotome for autoradiography and immunohistochemistry. In study III, all sections were 20 µm in thickness. In both studies, the 20 µm sections were placed in an exposure cassette, the distribution of radioactivity was recorded using a phosphoimager (Fuji BAS-5000, Fuji Photo Film) and images were analysed for count densities (photostimulated luminescence per unit area, PSL/mm^2) with analysing program TINA 2.1 (Raytest Isotopenmessgeräte Strubenhardt, Germany) or AIDA (Image Analyzer v. 4.2.2, Raytest Isotopenmessgeräte, Straubenhardt, Germany). The same tissue sections were then stained with hematoxylin and eosin for histological analysis.

Layers from histological images and autoradiography were overlaid using Adobe PhotoShop CS2 (CA, USA). As the same sections had been previously used for autoradiography, specific morphological structures were accurately localized. Count densities for background areas were subtracted from the image data. The differences in count densities were reported as ratios between endocrine versus exocrine pancreas.

5.1.4. PET imaging with animal PET/CT (III)

In study III, animal PET scans were carried out with an Inveon Multimodality PET/CT scanner (Siemens Medical Solutions USA, Knoxville, TN, USA). The following transmission scans for attenuation correction using the CT modality, 60-min dynamic PET scans in three-dimensional list mode were started at the same time with an intravenous bolus injection of [^{18}F]FDOPA at a dose of 32.8 ± 7.6 MBq (Fig. 8). The time frames used for the dynamic PET studies were 30 x 10 s, 15 x 60 s, 4 x 300 s, and 2 x 600 s. Images were reconstructed using the two-dimensional filtered back projection algorithm.

5.1.5. Image acquisition and processing with PET/(CT) (II)

The study subjects were positioned in a supine position inside the PET camera. GE Advance Scanner (General Electric Medical Systems, Milwaukee, WI, USA) or Discovery VCT PET/CT scanner (General Electric Medical Systems, Milwaukee, WI, USA) were used for imaging. Photon attenuation was measured with a 5-min transmission scan. Either CT or the preceding MRI was used for anatomical reference. The subjects who were studied with [^{11}C]methionine first, a dynamic scan (40 min; 4 x 30, 3 x 60, 5 x 180, 4 x 300 s frames) was obtained. [^{18}F]FDG scanning was started more than 2 h (6 x ^{11}C half-life) after the [^{11}C]methionine injection to allow decay of the ^{11}C-radioactivity. Dynamic [^{18}F]FDG-PET scan (60 min; 4 x 30, 3 x 60, 5 x 180, 4 x 300, 2 x 600 s frames) was initiated at the time of the injection. Plasma radioactivity was measured with an automatic gamma counter (Wizard 1480 3", PerkinElmer-Wallac, Turku, Finland). During the PET studies, normoglycemia was maintained using a variable-rate infusion of 20% glucose or an euglycemic insulin clamp was started with a low insulin dose (0.2 mU/kg/min) (DeFronzo *et al.,* 1979). All data were corrected for dead-time, decay, and measured photon attenuation and reconstructed in a 128 x 128 matrix with a Hann-filter of 0.3-0.5 cycles per sec. Image manipulation and data handling were performed on SUN SPARC workstations (Sun Microsystems, Mountain View, CA).

5.2. Analysis of PET data (II and III)

5.2.1. Regions of interest (II)

In study II, regions of interest (ROIs) were placed in the body and head of the pancreas as well as in the erector spinae muscle, according to the anatomical reference of MRI or CT.

In studies using MRI to locate the pancreas in PET images, regions of interest were placed in the transaxial MRI picture with the same zoom as the PET images. ROIs were copied from MRI sections to the corresponding planes in the [^{11}C]methionine image to confirm their correct positioning, and then ROIs were copied to the [^{18}F]FDG planes using the same zoom and thickness. The pancreatic tissue uptake of PET images was always correlated side by side with the anatomical reference images of MRI combined with [^{11}C]methionine scan or the corresponding CT when the PET/CT modality was used.

5.2.2. Regions of interest (III)

Volumes of interest were manually drawn on the rat pancreas and liver as verified with corresponding CT images using Inveon Research Workplace Image Analysis software v. 4.0 (Siemens Medical Solutions, USA). The obtained radioactivity concentrations were normalized to the injected dose and injection time, and time-radioactivity curves were obtained for all volumes of interest.

5.3. Analysis of methionine uptake using [^{11}C]methionine, and glucose uptake using [^{18}F]FDG (II)

Radioactivity of [^{11}C]methionine and [^{18}F]FDG measured in arterialized venous blood samples collected during each timeframe, were used as input function. The three compartment model of [^{11}C]methionine and [^{18}F]FDG kinetics (Sokoloff *et al.*, 1977) and graphical analysis according to Patlak & Blasberg (1985) were used to quantify the fractional uptake rates. The plasma curve was used for graphic analysis of [^{18}F]FDG and [^{11}C]methionine influx as described by Leskinen *et al.* (1992). The slopes of the plot (K_i) in graphical analysis are equal to the utilization rate constants of [^{11}C]methionine and [^{18}F]FDG. The rate of glucose uptake (per 100 g tissue per min) was obtained by multiplying K_i by the plasma glucose concentration divided by the lumped constant (LC) which is a correction factor for the tissue.

5.3.1. Lumped constant for [^{18}F]FDG in pancreas

Quantitation of the glucose uptake in pancreas with [^{18}F]FDG PET requires an appreciation of the rate of the uptake of [^{18}F]FDG relative to glucose from plasma into the tissue metabolite pools. The lumped constant (LC) accounts for ratio between [^{18}F]FDG and glucose uptake into the tissue. A lumped constant value of 1.0 for pancreas and 1.2 for skeletal muscle was used, as described (Nuutila *et al.*, 2000).

5.4. Enzyme inhibition of [^{18}F]FDOPA metabolism (III)

The metabolism of [^{18}F]FDOPA is regulated by several enzymes. Metabolism of [^{18}F]FDOPA is comparable to FDOPA metabolism which has been presented above (Fig 6.).

5.5. Analysis of radioactive metabolites

5.5.1. [^{11}C]Methionine metabolites in blood (II)

Radioactive metabolites of [^{11}C]methionine in the plasma were analyzed at 0, 20 and 40 min after the injection. The low molecular weight fraction of [^{11}C]methionine radiometabolites in plasma were separated by fast-gel filtration using Sephadex PD-10 column (Pharmacia Fine Chemicals, Uppsala, Sweden).

5.5.2. [^{18}F]FDOPA metabolites in the pancreas (III)

Radioactive metabolites in pancreas homogenates were analyzed with high performance liquid chromatography (HPLC). Authentic standards (Eskola *et al.*, 2012, Lehtiniemi *et al.,* 2012) of [^{18}F]FDOPA, 3,4-dihydroxy-6-[^{18}F]fluorophenylacetic acid, 6-[^{18}F] fluorohomovanillic acid, and 6-[^{18}F]fluoro-3-methoxytyramine were used to identify retention orders in the chromatographic system. Pancreas samples were homogenized in HPLC mobile phase, and the supernatant was separated by centrifugation.

5.5.3. Immunohistochemistry (I)

The 10 µm thick cryostat sections alternately cut with 20 µm for autoradiography, were used for the CD4 immunohistology. The purified rat anti-mouse CD4 (L3T4, clone RM4-5, isotype Rat (DA) IgG2a,κ) was purchased from Pharmingen (San Diego, CA, USA). The fluorescent isothiocyanate (FITC)-conjugated polyclonal rabbit anti-rat immunoglobulin was purchased from Dako Immunochemicals (Glosrup, Denmark). Immunostaining was performed as described by Ylinen *et al.* (2000). The sections were analysed using a digital microscope with an epi-illuminator and Olympus U-RFL-T FITC filter (Olympus).

5.6. Magnetic resonance imaging (MRI) (II)

The abdominal region was imaged with GE Signa Horitzon LX Echo Speed 1.5T (General Electric Medical System) MR imager using a body coil. Transverse T1-weighted field echo images with TR (Time of Repetition) of 124 ms and TE (Time of Echo) of 5 ms were obtained with the same pixel size as the PET images. Images were acquired during short breath-hold in the mid-expirium. The upper and lower borders of the imaged area were marked on the skin of the subject to ensure correspondence between MRI and PET imaging. The subjects fasted for at least 6 hours before the MRI scan to minimize bowel movements.

5.7. Bioanalytical methods (I, II and III)

In study I blood samples were taken immediately after animals were killed by cardiac puncture into heparinized tubes. Plasma was then separated by centrifugation and plasma

glucose analysed by the glucose oxidase method with an Analox GM7 glucose analyser (Analox Instruments, London, UK). In study III blood glucose was measured from a drop of blood from a tail vein at 0 min, 30 min, or 60 min after pretreatment by using an ACCU-CHEK Aviva glucose meter (Roche Diagnostics, Mannheim, Germany).

In study II, glycosylated hemoglobin (HbA_{1c}) and plasma C-peptide were measured from patients with T1D at the time of diagnosis. In the control subjects blood samples for HbA_{1c} and C-peptide, and furthermore for all participants analyses were conducted for T1D associated autoantibodies, glucose and insulin in serum or plasma drawn before the PET scanning after a 10- to 12-hour overnight fast. ICA was measured using a standard indirect immunofluorescence assay on a section of frozen human pancreas from a blood group O donor (Bottazzo *et al.*, 1974, Karjalainen, 1990). ICA-positive sera were diluted sequentially to find end-point titers, and the results were expressed in Juvenile Diabetes Foundation units (JDFU). The detection limit of the assay is 2.5 JDFU. Autoantibodies to IAA, GADA and IA-2A were measured as described (Kupila *et al.,* 2001). Plasma samples for immunoreactive free insulin were immediately precipitated with polyethylene glycol (Arnqvist *et al.,* 1987). Fasting levels of insulin and plasma C-peptide were assessed by radioimmunoassay using commercial kits (Pharmacia Insulin RA kit, Pharmacia Diagnostica, Uppsala, Sweden and Euria-C-peptide, Eurodiagnostica, Malmö, Sweden). HbA_{1c} was measured with high performance liquid chromatography (Variant Analyser, Bio-Rad, CA, USA) with reference values of 4.0-6.0%. The glucose concentration in arterialized venous blood was determined every 10 min with a glucose oxidase method (Analox GM7 Analyser, Analox Instruments, Hammersmith, England). Heart rate and blood pressure were monitored every 15 min during the PET studies.

5.8. Statistics

In study I and II, the statistical analysis was performed using SAS System for Windows release 8.0 and SAS System for Windows release 8.2, respectively (SAS, Cary, NC, USA). Shapiro-Wilks test was performed to test for the normal distribution and one-way analysis of variance (ANOVA) was used as a parametric method. In studies I-III, data are presented as mean ± SD. The Pearson correlation test was used for analysis of correlation. In study III statistical analysis was performed with SAS System for Windows, version 9.2 (SAS Institute Inc., Cary, NC). The differences in the ^{18}F-uptake between pre-treatment groups were first compared using the non-parametric Kruskal-Wallis test. In further pairwise comparisons Bonferroni-corrected Mann-Whitney U-test was used. In all of the analysis, the level of statistical significance was set at $p < 0.05$.

6. RESULTS

6.1. Radioactivity distribution in pancreas in rodents

6.1.1. Distribution of [^{18}F]FDG in NOD mouse pancreas (I)

In the autoradiogram of healthy BALB/c mice [^{18}F]FDG uptake to the endocrine islets was very similar compared to the exocrine pancreas. Haematoxylin-eosin-stained sections accurately showed the borders of the islets which otherwise could not be identified from the autoradiogram (Fig 2b in publication I).

In NOD mice [^{18}F]FDG accumulated homogenously to the exocrine pancreas, resembling the accumulation in the healthy BALB/c mice. The average [^{18}F]FDG accumulation to the exocrine pancreas of the BALB/c mice was higher than of the NOD mice. In the endocrine pancreas, [^{18}F]FDG accumulated to almost all islets in the NOD mice in quantities markedly exceeding those measured in the BALB/c mice (Fig. 2 in publication I). Uptake into the islets without insulitis i.e. healthy islets was not enhanced. The mean accumulation of [^{18}F]FDG to the NOD mice islets showed 1.6-fold (1.0- to 2.3-fold) higher ratios ([^{18}F]FDG uptake to the islets vs. uptake to the exocrine pancreas) than the BALB/c islets (mean ratios 1.6 ± 0.4 vs. 1.0 ± 0.1 in NOD vs. BALB/c mice, respectively, p = 0.001).

6.1.2. Biodistribution of [^{18}F]FDG in NOD mice (I)

[^{18}F]FDG uptake to the pancreas, liver, skeletal muscle, frontal cortex, and blood was calculated in all of the mice for whom plasma glucose concentrations were available. NOD and BALB/c mice which had glucose concentration less than 15 mmol/l were included in the study. Plasma glucose levels and the biodistribution measurements are listed in Table 4.

Table 4. Plasma glucose values and [^{18}F]FDG accumulations as percentage of injected dose/g tissue (%ID/g) in the blood and tissues of NOD and the BALB/c mice at 90 min after the tracer injection.

	Plasma Glucose	[^{18}F]FDG uptake (%ID/g tissue)				
	(mmol/l)	Pancreas	Skeletal muscle	Liver	Frontal Cortex	Blood
NOD	8 ± 4	1.3 ± 0.4	1.5 ± 0.8	1.0 ± 0.3	17 ± 6	0.6 ± 0.2
BALB/c	8 ± 2	2.2 ± 1.0	4.2 ± 1.9	1.9 ± 1.0	21 ± 13	1.2 ± 0.8
p-value	N.S.	0.002	<0.001	0.001	N.S.	<0.01

[^{18}F]FDG concentration in the blood was markedly higher in the BALB/c mice than in the NOD mice at 90 min after the tracer injection. The biodistribution measurements showed that amounts of ^{18}F-radioactivity in the pancreas, liver, and skeletal muscle were higher in the BALB/c than in the NOD mice, but the level of [^{18}F]FDG uptake to the frontal cortex of the brain was similar in both strains of mice (Table 4).

6.1.3. Histochemistry and immunostaining of the NOD mice pancreas (I)

Analysis of the severity of lymphocyte infiltration in the islets of Langerhans in the NOD mice at different ages (Fig. 10) revealed that already at the age of 8 weeks, 65% of the islets were infiltrated. The infiltration of lymphocytes in individual islets at any ages of NOD mice varied from mild to severe; the majority of the islet-infiltrating cells in the pancreas were $CD4^+$ lymphocytes as documented previously by Signore *et al.* (1989). This $CD4^+$ predominance remained through the development of insulitis, and showed no correlation with the age at least within the age range studied here. The proportion of infiltrated islets increased up to 90% as mice grew older. There was no evidence of insulitis in the pancreas of the BALB/c mice. The pancreatic β-cell content was not measured in this study.

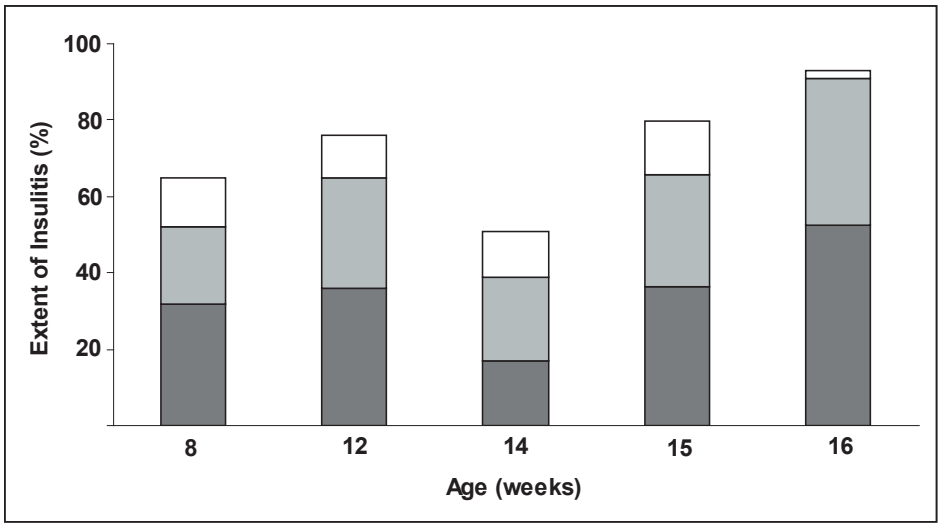

Figure 10. The extent of insulitis is presented by bars representing the percentage of infiltrated islets in NOD mice at different ages. Dark grey bars represent islets with severe infiltration, light grey medium infiltration, and open bars mild infiltration.

6.1.4. Distribution of [^{18}F]FDOPA in the rat pancreas after enzyme inhibition (III)

^{18}F-radioactivity distribution in the pancreatic sections of healthy rats was homogenous at 30 min after the [^{18}F]FDOPA admistration. Radioactivity did not accumulate in the pancreatic islets but the uptake was higher towards the head of the pancreas when COMT inhibition was used alone or in combination with MAO-A. The same effect was not seen with other enzyme inhibitors.

6.1.5. [^{18}F]FDOPA uptake in the rat pancreas (III)

^{18}F-radioactivity in the pancreas was 3.4-fold higher than blood activity (0.55 ± 0.22 %ID/g *vs.* 0.16 ± 0.03 %ID/g, $p = 0.016$) when [^{18}F]FDOPA was used without

any enzyme inhibition. MAO-A or MAO-B inhibition did not change the ^{18}F-uptake (p = 0.37 and p = 1.00, respectively) in the pancreas as compared with the vehicle. AADC inhibition elevated the amount of ^{18}F-radioactivity in all organs; ^{18}F uptake in the pancreas was enhanced by 3.2-fold (1.76 ± 0.31 %ID/g *vs.* 0.55 ± 0.22 %ID/g, p = 0.012). When animals were pretreated with COMT, ^{18}F-radioactivity in the pancreas increased by 2.8-fold (p = 0.008) as compared to vehicle treated; no increase in the amount of radioactivity was detected in the other organs. Pretreatment with combined COMT and MAO-B inhibitors enhanced the amount of radioactivity in the pancreas 5.2-fold (1.81 ± 0.35 vs. 0.55 ± 0.22, p = 0.006) compared with vehicle.

If MAO-A was combined with COMT inhibitor, then there was a significant enhancement in the uptake to the pancreas (3.7 ± 1.0 %ID/g vs. 1.5 ± 0.3 %ID/g, p = 0.024) compared with the treatment with the COMT blocker alone. Combination of COMT and MAO-A inhibition enhanced pancreatic radioactivity 6.7-fold (p = 0.032) compared to rats treated with vehicle (control) only. A slightly increased uptake was seen in pancreas after combination of COMT and AADC inhibition as compared to vehicle, but this increase did not reach statistical significance (2.39 ± 0.2 vs 0.55 ± 0.22, p = 0.057).

6.1.6. In vivo PET-imaging of rat pancreas (III)

In the PET images, the kidneys and pancreas exhibited high ^{18}F activity and were therefore readily visible after the pretreatments (Fig. 5b and c in publication III). Time-activity curves normalized to the injected activity indicated fast tracer uptake and slow clearance for pancreas and liver. When [^{18}F]FDOPA was used with vehicle only, the pancreas was difficult to localize in the PET-image and in that situation anatomical reference by CT helped to localize specific morphological structures. [^{11}C]methionine PET was performed as a reference to reveal the localization of the pancreas, since pancreas may be difficult to locate with PET in the abdominal area if radioactivity is low.

6.2. [^{18}F]FDOPA metabolite analysis (III)

HPLC radiochromatograms from the radiometabolite studies are shown in Figure 6 in publication III. Several radiolabelled metabolites of [^{18}F]FDOPA were identified. The following retention times (R_t) were analyzed from the radiochromatograms; [^{18}F]FDOPA (R_t = 5 min), [^{18}F]3-OMFD (R_t = 7 min), [^{18}F]FDOPAC (R_t = 8 min), [^{18}F]FDA (R_t = 12 min), [^{18}F]FHVA (R_t = 13 min), and [^{18}F]3-OMFT (R_t = 24 min).

In the pancreas of vehicle-treated rats, the main metabolite was [^{18}F]3-OMFD, as well as after inhibition of AADC. Combined inhibition of AADC and COMT retained [^{18}F]FDOPA in the pancreas as a main source of ^{18}F activity. The major metabolite after COMT inhibition alone or with MAO-A blockade was [^{18}F]FDOPAC, while after MAO-A inhibition, [^{18}F]3-OMFD was again predominantly identified.

6.3. Glucose uptake into the human pancreas (II)

In the patients with newly diagnosed T1D glucose uptake into the pancreas was markedly higher than in the healthy subjects (22.9 ± 6.4 vs. 17.8 ± 6.0 μmol/kg min, $p = 0.039$). Glucose uptake appeared high in the pancreas in the patients who were studied shortly after the diagnosis of T1D, declining thereafter in the course of T1D (R = -0.58, $p = 0.024$) (Fig 3A in publication II). Six months after the diagnosis, glucose uptake into the pancreas returned to the equivalent value of healthy subjects.

The highest glucose uptake into the pancreas (38.9 μmol/kg min) was found in the patient in whom T1D was diagnosed at a very early stage in a normal routine checkup at the age of 40 years. He had abnormal oral glucose tolerance test (OGTT) and therefore insulin medication was started. He was positive for three out of four T1D-specific autoantibodies. The PET study was performed seven months after the initiation of daily subcutaneous insulin. However, at the time of scanning, he only needed a daily dose of 2 IU of short-acting insulin at breakfast and was considered to be in remission. Therefore his pancreatic glucose uptake was not included in the analysis of the original publication. If he were to be included in the analysis, mean glucose uptake to the pancreas of newly diagnosed T1D patients would increase even higher value, to 24.1 ± 7.6 μmol/kg min (Fig. 11).

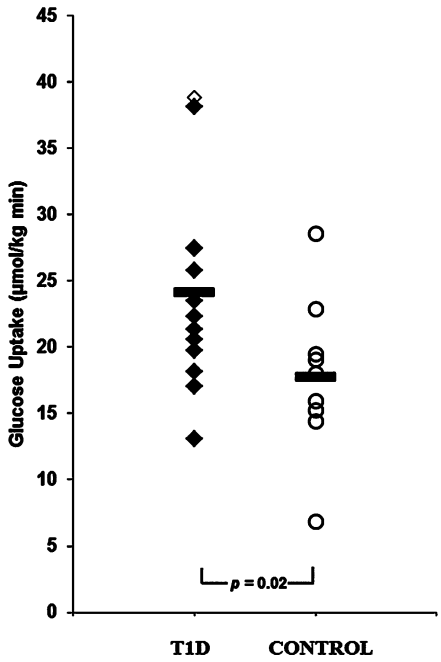

Figure 11. Glucose uptake to the pancreas of newly diagnosed T1D patients (♦) and healthy subjects (control) (○) measured by [^{18}F]FDG and PET. The results of one T1D patient originally excluded from the study has been included in the analysis (◊). Mean glucose uptake values are compared between T1D and control subjects (*p*-value).

Glucose uptake to the pancreas was not associated with the daily subcutaneous insulin dose used by diabetic patients, plasma insulin concentrations, or T1D specific autoantibody titres. Pancreatic glucose uptake values of T1D patients correlated with fasting C-peptide concentrations ($R = 0.62$, $p < 0.05$) but there was no association with HbA_{1C} values at the time of diagnosis ($R = -0.35$, $p = 0.26$).

6.4. Amino acid uptake in human pancreas using [^{11}C]methionine (II)

Methionine uptake of the pancreas was measured in nine patients with newly diagnosed T1D and seven healthy control subjects, as the [^{11}C]methionine scan was done in these patients for anatomical reference before it became possible to use PET/CT device. Mean methionine uptake tended to be higher in healthy subjects compared to T1D patients (4.6 ± 2.4 vs. 3.7 ± 1.9 µmol/kg min, p = n.s.) (Fig. 12). In addition, methionine uptake was not associated with pancreatic glucose uptake or with the duration of T1D.

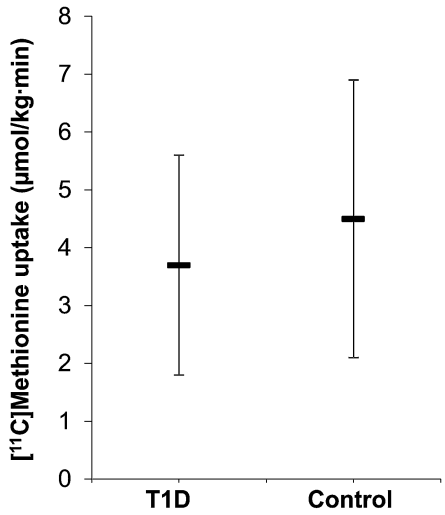

Figure 12. Mean [^{11}C]methionine uptake to the pancreas of newly diagnosed T1D patients (T1D) and healthy control subjects (Control) determined with PET. Statistical difference of mean [^{11}C]methionine uptake between groups was not significant (p = n.s.).

7. DISCUSSION

7.1. Methodological aspects

7.1.1. Human subjects

The human experiments involved young non-obese men who were either healthy or newly diagnosed with T1D. Therefore, the results may not be generalizable to women or children. When evaluating the PET scan of the human pancreas in study II, it should be noted that the pancreas moves concurrently with breathing, potentially leading to "blurring" of the pancreas image. This scan takes 40 or 60 minutes, and thus it is not possible for the subject to hold their breath. In contrast, CT scans are fast and can be performed while the subject holds their breath in mid-expirium.

7.1.2. Animal models for the study of T1D

Although pancreatic anatomy, physiology, and molecular biology differ between NOD mice and humans (Table 1), the use of NOD mice has substantially advanced our understanding of the histology, pathology, and genetics associated with autoimmunity. NOD mice exhibit polygenic control of diabetogenesis, coupled with the requirement for a diabetogenic susceptibility gene linked to the MHC complex. This suggests that the form of diabetes in NOD mice is genetically similar to T1D in humans (Leiter *et al*., 1987). Future research may focus on confirming that the mechanisms found in NOD mice also exist in humans (Ludvigsson, 2014). The NOD mouse model is clearly not completely translatable to human T1D, as illustrated by the velocity of disease onset and the relative ease of disease prevention and reversal in this animal model (Thayer *et al*., 2010). Additionally, NOD mice do not enjoy a "honeymoon period" comparable to that observed in humans after the initiation of insulin treatment (Akirav *et al*., 2009).

In four animal models of spontaneous T1D—the NOD mouse, BioBreeding (BB) rat, Komeda rat, and LEW.1AR1-*iddm* rat—immunohistochemistry and in situ RT-PCR of immune cell infiltrate and the cytokine pattern in pancreatic islets were examined in relation to T1D development in humans. After T1D manifestation, the main immune cell types—$CD8^+$ T cells, $CD68^+$ macrophages, and $CD4^+$ T cells—were observed with declining frequencies in infiltrated islets of all diabetic pancreases. Resembling the situation in humans, the major proinflammatory cytokines TNF-α and IL-1β were expressed in the pancreas of the NOD mouse, BB rat, and LEW.1AR1-*iddm* rat models. Ki67 expression was increased in all models, suggesting an ongoing effort to counteract apoptotic β-cell loss in the presence of continuing autoimmune attack, which may indicate that β-cells have a regenerative capacity (Jörns *et al*., 2014). Jörns and colleagues concluded that, other animal models with the exception of the Komeda rat, mirror well the situation in humans

with T1D. Taking these findings into consideration, the disease mechanisms obtained in the animal models still need to be translated to human T1D with considerable caution.

7.2. [^{18}F]FDG uptake into the pancreas and islets in NOD mice with insulitis (I)

In study I, [^{18}F]FDG accumulation was up to 2.3 times higher in the islets of Langerhans in prediabetic and diabetic NOD mice with active insulitis compared to the surrounding exocrine pancreas or the islets without insulitis. All NOD mice with insulitis also exhibited entirely intact islets, often several in the same tissue section, which complicated their visualization. The [^{18}F]FDG accumulation showed a poor association with the age of the NOD mice, since the extent of insulitis varied widely within individual islets across all age groups (Fig. 5 in publication I). It was impossible to localize islets without insulitis on autoradiographs, and thus haematoxylin-eosin staining of the sections was essential for their identification.

Biodistribution measurements revealed significantly higher ^{18}F-radioactivity in blood, pancreas, skeletal muscle, and liver among BALB/c mice than in NOD mice. However, [^{18}F]FDG uptake in the frontal cortex of the brain was similar in both strains of mice. Urine levels of [^{18}F]FDG were not determined; however, a few NOD mice were slightly hyperglycemic and the subsequent mild glucosuria may explain the [^{18}F]FDG loss through urine. This would be in line with earlier findings in rats with streptozotocin-induced diabetes (Malaisse *et al*., 2000). In study I, mice with glucose levels above 15 mmol/l were excluded to minimize inter-individual variation.

At the beginning of insulitis, only a small portion of the islets are infiltrated with lymphocytes. In study I, 8-week-old NOD mice showed a mean proportion of 65% infiltrated islets, with the severity varying from mild to harsh. Over the next ten weeks, the mean percentage of infiltrated islets increased to 90%, and the insulitis became more severe. When NOD mice develop diabetes, they show generalized and severe islet destruction with heavy lymphocytic infiltrates (Shimada *et al*., 1996). It has been hypothesized that β-cell destruction occurs late in the course of the inflammatory process, within a short time period. NOD mice with symptomatic T1D continue to show actively metabolizing lymphocytic infiltrations in the islets, supporting the theory that insulitis may continue even after development of clinical autoimmune diabetes. The results from study I, support the assumption that the inflammatory activity of the infiltrating lymphocytes decreases once the maximum extent of infiltration has been reached (Fig 4. in publication I).

Earlier immunological studies have demonstrated that persistent antigen stimulation leads T-cells (particularly CD4$^+$ T-cells) to undergo an initial phase of expansion, followed by a hypofunctional phase characterized by hyporesponsive T-cells (Aly & Gottlieb, 2009). Inflammatory CD4+ T-cells express GLUT1, GLUT3, GLUT6, and GLUT8. Although multiple GLUTs are expressed, GLUT1 deficiency is sufficient to selectively

impair metabolism and function of thymocytes and effector T-cells (Macintyre *et al*., 2014). Activated T lymphocytes have a high glucose demand and thus, tight regulation of glucose uptake is required to maintain immune homeostasis. Activated T-cells are dependent on glucose as their main source of energy, which they derive mainly through glycolysis. In T-cell metabolic reprogramming, GLUT1 serves the selective cell-intrinsic function of driving T-cell glycolysis for growth, expansion, and inflammatory disease. T-cell receptor stimulation is responsible for increased GLUT1 protein level, whereas CD28 co-stimulation is necessary for GLUT1 trafficking to the cell surface (Maciver *et al*., 2008). Isolated resting human lymphocytes and monocytes reportedly express GLUT 1 and GLUT 3 glucose transporters, with GLUT 1 protein levels being higher in lymphocytes than monocytes (Fu *et al*., 2004). These molecular alterations are in agreement with the findings of study I, showing that [^{18}F]FDG uptake was high in active lymphocytes but subsequently diminished in inactive lymphocytes, despite the large lymphocyte population found in and around islets of Langerhans.

7.3. Pancreatic biodistribution of [^{18}F]FDOPA in healthy rats (III)

Several studies have shown that normal pancreatic cells can take up L-DOPA; however, the relatively low β-cell binding specificity impairs [^{18}F]FDOPA PET to assess the β-cell mass in diabetic patients (Wu & Kandeel, 2010). When comparing different tracers for imaging β-cell mass, the specificity ratio of [^{18}F]FDOPA has been shown to be higher for the endocrine pancreas relative to exocrine cells (Sweet *et al*., 2004). The administration of enzyme inhibitors prior to [^{11}C]DOPA reportedly changes the ^{11}C-radioactivity in the pancreas (Bergström *et al*., 1996 and 1997). Pretreatment with carbidopa enhances the sensitivity of [^{18}F]FDOPA for extra-adrenal abdominal paraganglioma and adrenal pheochromocytoma imaging, by increasing the tumor-to-background ratio of the tracer (Timmers *et al.*, 2007). Another study found that pretreatment with carbidopa fully masked [^{18}F]FDOPA uptake in two out of three patients with insulinoma and β-cell hyperplasia (Kauhanen *et al.*, 2008). Therefore, [^{18}F]FDOPA uptake in the healthy rat pancreas was determined following the administration of various premedications to improve our understanding of the nature of dopamine metabolism and tracer uptake in the normal pancreas.

L-DOPA and 5-hydroxytryptophan (5-HTP) have similar synthetic and metabolic pathways. AADC converts L-DOPA into dopamine, and 5-HTP into serotonin (*5-hydroxytryptamine* or 5-HT). MAO-A converts dopamine into 3,4-dihydroxyphenylacetic acid (DOPAC), and 5-HT into 5-hydroxyindolacetic acid (5-HIAA). In contrast to 5-HT, DA can be metabolized by MAO-B and catechol-O-methyltransferase (Soares da Silva *et al*., 1995). Radiolabeled 5-HTP accumulates in the form of serotonin in islets of Langerhans, as opposed to in the exocrine pancreatic parenchyma (Ekholm *et al*., 1971). An *in vitro* study of [^{11}C]5-HTP demonstrated high selective retention (8–55 times greater) in

human islets compared to exocrine cells (Eriksson *et al*., 2014). The uptake mechanism and the retention of [^{11}C]5-HTP have been evaluated *in vitro* in an exocrine human pancreas carcinoma cell line (PANC-1) and in an endocrine human insulinoma cell line (CM) (Di Gialleonardo *et al*., 2012). In these studies, Di Gialleonardo and co-workers demonstrated that the cell lines differed in tracer retention rather than uptake. [^{11}C]5-HTP was taken up, rapidly metabolized, and trapped inside the endocrine cells, whereas the washout occurred immediately in the exocrine cells.

Di Gialleonardo and co-workers also demonstrated that inhibition of AADC had no effect on [^{11}C]5-HTP uptake in either cell type, while inhibition of MAO-A increased the tracer accumulation in CM cells. PET studies demonstrated the achievement of [^{11}C]5-HTP selectivity in β-cells by inhibition of MAO-A in healthy rats, which led to increased retention of radioactive serotonin inside the β-cells (Di Gialleonardo *et al*., 2012). Eriksson and co-workers showed that pancreatic uptake of [^{11}C]5-HTP in nonhuman primates was markedly decreased by AADC inhibition, and was increased after MAO-A inhibition. In the rat pancreas, uptake was similarly modulated by MAO-A inhibition, and was reduced in animals with induced diabetes (Eriksson *et al*., 2014). The same group observed substantial [^{11}C]5-HTP accumulation in the pancreas of healthy control subjects, with large inter-individual variation. Pancreatic uptake of [^{11}C]5-HTP was substantially and significantly reduced (66%) in patients who had T1D for at least 10 years and showed negative C-peptide concentration. This reduction of [^{11}C]5-HTP uptake was most evident in the tail of the pancreas, where β-cells are normally the major islet constituent (Eriksson *et al*., 2014), supporting the potential use of [^{11}C]5-HTP for quantitative imaging of endocrine pancreas.

Among patients with Parkinson disease who are receiving a high dose of L-DOPA, the intracellular dopamine content in peripheral lymphocytes is reportedly three times higher than in lymphocytes of healthy controls (Rajda *et al*., 2005). It remains to be explored whether [^{18}F]FDOPA-PET could be used to visualize this kind of enhancement in insulitis.

Study III demonstrates that enzyme inhibition increased the uptake of [^{18}F]FDOPA-derived ^{18}F-radioactivity in the rat pancreas, with the radioactivity intensity distinctly varying depending on which enzyme inhibitors (or combinations of enzyme inhibitors) were used. Depending upon which enzymatic pathway was blocked, the presence of different radiolabelled metabolites in the pancreas was responsible for this increase in the uptake. Administration of a COMT inhibitor alone enhanced radioactivity uptake in the pancreas in a manner similar to that observed with AADC, with a four-fold increase compared to non-treated animals. Combined administration of COMT and MAO-A inhibitors resulted in the highest ^{18}F uptake in the pancreas: nearly 7-fold compared to the control. Surprisingly ^{18}F activity in the healthy rat pancreas was unaltered following the inhibition of either MAO-A or MAO-B enzymes alone. Furthermore, COMT inhibition combined with AADC or MAO-B did not achieve the uptake values obtained with COMT and MAO-A.

7.3.1. [^{18}F]FDOPA distribution in rat pancreas sections

In most cases, ^{18}F-radioactivity was homogenously distributed over the pancreatic AR sections. The islets of Langerhans in these sections were verified from images of the hematoxylin and eosin-stained sections (Fig. 13). The outlines of the islets were drawn onto the HE-stained sections and they were fitted with autoradiographical images. These overlaid images revealed that radioactivity did not accumulate in the pancreatic islets with any of the tested premedications. Therefore, [^{18}F]FDOPA uptake in the healthy pancreas didn't show the same endocrine vs. exocrine pancreas differentiation as observed with [^{11}C]5-HTP. However, the ^{18}F-uptake was higher towards the head of the pancreas when COMT inhibition was used alone or in combination with MAO-A. In the rat, the tail of the pancreas contains the highest number of islets (Elayat *et al*., 1995). Based on the anatomical heterogeneity and the findings of this study, it remains possible that the amounts of ^{18}F-radioactivity detected in the pancreas could be attributable to regional differences in either blood flow or blood perfusion (Ibukuro, 2001), as previously observed with [^{11}C]dihydrotetrabenazine ([^{11}C]DTBZ) (Fagerholm *et al*., 2010).

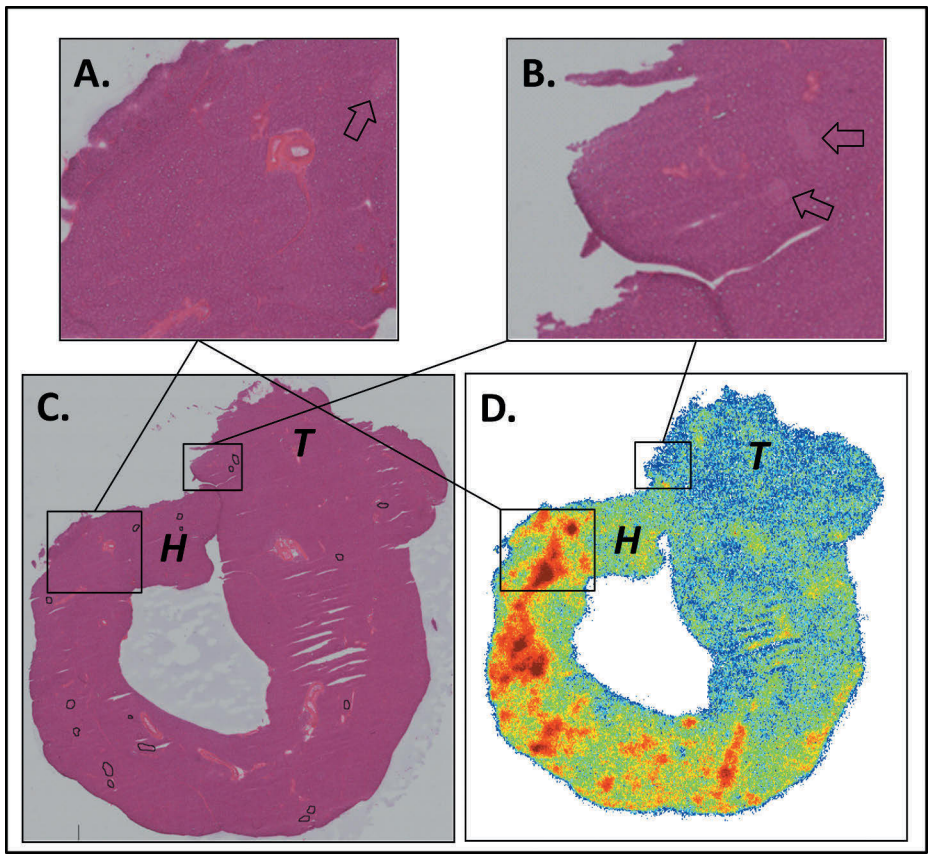

Figure 13. [^{18}F]FDOPA autoradiography (D.) and HE-stained anatomical reference (C.) of rat pancreas after MAO-B enzyme inhibition. Islets of Langerhans are marked with an arrow in enlarged figures (A. and B.) and they are circled in C. [^{18}F]FDOPA shows higher uptake (dark red in D.) towards the head (H). The tail of the pancreas is marked with T.

7.4. In vivo [^{18}F]FDOPA PET-imaging of rat pancreas

In addition to biodistribution measurements of [^{18}F]FDOPA in the pancreas, dynamic [^{18}F]FDOPA PET/CT was performed in a total of seven healthy rats. [^{18}F]FDOPA hybrid PET/CT was performed after vehicle (n = 1), AADC inhibitor (n = 3), and combined inhibition of COMT + MAO-A (n = 3). When [^{18}F]FDOPA was used with vehicle alone, the pancreas was difficult to localize in the PET-image; therefore, one rat was imaged with [^{11}C]methionine to confirm the pancreas location. The PET images showed high [^{18}F]FDOPA-related radioactivity in the kidneys and pancreas, which were therefore readily visible after the pretreatments. Time–activity curves, normalized to the injected activity, indicated fast tracer uptake and slow clearance for the pancreas and liver (Fig. 5 in publication III).

7.5. Radiometabolites of [^{18}F]FDOPA

All of the enzyme inhibitors used in study III have been previously documented to be present in pancreatic cells. Both AADC and COMT enzymes have been detected in insulin-producing β-cells (Karhunen *et al*., 1994, Rorsman *et al*., 1995). MAO-A and MAO-B are found in the human exocrine and endocrine pancreas (Pizzinat *et al.*, 1999). In rats, MAO-A is present in both the exocrine and endocrine pancreas, while MAO-B has been detected only in the islets of Langerhans (Saura *et al*., 1992). The administration of alloxan to induce diabetes mellitus in rats reportedly eliminates MAO activity from the islets (Adeghate & Parvez, 2004).

In study III, the combination of COMT and MAO-A inhibitors resulted in the highest ^{18}F-radioactivity values recorded in the pancreas, with the main metabolite being [^{18}F]FDOPAC. This metabolite also accumulated into the pancreas when COMT inhibition was used alone; however, the amount of ^{18}F-radioactivity was markedly lower with COMT inhibitor alone. In contrast, [^{18}F]3-OMFD was the main metabolite following the use of AADC or MAO-A inhibitors, or vehicle. Finally, when both COMT and AADC enzymatic routes were blocked, [^{18}F]FDOPA itself was the main radioactive component observed in the pancreas. Overall, when enzyme inhibitors are used in combination with [^{18}F]FDOPA, the ^{18}F uptake in the tissue reflects the activity of the various tracers that are metabolic end-products at certain time-points.

7.6. Pancreatic glucose uptake in newly diagnosed human T1D (II)

The [^{18}F]FDG-PET method has not been previously used to study the human pancreas in relation to T1D development. In study II, glucose uptake into the pancreas was enhanced in patients with newly diagnosed T1D, with the peak at the time of clinical diabetes diagnosis (or during remission in a single subject who was excluded from the published

data). Thereafter, the uptake values decreased to the levels of healthy subjects within 3 to 6 months. The time since development of clinical diabetes was strongly correlated with glucose uptake to the pancreas ($R = -0.58$; $p = 0.024$), suggesting that enhanced glucose uptake in the pancreas may reflect the glucose uptake of the activated lymphocytes in the tissue. Changes in blood flow alter the outcomes of functional imaging methods (such as functional MRI), but do not necessarily influence PET tracer uptake (targeted tracer). Differences in tissue vasculature and the activity of transporter systems reportedly contribute to genotype-related standardized uptake values (Van Berkel *et al*., 2014). In humans, no technique is available for specific studies of islet blood perfusion. However, the perfusion of the whole pancreas as measured by magnetic resonance perfusion imaging was the same in healthy control subjects and T1D subjects (Hirshber *et al*., 2009). In study I, diminished ^{18}F-activity in lymphocytes were observed at the final stage of insulitis, which could explain the findings in study II where T1D patients showed reduced glucose uptake in relation to the time after T1D diagnosis.

Theories propose that after T1D diagnosis and the onset of insulin therapy, the number of insulin-producing β-cells decreases. In cases of substantial residual C-peptide secretion, the period after T1D diagnosis is called "the honeymoon phase", which may last from weeks to months (Chase *et al*., 2004). According to the International Society for Pediatric and Adolescent Diabetes (ISPAD) Guidelines 2006/2007, the honeymoon phase is defined as the period during which the patient requires less than 0.5 units of insulin per kilogram of body weight per day, and has HbA_{1c} of less than 7% (Couper & Donaghue, 2007). The honeymoon phase can be followed by partial or complete remission. During this period, some of the β-cells have not yet been completely destroyed, and produce unpredictable amounts of insulin. It has been claimed that episodes of β-cell destruction could potentially be followed by episodes of repair and regeneration (In't Veld, 2007).

Emerging evidence suggests that the dogma that all β-cells are destroyed in longstanding T1D is probably incorrect for many patients (Gotthardt *et al*., 2014). Studies of NOD mice (Strandell *et al*., 1990) and T1D patients (Marchetti *et al*., 2000) have shown that a population of functionally suppressed but still viable β-cells remains following T1D diagnosis. These cells can produce and secrete insulin as shown by C-peptide measurement and, most importantly, they can survive for decades after T1D diagnosis (Oram *et al*., 2014). Among T1D children (age range, 0.9–14.7 years), for every 1-year increase in age at T1D diagnosis, the odds of detectable fasting C-peptide increased 1.2 times (Sorensen *et al*., 2012), suggesting that the course of pathogenesis differs between individuals at different ages. Residual β-cells sufficient to raise the C-peptide level to just above the detection limit will not substantially affect the clinical outcome, but may stimulate further autoantibody formation. With recent reports that these remaining pancreatic cells are functional, it is now clear that T1D patients might benefit from new immunotherapies and should be included in clinical trials (Faustman, 2014). It also

appears that [18F]FDG-PET may be useful for quantitative imaging of the extent of insulitis in humans. Additional studies are needed to determine whether glucose uptake is enhanced in subjects with positive T1D-specific autoantibodies but who have not yet developed clinical diabetes.

7.7. Newly diagnosed T1D and pancreatic [11C]methionine uptake

In humans, pancreatic [11C]methionine uptake showed a different temporal pattern compared to glucose uptake. Previous studies have indicated that amino acids are less actively taken up by inflammatory cells than glucose (Kubota K. *et al*., 1984, Kubota R. *et al*., 1992). High methionine uptake in the pancreas has been linked to exocrine pancreas function, which involves the production of enzymes, such as trypsin and chymotrypsin, for the breakdown of ingested proteins, fats, and carbohydrates. A biodistribution study investigated [11C]methionine in non-tumor-involved organs of children and young adults with known or suspected malignancies, and found the highest [11C]methionine uptake in the pancreas, followed by the liver, kidneys, and spleen (Harris *et al.,* 2013).

In study II, [11C]methionine uptake in the pancreas was about 20% higher among control subjects compared to diabetic patients, but this difference was not statistically significant. It is possible that patients with diabetes may have been in a mild catabolic state due to fasting, which could explain their decreased [11C]methionine uptake into the pancreas. Interestingly, children who are islet autoantibody-positive but have not developed T1D, have displayed 17% lower median concentrations of [11C]methionine in the plasma compared with children who are islet autoantibody-negative (Pflueger *et al*., 2011). In that study, [11C]methionine was the only essential amino acid to show this kind of association with islet autoimmunity, and this observation was attributed to changes in whole-body methionine metabolism. Overall, the present results obtained with glucose and methionine tracers support the speculation of the presence of local inflammation, typically characterized by higher uptake of [18F]FDG than of [11C]methionine.

8. SUMMARY AND CONCLUSIONS

Over the past decade, researchers have been working to develop a non-invasive method to image either insulitis or the remaining mass of functioning pancreatic β-cells. However, the pancreas is challenging to access. Furthermore, T1D-related changes in the endocrine pancreas are difficult to investigate due to the long clinically silent period that precedes the onset of clinical diabetes, during which lymphocytes traffic to the islets and mediate the progressive destruction of β-cells. A non-invasive imaging method could be a useful tool for both research and clinical investigation into the course of T1D development, as well as T2D development in some cases. New hybrid imaging techniques, such as PET/CT and PET/MRI, provide improved anatomical localization of the functional imaging, and are already more advanced than the methods used in study II. This progress to date makes the presently reported findings even more valuable. In combination with new more specific tracers, these new imaging techniques could lead to improved early identification of subjects at an increased risk of progression to overt T1D.

Until recently, interventional studies of T1D have focused on primary prevention (prior to any evidence of autoimmunity) and secondary prevention (after the development of islet autoantibodies) (Skyler, 2013). Both primary and secondary interventions are performed before disease onset with the aim of arresting the immune process, and thus preventing or delaying clinical disease. As residual β-cell survival has now been reported even years after T1D diagnosis, tertiary intervention has become equally important. Tertiary intervention trials are undertaken at or after disease onset, with the aim of halting the destruction of remaining β-cells, and of potentially allowing these residual β-cells to recover function, with the hope of lessening the severity of clinical manifestations and disease progression (Skyler, 2013).

I. Here the feasibility was evaluated for combining [^{18}F]FDG and autoradiography to assess [^{18}F]FDG uptake in activated lymphocytes in islets of Langerhans (insulitis) in NOD mice. [^{18}F]FDG has not previously been used for imaging insulitis in T1D animal models or humans. The [^{18}F]FDG uptake in inflamed islets was markedly enhanced. Since all NOD mice with insulitis had also entirely intact islets, and the extent of the insulitis varied markedly within individual islets, the [^{18}F]FDG accumulation was poorly associated with the age of the NOD mice. Nevertheless, [^{18}F]FDG can be used to visualize the extent of lymphocytic infiltration in the islets at all stages of prediabetes in the NOD mice using autoradiography.

II. [^{11}C]Methionine and [^{18}F]FDG PET were used to evaluate visualization of insulitis affecting the islets of Langerhans in the pancreas of newly diagnosed T1D adult patients. In patients with T1D, glucose uptake into the pancreas exhibited high interindividual

variation, with higher uptake observed at or soon after the time of diagnosis. [^{11}C]methionine uptake in the pancreas was slightly higher in control subjects compared to diabetic patients, but this difference was not statistically significant. It appears that [^{18}F]FDG-PET may be used to estimate the extent of insulitis in humans. Advantages of [^{18}F]FDG-PET include its availability, and wide experience with PET imaging. Progression towards T1D seems to occur with inter-individual phenotypic differences; therefore, [^{18}F]FDG may be suitable for visualization of inflammation in different types.

III. [^{18}F]FDOPA distribution and metabolism in the pancreas of healthy rats was evaluated to determine whether this tracer could be used to image β-cell mass and/or endocrine pancreas. Pretreatment with individual enzymatic inhibitors and their combinations significantly affected pancreatic uptake of ^{18}F-radioactivity. This approach enabled better discrimination between the pancreas and the surrounding tissues. However, the use of these pretreatments did not enhance the visualization of islets in the exocrine pancreas. When [^{18}F]FDOPA is combined with various enzymatic inhibitors, the ^{18}F-uptake in the tissue generally reflects the uptake of different radiometabolites, which vary according to cell type. The use of [^{18}F]FDOPA with or without enzymatic inhibition must be considered when planning experimental settings, since a method that is applicable for some clinical research demands may produce misleading results in other situations. The present results may be important for the interpretation of clinical examinations, including for diseases such as neuroendocrine tumors and congenital hyperinsulinism.

In conclusion, enhanced [^{18}F]FDG uptake related to insulitis in the NOD mouse can already be reliably visualized with autoradiography in *ex vivo* studies. The results of study II indicate that [^{18}F]FDG PET can be used to estimate the extent of insulitis in humans. Further clinical studies are needed to determine the optimal time to perform [^{18}F]FDG PET imaging before the clinical diagnosis of T1D, as the extent of insulitis may be more pronounced weeks and perhaps even months before T1D diagnosis. Compared to imaging β-cell destruction, the ability to image insulitis could offer opportunities for earlier prediction of T1D. Confirming the validity of this imaging approach will require repeated [^{18}F]FDG PET studies in non-diabetic subjects with increased risk of developing T1D. Increased radioactivity uptake of [^{18}F]FDOPA and a change in the radiometabolic profile were found in the pancreas, allowing better discrimination between the pancreas and surrounding tissues of the rat. However, these manipulations still could not separate islets from the exocrine pancreas.

ACKNOWLEDGEMENTS

This study was carried out in the Department of Pediatrics, University of Turku, Finland in collaboration with the Turku PET Centre, Finland during the years 2003-2014.

I am very grateful to my supervisor Professor Olli Simell for introducing me into the world of scientific thinking and working. It has been a priviledge to do my doctoral thesis under his supervision. Thank you for guiding me into the fascinating world of type 1 diabetes pathogenesis, and supporting me during these years. Your expertise in scientific writing and comments have always been excellent.

I wish to thank my second supervisor Docent Merja Haaparanta-Solin for providing excellent working facilities and an inspirational environment for carrying out my doctoral thesis. Her ability to simplify complicated matters has provided practical guidance through the animal PET methodology and data analyzing. Thank you Merja for the supportive attitude during this study and for several nonscientific chatting moments we have had over these years.

Professor Timo Otonkoski and Docent Olof Eriksson are gratefully acknowledged for the review of my thesis manuscript and for their valuable comments, constructive criticisms, and expert advice during the preparation of the final manuscript. I am also sincerely thankful for Professor Alberto Signore for the honor of having him as my opponent.

I would like to thank my thesis supervision committee members, Professor Pirjo Nuutila and Docent Erkki Svedström for the advice and criticism of my thesis. I wish to thank Pirjo for giving me unique opportunity to do scientific work in such a brilliant research group she has been creating. I am very grateful to Erkki for technical assistance, and for all of the advice to understand the basics of MRI imaging methods.

I am priviledged to have excellent co-authors. I want to express my warm thanks to Patricia Iozzo, Anne Roivainen, Heikki Minn, and especially Kirsi Virtanen for her guidance and support during the beginning of my thesis. I also wish to thank Marco Bucci for his technical assistance and experties in data processing. I want to thank Kjell Någren, Tapio Viljanen, and Semi Helin for their contribution to my thesis. I wish to thank Tove Grönroos, Sarita Forsback, Johanna Tuomela, Laura Haavisto, and Anniina Snellman for pleasant and enthusiastic working atmosphere during animal studies. I am grateful to Processor Juhani Knuuti, the director of Turku PET Centre for creating an inspiring atmosphere and excellent working facilities in the Turku PET centre. I express my sincere thanks to Professor Tapani Rönnemaa for his supportive attitude and for constructive comments. I wish to warmly thank Professor Olof Solin for support and encouragement during this thesis, as well as for our chats during the years.

I wish to thank the staff of the Accelerator Laboratory for radionuclide production, the staff of the Radiopharmaceutical Chemistry Laboratory for radiotracer production. I am grateful to all personnel in Turku PET Centre, especially Minna Aatsinki, Marjo Tähti, Mika Teräs, Marko Seppänen, and Mirja Jyrkinen for a flexible and pleasant working atmosphere. I want to express my warm thanks for all the present and former members of the MediCity Research group: Veronica Fagerholm, Päivi Marjamäki, Aake Honkaniemi, Tarja Marttila, Elisa Riuttala, Leena Tokoi-Eklund, Marko Vehmanen, Francisco López Picón, and Hanna Kukkula. Thank you for all for being nice colleagues during my studies.

I wish to express my warm gratitude to staff members in the Department of Radiology in Turku University Hospital, especially Heikki Oivanen, Markku Komu, Jani Saunavaara, and Mikko Kankaanpää for their kind help and collaboration with MRI.

My sincerest appreciation goes to the personnel of the DIPP project: Ville Simell, Aaro Simell, Riikka Sihvo and Minna Romo. I express my warmest thanks to Tuula Simell for valuable advice and help over all these years.

I owe my deepest gratitude to all the subjects who volunteered to participate in this study.

I am very grateful to all my colleagues in the Pediatric Clinic at Seinäjoki Central Hospital and Turku University Hospital for their supportive attitudes and advice during my pediatric specialization.

I would like to thank Joonas Salusjärvi for the artwork in the dedication page. The scene represents winter night in the fields of South Ostrobothnia, Finland.

I would like to express my sincere thanks to my parents Marita and Lauri, and for my sister Terhi for their support throughout my life and their interest towards my scientific work.

Most of all, I owe my loving gratitude to my family. I am thankful to my wife Mervi for her love and patience, and for providing the opportunities for me to work on this study. Her constant support has been essential for the finishing of this project. Thank You for always believing in me. I am also blessed with the greatest joy of my life, our children Elias and Iiris.

The following foundations are thankfully acknowledged for their support: Instrumentarium Reseach Foundation, Research Foundation of Orion Corporation, Foundation for Pediatric Research, Finland, Special Federal Reseach Fund for University Hospitals in Finland, Diabetes Research Foundation, The Academy of Finland. The DIPP project was also supported by the Juvenile Diabetes Research Foundation and Sigrid Juselius Foundation.

Turku, in October 2014

REFERENCES

Adeghate E. & Parvez H. (2004) The effect of diabetes mellitus on the morphology and physiology of monoamine oxidase in the pancreas. *Neurotoxicology* **25**, 167-173

Ahrén B. (2000) Autonomic regulation of islet hormone secretion Implications for health and disease. *Diabetologia* **43**, 393-410

Akirav E., Koshner J.A. & Herold K.C. (2008) The beta-cell mass and type 1 diabetes: going, going and gone? *Diabetes* **57**, 2883–2888

Aly H. & Gottlieb P. (2009) The honeymoon phase: intersection of metabolism and immunology. *Curr Opin Endocrinol Diabetes Obes*. **16**, 286-92

Andralojc K., Srinivas M., Brom M., Joosten L., de Vries I.J., Eizirik D.L., Boerman O.C., Meda P. & Gotthardt M. (2012) Obstacles on the way to the clinical visualisation of beta cells: looking for the Aeneas of molecular imaging to navigate between Scylla and Charybdis. *Diabetologia*. **55**, 1247-57

Antkowiak P.F., Tersey S.A., Carter J.D., Vandsburger M.H., Nadler J.L., Epstein F.H. & Mirmira R.G. (2009) Noninvasive assessment of pancreatic B-cell function *in vivo* with manganese-enhanced magnetic resonance imaging *Am J Physiol Endocrinol Metab* **296**, 573–578

Arnqvist H., Olsson P.O. & Von Schenck H. (1987) Free and total insulin as determined after precipitation with polyethylene glycol: analytical characteristics and effects of sample handling and storage. *Clin Chem*. **33**, 93-96

Atkinson M.A. & Eisenbarth G.S. (2001) Type 1 diabetes: new perspectives on disease pathogenesis and treatment. *The Lancet* **358**, 221-229

Bach J.F.(1994) Insulin-dependent diabetes mellitus as an autoimmune disease. *Endocr Rev.* **15**, 516-42.

Ballian N. & Brunicardi F.C. (2007) Islet vasculature as a regulator of endocrine pancreas function. *World J Surg*. **31**, 705-14

Barone R., Procaccini E., Chianelli M., Annovazzi A., Fiore V., Hawa M., Nardi G., Ronga G., Pozzilli P. & Signore A. (1998) Prognostic relevance of pancreatic uptake of technetium-99m labelled human polyclonal immunoglobulins in patients with type 1 diabetes. *Eur J Nucl Med.* **25**, 503-508

Bedoya F.J., Wilson J.M., Ghosh A.K., Finegold D. & Matschinsky F.M. (1986) The Glucokinase Glucose Sensor in Human Pancreatic Islet Tissue. *Diabetes* **35**, 61-67

Bell G.I., Kayano T., Buse J.B., Burant C.F., Takada J., Lin D., Fukumoto H. & Seino S. (1990) Molecular biology of mammalian glucose transporters. *Diabetes Care* **13**, 198-208

Bergström M., Lu L., Marquez M., Fasth K.J., Bjurling P., Watanabe Y., Eriksson B. & Langstrom B. (1997) Modulation of organ uptake of 11C-labelled L-DOPA. *Nucl Med Biol.* **24**, 15-19

Bergström M., Lu L., Marquez M., Moulder R., Jacobsson G., Ogren M., Eriksson B., Watanabe Y. & Langstrom B. (1996) Catechol-O-methyltransferase inhibition increases the uptake of 11C-3-(3,4-dihydroxyphenyl)-L-alanine in the rat pancreas. *Scand J Gastroenterol.* **31**, 1216-1222

Blakemore S.J., Aledo J.C., James J., Campbell F.C., Lucocq J.M. & Hundal HS (1995) The GLUT5 hexose transporter is also localized to the basolateral membrane of the human jejunum. *Biochem J*. **309**, 7-12

Blomberg B.A., Moghbel M.C., Saboury B., Stanley C.A. & Alavi A. (2013) The value of radiologic interventions and (18)F-DOPA PET in diagnosing and localizing focal congenital hyperinsulinism: systematic review and meta-analysis. *Mol Imaging Biol.* **15**, 97-105

Bockman D.E. (2007) Nerves in the pancreas: what are they for? *The American Journal of Surgery* **194**, S61–S64

Bonner-Weir S. (1994) Regulation of pancreatic beta-cell mass in vivo. *Recent Prog. Horm. Res*. **49**, 91–104

Bosco D., Armanet M., Morel P., Niclauss N., Sgroi A., Muller Y.D., Giovannoni L., Parnaud G. & Berney T. (2010) Unique arrangement of alpha- and beta-cells in human islets of Langerhans. *Diabetes* **59**, 1202-10

Bottazzo G.F., Dean B.M., McNally J.M., MacKay E.H., Swift P.G. & Gamble D.R. (1985) In situ characterization of autoimmune phenomena and expression of HLA molecules in the pancreas in diabetic insulitis. *N Engl J Med.* **313**, 353–360

Bottazzo G.F., Florin-Christensen A. & Doniach D. (1974) Islet-cell antibodies in diabetes mellitus with autoimmune polyendocrine deficiencies. *Lancet* **2**, 1279-1283

Brom M., Woliner-van der Weg W., Joosten L., Frielink C., Bouckenooghe T., Rijken P., Andralojc K., Göke B.J., de Jong M., Eizirik D.L., Béhé M., Lahoutte T., Oyen W.J., Tack C.J., Janssen M., Boerman O.C.

& Gotthardt M. (2014) Non-invasive quantification of the beta cell mass by SPECT with ^{111}In-labelled exendin. *Diabetologia*. Epub ahead of print

Brugman S., Klatter F.A., Visser J.T., Wildeboer-Veloo A.C., Harmsen H.J., Rozing J. & Bos N.A. (2006) Antibiotic treatment partially protects against type 1 diabetes in the Bio-Breeding diabetes-prone rat. Is the gut flora involved in the development of type 1 diabetes? *Diabetologia* **49**, 2105–2108

Cabrera O., Berman D.M., Kenyon N.S., Ricordi C., Berggren P.O. & Caicedo A. (2006) The unique cytoarchitecture of human pancreatic islets has implications for islet cell function. *Proc Natl Acad Sci U S A*. **103**, 2334-9

Case R.M. (2006) Is the Rat Pancreas an Appropriate Model of the Human Pancreas? *Pancreatology* **6**, 180–190

Chase H.P., MacKenzie T.A., Burdick J., Fiallo-Scharer R., Walravens P., Klingensmith G. & Rewers M. (2004) Redefining the clinical remission period in children with type 1 diabetes. *Pediatr Diabetes* **5**, 16–19

Chianelli M., Parisella M.G., Visalli N., Mather S.J., D'Alessandria C., Pozzilli P. & Signore A. (2008) Pancreatic scintigraphy with 99mTc-interleukin-2 at diagnosis of type 1 diabetes and after 1 year of nicotinamide theraphy. *Diabetes/metabolism research and reviews* **24**, 115-122

Concannon P., Rich S.S. & Nepom G.T. (2009) Genetics of Type 1A Diabete. *N Engl J Med.* **360**, 1646-54

Connolly B.M., Vanko A., McQuade P., Guenther I., Meng X., Rubins D., Waterhouse R., Hargreaves R., Sur C. & Hostetler E. (2012) Ex Vivo Imaging of Pancreatic Beta Cells using a Radiolabeled GLP-1 Receptor Agonist. *Mol Imaging Biol.* **14**, 79-87

Couper J.J. & Donaghue K.C. (2007) Phases of diabetes. ISPAD clinical practice consensus guidelines 2006/2007. *Pediatr Diabetes* **8**, 44–47

Czech M.P. & Corvera S. (1999) Signaling mechanisms that regulate glucose transport. *J Biol Chem.* **274**, 1865–1868

Czech M.P., Clancy B.M., Pessino A., Woon C.W. & Harrison S.A. (1992) Complex regulation of simple sugar transport in insulin-responsive cells. *Trends Biochem Sci*. **17**, 197-201

De Lonlay P., Simon-Carre A., Ribeiro M.J., Boddaert N., Giurgea I., Laborde K., Bellanné-Chantelot C., Verkarre V., Polak M., Rahier J., Syrota A., Seidenwurm D., Nihoul-Fékété C., Robert J.J., Brunelle F. & Jaubert F. (2006) Congenital hyperinsulinism: pancreatic [18F]fluoro-L-dihydroxyphenylalanine (DOPA) positron emission tomography and immunohistochemistry study of DOPA decarboxylase and insulin secretion. *J Clin Endocrinol Metab*. **91**, 933-940.

DeFronzo R.A., Tobin J.D. & Andres R. (1979) Glucose clamp technique: a method for quantifying insulin secretion and resistance. *Am J Physiol.* **237**, 214-223

Denis M.C., Mahmood U., Benoist C., Mathis D. & Weissleder R. (2004) Imaging inflammation of the pancreatic islets in type 1 diabetes. *Proc Natl Acad Sci U S A* **101**, 12634-9

Di Gialleonardo V., Signore A., Scheerstra E.A., Visser A.K., van Waarde A., Dierckx R.A. & de Vries E.F. (2012) ^{11}C-hydroxytryptophan uptake and metabolism in endocrine and exocrine pancreas. *J Nucl Med.* **53**, 1755-1763

Diabetes control and complications trial research group. *NEJM* 1993; 329, 977-86

DIAMOND Project Group (2006) Incidence and trends of childhood type 1 diabetes worldwide 1990-1999. *Diabet Med.* **23**, 857–66

Eisenbarth G.S. (1986) Type I diabetes mellitus: a chronic autoimmune disease. *N Engl J Med.* **314**, 1360-8

Eisenberg M.L., Maker A.V, Slezak L.A., Nathan J.D., Sritharan K.C., Jena B.P., Geibel J.P. & Andersen D.K. (2005) Insulin Receptor (IR) and Glucose Transporter 2 (GLUT2) Proteins Form a Complex on the Rat Hepatocyte Membrane. *Cell Physiol Biochem.* **15**, 51-58

Eisenhofer G., Kopin I.J. & Goldstein D.S. (2004) Catecholamine metabolism: a contemporary view with implications for physiology and medicine. *Pharmacol Rev.* **56**, 331-349

Eizirik D.L., Colli M.L. & Ortis F. (2009) The role of inflammation in insulitis and beta cell loss in type 1 diabetes. *Nature Reviews* **5**, 219-26

Ekholm R., Ericson L.E. & Lundquist I. (1971) Monoamines in the pancreatic islets of the mouse. Subcellular localization of 5-hydroxytryptamine by electron microscopic autoradiography. *Diabetologia* **7**, 339-348

Elayat A.A., El-Naggar M.M. & Tahir M. (1995) An immunocytochemical and morphometric study of the rat pancreatic islets. *J. Anat*. **186**, 629-637

El-Chemaly S., Malide D., Yao J., Nathan S.D., Rosas I.O., Gahl W.A., Moss J. & Gochuico B.R. (2013) Glucose transporter-1 distribution in fibrotic lung disease: association with [^{18}F]-2-fluoro-2-deoxyglucose-PET scan uptake, inflammation, and neovascularization. *Chest* **143**, 1685-91

Elding Larsson H., Vehik K., Gesualdo P., Akolkar B., Hagopian W., Krischer J., Lernmark Å., Rewers M., Simell O., She J.X., Ziegler A. & Haller M.J. (2014) Children followed in the TEDDY study are diagnosed with type 1 diabetes at an early stage of disease. *Pediatr Diabetes*. **15**, 118-26

Ellis H. (2013) Anatomy of the pancreas. *Surgery* **31**, 263-266

Ericson K., Blomqvist G., Bergström M., Eriksson L. & Stone-Elander S. (1987) Application of a kinetic model on the methionine accumulation in the intracranial tumours studied with positron emission tomography. *Acta Radiol.* **28**, 505-509

Ericson L.E., Håkanson R. & Lundquist I. (1977) Accumulation of dopamine in mouse pancreatic B-cells following injection of L-DOPA. Localization to secretory granules and inhibition of insulin secretion. *Diabetologia* **13**, 117-124

Eriksson O., Espes D., Selvaraju R.K., Jansson E., Antoni G., Sörensen J., Lubberink M., Biglarnia A., Eriksson J.W., Sundin A., Ahlström H., Eriksson B., Johansson L., Carlsson P.O. & Korsgren O. (2014) The Positron Emission Tomography ligand [11C]5-Hydroxy-Tryptophan can be used as a surrogate marker for the human endocrine pancreas. *Diabetes* May 21 [Epub ahead of print]

Eriksson O., Selvaraju R.K., Johansson L., Eriksson J.W., Sundin A., Antoni G., Sörensen J., Eriksson B. & Korsgren O. (2014) Quantitative imaging of serotonergic biosynthesis and degradation in the endocrine pancreas. *J Nucl Med*. **55**, 460-5

Eskola O., Grönroos T.J., Naum A., Marjamäki P., Forsback S., Bergman J., Länkimäki S., Kiss J., Savunen T., Knuuti J., Haaparanta M. & Solin O. (2012) Novel electrophilic synthesis of 6-[(1)(8) F]fluorodopamine and comprehensive biological evaluation. *Eur J Nucl Med Mol Imaging* **39**, 800-810

Esqueda A.C., López J.A., Andreu-de-Riquer G., Alvarado-Monzón J.C., Ratnakar J., Lubag A.J., Sherry A.D. & De León-Rodríguez L.M. (2009) A new gadolinium-based MRI zinc sensor. *J Am Chem Soc*. **131**, 11387-91

Fagerholm V., Mikkola K.K., Ishizu T., Arponen E., Kauhanen S., Någren K., Solin O., Nuutila P. & Haaparanta M. (2010) Assessment of islet specificity of dihydrotetrabenazine radiotracer binding in rat pancreas and human pancreas. *J Nucl Med*. **51**, 1439-46

Fan Y., Rudert W.A., Grupillo M., He J., Sisino G. & Trucco M. (2009) Thymus-specific deletion of insulin induces autoimmune diabetes. *EMBO J.* **28**, 2812–2824

Faustman D.L. (2014) Why were we wrong for so long? The pancreas of type 1 diabetic patients commonly functions for decades. *Diabetologia* **57**, 1-3

Firnau G, Nahmias C, Garnett S. (1973) The preparation of (18F)5-fluoro-DOPA with reactor-produced fluorine-18. *Int J Appl Radiat Isot*. **24**, 182-184.

Forsback S., Eskola O., Haaparanta M., Bergmann J. & Solin O. (2008) Electrophilic synthesis of 6-[18F] fluoro-L-DOPA using post-target produced [18F]F2. *Radiochim Acta* **96**, 845-848

Foulis A.K. & Stewart J.A. (1984) The pancreas in recent-onset type 1 (insulin-dependent) diabetes mellitus: insulin content of islets, insulitis and associated changes in the exocrine acinar tissue. *Diabetologia* **26**, 456–461

Foulis A.K., Liddle C.N., Farquharson M.A., Richmond J.A. & Weir R.S. (1986) The histopathology of the pancreas in type 1 (insulindependent) diabetes mellitus: a 25-year review of deaths in patients under 20 years of age in the United Kingdom. *Diabetologia* **29**, 267–274

Fu W., Wojtkiewicz G., Weissleder R., Benoist C. & Mathis D. (2012) Early window of diabetes determinism in NOD mice, dependent on the complement receptor CRIg, identified by noninvasive imaging. *Nature immunology* **13**, 361-8

Fu Y., Maianu L., Melbert B.R. and Garvey W.T. (2004) Facilitative glucose transporter gene expression in human lymphocytes, monocytes, and macrophages: a role for GLUT isoforms 1, 3, and 5 in the immune response and foam cell formation *Blood Cells, Molecules, and Diseases* **32**, 182–190

Fu Z., Gilbert E.R. & Liu D. (2013) Regulation of Insulin Synthesis and Secretion and Pancreatic Beta-Cell Dysfunction in Diabetes. *Current Diabetes Reviews* **9**, 25-53

Gaglia J.L., Guimaraes A.R., Harisinghani M., Turvey S.E., Jackson R., Benoist C., Mathis D. & Weissleder R. (2011) Noninvasive imaging of pancreatic islet inflammation in type 1A diabetes patients. *J Clin Invest*. **121**, 442–445

Gale E.A., Bingley P.J., Emmett C.L. & Collier T.; European Nicotinamide Diabetes Intervention Trial (ENDIT) Group. (2004) European Nicotinamide Diabetes Intervention Trial (ENDIT): a randomised controlled trial of intervention before the onset of type 1 diabetes. *Lancet* **363**, 925-31.

Gazdar A.F., Helman L.J., Israel M.A., Russell E.K., Linnoila R.I., Mulshine J.L., Schuller H.M. & Park J.G. (1988). Expression of neuroendocrine cell markers L-dopa decarboxylase, chromogranin A, and dense core granules in human tumors of

endocrine and nonendocrine origin. *Cancer Res*. **48**, 4078-4082.

Gepts W. (1965) Pathologic anatomy of the pancreas in juvenile diabetes mellitus. *Diabetes* **14**, 619–633

Glaudemans A.W.J.M., Quintero A.M. & Signore A. (2012) PET/MRI in infectious and inflammatory diseases: will it be a useful improvement? *Eur J Nucl Med Mol Imaging* **39**, 745-749

Goland R., Freeby M., Parsey R., Saisho Y., Kumar D., Simpson N., Hirsch J., Prince M., Maffei A., Mann J.J., Butler P.C., Van Heertum R., Leibel1 R.L., Ichisey M. & Harrisy P.E. (2009) 11C-Dihydrotetrabenazine PET of the Pancreas in Subjects with Long-Standing Type 1 Diabetes and in Healthy Controls. *J Nucl Med.* **50**, 382–389

Gotthardt M., Eizirik D.L., Cnop M. & Brom M. (2014) Beta cell imaging - a key tool in optimized diabetes prevention and treatment. *Trends Endocrinol Metab*. Apr 10 [Epub ahead of print]

Green J., Ellis F., Shallcross T. & Bramley P. (1990) Invalidity of hand heating as a method to arterialize venous blood. *Clin Chem.* **36**, 719-722

Hamacher K., Coenen H.H. & Stocklin G. (1986) Efficient stereospecific synthesis of no-carrier-added 2-[18F]-fluoro-2-deoxy-D-glucose using aminopolyether supported nucleophilic substitution. *J Nucl Med.* **27**, 235-238

Harjutsalo V., Sjöberg L. & Tuomilehto J. (2008) Time trends in the incidence of type 1 diabetes in Finnish children. *Lancet* **371**, 1777–1782

Harris S.M., Davis J.C., Snyder S.E., Butch E.R., Vavere A.L., Kocak M. & Shulkin B.L. (2013) Evaluation of the biodistribution of 11C-methionine in children and young adults. *J Nucl Med*. **54**, 1902-1908

Hatamori N., Yokono K., Nagata M., Doi K. & Baba S. (1989) Interleukin 2/interleukin 2 receptor system in type 1 diabetes. *Diabetes Res Clin Pract.* **7**, 67-72

Henquin J.C., Charles S., Nenquin M., Mathot F. & Tamagawa T. (1982) Diazoxide and D600 inhibition of insulin release: distinct mechanisms explain the specificity for different stimuli. *Diabetes* **31,** 776–783

Henquin J.C., Ravier M.A., Nenquin M., Jonas J.C. & Gilon P. (2003) Hierarchy of the β-cell signals controlling insulin secretion. *European Journal of Clinical Investigation* **33**, 742–750

Higashi K., Ueda Y., Sakurai A., Wang X.M., Xu L., Murakami M., Seki H., Oguchi M., Taki S., Nambu Y., Tonami H., Katsuda S. & Yamamoto I. (2000) Correlation of Glut-1 glucose transporter expression with. *Eur J Nucl Med*. **27**, 1778-85

Hirshberg B., Qiu M., Cali A.M., Sherwin R., Constable T., Calle R.A. & Tal M.G. (2009) Pancreatic perfusion of healthy individuals and type 1 diabetic patients as assessed by magnetic resonance perfusion imaging. *Diabetologia* **52**, 1561-5

Hong F., Liu L., Fan R.F., Chen Y., Chen H., Zheng R.P., Zhang Y., Gao Y. & Zhu J.X. (2014) New perspectives of vesicular monoamine transporter 2 chemical characteristics in mammals and its constant expression in type 1 diabetes rat models. *Translational Research* **163**, 171-82

Horton R.W., Meldrum B.S. & Bachelard H.S. (1973) Enzymic and cerebral metabolic effect of 2-deoxy-D-glucose. *Neurochem.* **21**, 507-520

Ibukuro K. (2001) Vascular anatomy of the pancreas and clinical applications. *Int J Gastrointest Cancer* **30**, 87-104

Imagawa A. (2000) A Novel Subtype of Type 1 Diabetes Mellitus Characterized by a Rapid Onset and an Absence of Diabetes-related Antibodies. *The New England Journal of Medicine* **342**, 301-7

In't Veld P. (2011) Insulitis in human type 1 diabetes The quest for an elusive lesion *Islets* **3**, 131-138

In't Veld P., Lievens D., De Grijse J., Ling Z., Van der Auwera B., Pipeleers-Marichal M., Gorus F. & Pipeleers D. (2007) Screening for Insulitis in Adult Autoantibody-Positive Organ Donors. *Diabetes* **56**, 2400-2404

Jones A.G. & Hattersley A.T. (2013) The clinical utility of C-peptide measurement in the care of patients with diabetes. *Diabet Med.* **30**, 803-17

Jörns A., Arndt T., Zu Vilsendorf A.M., Klempnauer J., Wedekind D., Hedrich H.J., Marselli L., Marchetti P., Harada N., Nakaya Y., Wang G.S., Scott F.W., Gysemans C., Mathieu C. & Lenzen S. (2014) Islet infiltration, cytokine expression and beta cell death in the NOD mouse, BB rat, Komeda rat, LEW.1AR1-iddm rat and humans with type 1 diabetes. *Diabetologia* **57**, 512-21

Kalliokoski T., Svedström E., Saunavaara J., Roivainen A., Kankaanpää M., Oivanen H., Nuutila P & Simell O. (2011) Imaging of Insulitis in NOD Mice with IL-2-Gd-DTPA and 1.5 T MRI. *Advances in Molecular Imaging* **1**, 43-49

Karhunen T., Tilgmann C., Ulmanen I., Julkunen I. & Panula P. (1994) Distribution of catechol-O-methyltransferase enzyme in rat tissues. *J Histochem Cytochem.* **42**, 1079-1090

Karjalainen J.K. (1990) Islet cell antibodies as predictive markers for IDDM in children with high background incidence of disease. *Diabetes* **39**, 1144-1150

Katzen H.M., Soderman D.D. & Wiley C.E. Multible forms of hexokinase. (1970) *J Biol Chem.* **245**, 4081-4096

Kauhanen S., Seppanen M. & Nuutila P. (2008) Premedication with carbidopa masks positive finding of insulinoma and beta-cell hyperplasia in [(18)F]-dihydroxy-phenyl-alanine positron emission tomography. *J Clin Oncol*. **26**, 5307-5308.

Kauhanen S., Seppänen M., Minn H., Gullichsen R., Salonen A., Alanen K., Parkkola R., Solin O., Bergman J., Sane T., Salmi J., Välimäki M. & Nuutila P. (2007) Fluorine-18-L-dihydroxyphenylalanine (18F-DOPA) positron emission tomography as a tool to localize an insulinoma or beta-cell hyperplasia in adult patients. *J Clin Endocrinol Metab*. **92**, 1237-1244.

Kauhanen S., Seppänen M., Ovaska J., Minn H., Bergman J., Korsoff P., Salmela P., Saltevo J., Sane T., Välimäki M. & Nuutila P. (2009) The clinical value of [18F]fluoro-dihydroxyphenylalanine positron emission tomography in primary diagnosis, staging, and restaging of neuroendocrine tumors. *Endocr Relat Cancer* **16**, 255-265.

Knip M., Åkerblom H.K., Becker D., Dosch H.M., Dupre J., Fraser W., Howard N., Ilonen J., Krischer J.P., Kordonouri O., Lawson M.L., Palmer J.P., Savilahti E., Vaarala O. & Virtanen S.M. (2014) Hydrolyzed infant formula and early β-cell autoimmunity: a randomized clinical trial. *JAMA* **311**, 2279-87

Kobayashi H. (2004) Expression of glucose transporter 4 in the human pancreatic islet of Langerhans. *Biochem Biophys Res Commun.* **314**, 1121–1125

Kobayashi M., Hashimoto F., Ohe K., Nadamura T., Nishi K., Shikano N., Nishii R., Higashi T., Okazawa H. & Kawai K. (2012) Transport mechanism of 11C-labeled L- and D-methionine in human-derived tumor cells. *Nuclear Medicine and Biology* **39**, 1213–1218

Kubota K., Yamada K., Fukada H., Endo S., Ito M., Abe Y., Yamaguchi T., Fujiwara T., Sato T. & Ito K. (1984) Tumor detection with carbon-11-labelled amino acids. *Eur J Nucl Med.* **9**, 136-140

Kubota R., Yamada S., Kubota K., Ishiwata K., Tamahashi N. & Ido T. (1992) Intratumoral distribution of fluorine-18-fluorodeoxyglucose in vivo: high accumulation in macrophages and granulation tissues studied by microautoradiography. *J Nucl Med.* **33**, 1972-1980

Kulmala P., Savola K., Petersen J.S., Vahasalo P., Karjalainen J., Lopponen T., Dyrberg T., Akerblom H.K. & Knip M. (1998) Prediction of insulin-dependent diabetes mellitus in siblings of children with diabetes: a population-based study. *J Clin Invest.* **101**, 327–336

Kupila A., Keskinen P., Simell T., Erkkilä S., Arvilommi P., Korhonen S., Kimpimäki T., Sjöroos M., Ronkainen M., Ilonen J., Knip M. & Simell O. (2002) Genetic risk determines the emergence of diabetes-associated autoantibodies in young children. *Diabetes* **51**, 646-51

Kupila A., Muona P., Simell T., Arvilommi P., Savolainen H., Hämäläinen A.M., Korhonen S., Kimpimäki T., Sjöroos M., Ilonen J., Knip M. & Simell O. (2001) Feasibility of genetic and immunological prediction of Type 1 Diabetes in a population-based birth cohort. *Diabetologia* **44**, 290-297

Lackovic Z. & Neff N. (1983) Evidence that dopamine is a neurotransmitter in peripheral tissues. *Life Sciences* **32**, 1665-1674

Laitinen O.H., Honkanen H., Pakkanen O., Oikarinen S., Hankaniemi M.M., Huhtala H., Ruokoranta T., Lecouturier V., André P., Harju R., Virtanen S.M., Lehtonen J., Almond J.W., Simell T., Simell O., Ilonen J., Veijola R., Knip M. & Hyöty H. (2014) Coxsackievirus B1 is associated with induction of β-cell autoimmunity that portends type 1 diabetes. *Diabetes* **63**, 446-55.

Lehtiniemi P., Forsback S., Kirjavainen A., Haavisto L., Haaparanta M. & Solin O. (2012) Electrophilic fluorination of five metabolites of [18F]FDOPA. *The quarterly journal of nuclear medicine* **56**, 38

Leiter E.H., Prochazka M. & Coleman D.L. (1987) The non-obese diabetic (NOD) mouse. *Am J Pathol*. **128**, 380–383

Lempäinen J., Tauriainen S., Vaarala O., Mäkelä M., Honkanen H., Marttila J., Veijola R., Simell O., Hyöty H., Knip M. & Ilonen J. (2012) Interaction of enterovirus infection and cow's milk-based formula nutrition in type 1 diabetes-associated autoimmunity. *Diabetes Metab Res Rev*. **28**, 177-85

Leskinen K., Nagren K., Lehikoinen P., Ruotsalainen U., Teras M. & Joensuu H. (1992) Carbon-11-methionine and PET is an effective method to image head and neck cancer. *J Nucl Med*. **33**, 691-695

Leturque A., Brot-Laroche E., Le Gall M., Stolarczyk E. & Tobin V. (2005) The role of GLUT2 in dietary sugar handling. *J Physiol Biochem.* **61**, 529-37.

Li Y.V. (2014) Zinc and insulin in pancreatic beta-cells. *Endocrine* **45**, 178-89

Lifson N., Lassa C.V. & Dixit P.K. (1985) Relation between blood flow and morphology in islet organ of rat pancreas. *Am J Physiol*. **249**, E43-8.

Ludvigsson J. (2014) Is it time to challenge the established theories surrounding type 1 diabetes? *Acta Paediatr*. **103**, 120–123

Lundquist I., Panagiotidis G. & Stenström A. (1991) Effect of L-dopa administration on islet monoamine oxidase activity and glucose-induced insulin release in the mouse. *Pancreas* **6**, 522-527

Maahs D.M., West N.A., Lawrence J.M. & Mayer-Davis E.J. (2010) Epidemiology of Type 1 Diabetes. *Endocrinol Metab Clin N Am.* **39**, 481–497

Macdonald M.J. (1993) Estimates of Glycolysis, Pyruvate (De)Carboxylation, Pentose Phosphate Pathway, and Methyl Succinate Metabolism in Incapacitated Pancreatic Islets. *Arch Biochem Biophys.* **305**, 205-14.

Macintyre A.N., Gerriets V.A., Nichols A.G., Michalek R.D., Rudolph M.C., Deoliveira D., Anderson S.M., Abel E.D., Chen B.J., Hale L.P. & Rathmell J.C. (2014) The Glucose Transporter Glut1 Is Selectively Essential for CD4 T Cell Activation and Effector Function. *Cell Metab*. **20**, 61-72

Maciver N.J., Jacobs S.R., Wieman H.L., Wofford J.A., Coloff J.L. & Rathmell JC. (2008) Glucose metabolism in lymphocytes is a regulated process with significant effects on immune cell function and survival. *J Leukoc Biol.* **84**, 949–957

Maffei A., Liu Z., Witkowski P., Moschella F., Del Pozzo G., Liu E., Herold K., Winchester R.J., Hardy M.A. & Harris P.E. (2004) Identification of tissuerestricted transcripts in human islets. *Endocrinology* **145**, 4513–4521

Malaisse W, Maedler K. (2012) Imaging of the b-cells of the islets of Langerhans. *Diabetes Research and Clinical Practice* **98**, 11-18

Malaisse W.J., Damhaut P., Malaisse L., Ladriere L., Olivares E. & Goldman S. (2000) Fate of 2-deoxy-2-[18F]fluoro-D-glucose in control and diabetic rats. *Int J Mol Med.* **5**, 525-532

Mann R., Nasr N., Hadden D., Sinfield F., Abidi F. & Al-Sabah S. (2007) Peptide binding at the GLP-1 receptor. *Biochem Soc Trans.* **35**, 713–716

Marchetti P., Dotta F., Ling Z., Lupi R., Del Guerra S., Santangelo C., Realacci M., Marselli L., Di Mario U. & Navalesi R. (2000) Function of pancreatic islets isolated from a type 1 diabetic patient. *Diabetes Care* **23**, 701-3.

McCulloch L.J., van de Bunt M., Braun M., Frayn K.N., Clark A. & Gloyn A.L. (2011) GLUT2 (SLC2A2) is not the principal glucose transporter in human pancreatic beta cells: Implications for understanding genetic association signals at this locus. *Mol Genet Metab.* **104**, 648–653

Medarova Z., Castillo G., Dai G., Bolotin E., Bogdanov A. & Moore A. (2007) Noninvasive Magnetic Resonance Imaging of Microvascular Changes in Type 1 Diabetes. *Diabetes* **56**, 2677-82

Meglasson M.D. & Matschinsky F.M. (1984) New perspectives on pancreatic islet glucokinase, *Am J Physiol Endocrinol Metab.* **246**, E1-E13

Meisenberg G. & Simmons W.H. The Oxidation of Glucose. In: Underdown E. and Copland B., editors. *Principles of Medical Biochemistry*. Mosby Inc. 1998: 298-299

Melega W.P., Luxen A., Perlmutter M.M., Nissenson C.H., Phelps M.E. & Barrio J.R. (1990) Comparative *in vivo* metabolism of 6-[18F]fluoro-L-dopa and [3H]L-dopa in rats. *Biochem Pharmacol*. **39**, 1853-1860

Merger S.R., Leslie R.D. & Boehm B.O. (2013) Review Article: The broad clinical phenotype of Type 1 diabetes at presentation. *Diabet. Med*. **30**, 170–178

Mezey E., Eisenhofer G., Harta G., Hansson S., Gould L., Hunyady B. & Hoffman B.J. (1996) A novel nonneuronal catecholaminergic system: exocrine pancreas synthesizes and releases dopamine. *Proc Natl Acad Sci U S A* **93**, 10377-10382

Mikkola K., Yim C.B., Fagerholm V., Ishizu T., Elomaa V.V., Rajander J., Jurttila J., Saanijoki T., Tolvanen T., Tirri M., Gourni E., Béhé M., Gotthardt M., Reubi J.C., Mäcke H., Roivainen A., Solin O. & Nuutila P. (2014) 64Cu- and 68Ga-labelled [Nle(14),Lys(40)(Ahx-NODAGA)NH2]-exendin-4 for pancreatic beta cell imaging in rats. *Mol Imaging Biol*. **16**, 255-63

Miller R.E. (1981) Pancreatic Neuroendocrinology: Peripheral Neural Mechanisms in the Regulation of the Islets of Langerhans. *Endocr Rev.* **2**, 471-494

Moore A., Grimm J., Han B. & Santamaria P. (2004) Tracking the Recruitment of Diabetogenic $CD8^+$ T-Cells to the Pancreas in Real Time. *Diabetes* **53**, 1459-66

Moore A., Sun P., Cory D., Högemann D., Weissleder R. & Lipes M. (2002) MRI of Insulitis in Autoimmune Diabetes. *MRM* **47**, 751-758

Murakami T. (1993) The insulo-acinar portal and insulo-venous drainage systems in the pancreas of the mouse, dog, monkey and certain other animals: a scanning electron microscopic study of corrosion casts. *Arch Histol Cytol.* **56**, 127–147.

Murakami T., Miyake T., Tsubouchi M., Tsubouchi Y., Ohtsuka A. & Fujuti T. (1997) Blood Flow Patterns in the Rat Pancreas: A Simulative Demonstration

by Injection Replication and Scanning Electron Microscopy. *Microsc Res Tech.* **37**, 497–508

Naik R.G. & Palmer J.P.(2003) Latent autoimmune diabetes in adults (LADA). *Rev Endocr Metab Disord.* **4**, 233–41

Nalin L., Selvaraju R.K., Velikyan I., Berglund M., Andréasson S., Wikstrand A., Rydén A., Lubberink M., Kandeel F., Nyman G., Korsgren O., Eriksson O. & Jensen-Waern M. (2014) Positron emission tomography imaging of the glucagon-like peptide-1 receptor in healthy and streptozotocin-induced diabetic pigs. *Eur J Nucl Med Mol Imaging* Mar 19. [Epub ahead of print]

Nanni C., Rubello D. & Fanti S. (2006) 18F-DOPA PET/CT and neuroendocrine tumours. *Eur J Nucl Med Mol Imaging* **33**, 509-513.

Nauck M.A., Bartels E., Ørskov C., Ebert R. & Creutzfeldt W. (1993) Additive insulinotropic effects of exogenous synthetic human gastic inhibitory polypeptide and glucagon-like peptide-1-(7-36) amide infused at near-physiological insulinotropic hormone and glucose concentrations. *J Clin Endocrinol Metab.* **76**, 912–917

Normandin M.D., Petersen K.F., Ding Y., Lin S., Naik S., Fowles K., Skovronsky D.M., Herold K.C., McCarthy T.J., Calle R.A., Carson R.E., Treadway J.L. & Cline G. (2012) In Vivo Imaging of Endogenous Pancreatic b-Cell Mass in Healthy and Type 1 Diabetic Subjects Using ^{18}F-Fluoropropyl-Dihydrotetrabenazine and PET. *J Nucl Med.* **53**, 908–916

Norris J.M., Beaty B., Klingensmith G., Hoffman M., Chase P., Erlich H.A., Hamman R.F., Eisenbarth G.S. & Rewers M. (1996) Lack of association between early exposure to cow's milk protein and beta-cell autoimmunity. Diabetes Autoimmunity Study in the Young (DAISY). *JAMA* **276**, 609–14

Nuutila P., Peltoniemi P., Oikonen V., Larmola K., Kemppainen J., Takala T., Sipilä H., Oksanen A., Ruotsalainen U., Bolli G. & Yki-Järvinen H. (2000) Enhanced Stimulation of Glucose Uptake by Insulin Increases Exercise-Stimulated Glucose Uptake in Skeletal Muscle in Humans Studies Using [15O]O2, [15O]H2O, [18F]fluoro-deoxy-glucose, and Positron Emission Tomography. *Diabetes* **49**, 1084–1091

Någren K. & Halldin C. (1998) Methylation of amide and thiol functions with [11C]methyl triflate, examplified by [11C]NMSP, [11C]flumazenil and [11C]methionine. *J Labelled Compd Radiopharm.* **41**, 831-841

Någren K. (1993) Quality control aspects in the preparation of [11C]-methionine. PET studies on amino acid metabolism and protein synthesis, B.M.Mazoyer, W.D.Heiss & D.Comar (eds), Kluwer Academic Publishers, Dordrecht. 81-87

Näntö-Salonen K., Kupila A., Simell S., Siljander H., Salonsaari T., Hekkala A., Korhonen S., Erkkola R., Sipilä J.I., Haavisto L., Siltala M., Tuominen J., Hakalax J., Hyöty H., Ilonen J., Veijola R., Simell T., Knip M. & Simell O. (2008) Nasal insulin to prevent type 1 diabetes in children with HLA genotypes and autoantibodies conferring increased risk of disease: a double-blind, randomised controlled trial. *Lancet* **372**, 1746–1755

Oram R.A., Jones A.G., Besser R.E., Knight B.A., Shields B.M., Brown R.J., Hattersley A.T. & McDonald T.J. (2014) The majority of patients with long-duration type 1 diabetes are insulin microsecretors and have functioning beta cells *Diabetologia* **57**, 187-91

Otonkoski T., Näntö-Salonen K., Seppänen M., Veijola R., Huopio H., Hussain K., Tapanainen P., Eskola O., Parkkola R., Ekström K., Guiot Y., Rahier J., Laakso M., Rintala R., Nuutila P. & Minn H. (2006) Noninvasive diagnosis of focal hyperinsulinism of infancy with [18F]-DOPA positron emission tomography. *Diabetes* **55**, 13-8.

Ørskov C. (1992) Glucagon-like peptide-1, a new hormone on the entero-insular axis. *Diabetologia* **35**, 701–711

Palmer J.P. (2009) C-peptide in the natural history of type 1 diabetes. *Diabetes Metab Res Rev.* **25**, 325–328

Parikka V., Näntö-Salonen K., Saarinen M., Simell T., Ilonen J., Hyöty H., Veijola R., Knip M. & Simell O. (2012) Early seroconversion and rapidly increasing autoantibody concentrations predict prepubertal manifestation of type 1 diabetes in children at genetic risk. *Diabetologia* **55**, 1926-36

Patlak CS, Blasberg RG & Fenstermacher J.D. (1985) Graphical evaluation of blood-to-brain transfer constant from multiple time uptake data. Generalizations. *J Cereb Blood Flow Metab.* **5**, 584-590

Patterson C.C., Dahlquist G.G., Gyurus E., Green A. & Soltesz G. (2009) Incidence trends for childhood type 1 diabetes in Europe during 1989-2003 and predicted new cases 2005-20: a multicentre prospective registration study **373**, 2027–33

Pflueger M., Seppänen-Laakso T., Suortti T., Hyötyläinen T., Achenbach P., Bonifacio E., Orešič M. & Ziegler A.G. (2011) Age- and islet autoimmunity-associated differences in amino acid and lipid metabolites in children at risk for type 1 diabetes. *Diabetes* **60**, 2740-2747

Pizzinat N., Chan S.L., Remaury A., Morgan N.G. & Parini A. (1999) Characterization of monoamine oxidase isoforms in human islets of Langerhans. *Life Sci*. **65**, 441-448

Rajda C., Dibó G., Vécsei L. & Bergquist J. (2005) Increased dopamine content in lymphocytes from high-dose L-Dopa-treated Parkinson's disease patients. *Neuroimmunomodulation* **12**, 81-84.

Report of the Expert Committee on the Diagnosis and Classification of Diabetes Mellitus. (1997) *Diabetes Care* **20**, 1183-97

Rodriguez-Diaz R., Abdulreda M.H., Formoso A.L., Gans I., Ricordi C., Berggren P.O. & Caicedo A. (2011) Innervation patterns of autonomic axons in the human endocrine pancreas. *Cell Metab*. **14**, 45-54

Roep B.O., Atkinson M. & von Herrath M. (2004) Satisfaction (not) guaranteed: re-evaluating the use of animal models of type 1 diabetes. *Nature Reviews* **4**, 989-97

Roep B.O., Hiemstra H.S., Schloot N.C., De Vries R.R., Chaudhuri A., Behan P.O., Drijfhout J.W. (2002) Molecular mimicry in type 1 diabetes: immune cross-reactivity between islet autoantigen and human cytomegalovirus but not Coxsackie virus. *Ann N Y Acad Sci.* **958**, 163–165

Rolandsson O., Stigbrand T., Riklundahlstrom K., Eary J. & Greenbaum C. (2001) Accumulation of(125) iodine labeled interleukin-2 in the pancreas of NOD mice. *J Autoimmun*. **17**, 281-287

Rorsman F., Husebye E.S., Winqvist O., Björk E., Karlsson F.A. & Kämpe O. (1995) Aromatic-L-amino-acid decarboxylase, a pyridoxal phosphate-dependent enzyme, is a beta-cell autoantigen. *Proc Natl Acad Sci USA* **92**, 8626-9.

Rowe P.A. (2011) The pancreas in human type 1 diabetes. *Semin Immunopathol.* **33**, 29–43

Ruottinen H.M., Bergman J.R., Oikonen V.J., Haaparanta M.T., Solin O.H. & Rinne J.O. (2001) Determination of 6-[^{18}F]fluoro-L-dopa metabolites: importance in interpretation of PET results. In: Gjedde A, Hansen SB, Knudsen GM, Paulson OB, editors. *Physiological Imaging if the Brain with PET.* San Diego: Academic Press 413p. 179-186

Rutter G.A. (2004) Visualising insulin secretion. The Minkowski Lecture 2004. *Diabetologia* **47**, 1861–1872

Sadeharju K., Lönnrot M., Kimpimäki T., Savola K., Erkkilä S., Kalliokoski T., Savolainen P., Koskela P., Ilonen J., Simell O., Knip M. & Hyöty H. (2001) Enterovirus antibody levels during the first two years of life in prediabetic autoantibody-positive children. *Diabetologia* **44**, 818–23

Santer R., Schneppenheim R., Suter D., Schaub J. & Steinmann B. (1998) Fanconi–Bickel syndrome—the original patient and his natural history, historical steps leading to the primary defect, and a review of the literature. *Eur J Pediatr*. **157**, 783–797.

Sato Y., Ito T., Udaka N., Kanisawa M, Noguchi Y., Cushman S.W. & Satoh S. (1996) Immunohistochemical localization of facilitated-diffusion glucose transporters in rat pancreatic islets. *Tissue & Cell* **28**, 637—643

Saura J., Kettler R., Da Prada M. & Richards J.G. (1992) Quantitative enzyme radioautography with 3H-Ro 41-1049 and 3H-Ro 19-6327 in vitro: localization and abundance of MAO-A and MAO-B in rat CNS, peripheral organs, and human brain. *J Neurosci.* **12**, 1977-1999

Schranz D.B. & Lernmark A. (1998) Immunology in diabetes: an update. *Diabetes metab rev.* **14**, 3-29

Schuit F., Moens K., Heimberg H. & Pipeleers D. (1999) Cellular origin of hexokinase in pancreatic islets. *J Biol Chem.* **274**, 32803-9

Sekine N., Cirulli V., Regazzi R., Brown L.J., Gine E., Tamarit-Rodriguez J., Girotti M., Marie S., MacDonald M.J., Wollheim C.B., et al (1994) Low lactate dehydrogenase and high mitochondrial glycerol phosphate dehydrogenase in pancreatic beta-cells. Potential role in nutrient sensing. *J Biol Chem.* **269**, 4895–4902

Selvaraju R.K., Velikyan I., Johansson L., Wu Z., Todorov I., Shively J., Kandeel F., Korsgren O. & Eriksson O. (2013) In vivo imaging of the glucagonlike peptide 1 receptor in the pancreas with 68Ga-labeled DO3A-exendin-4. *J Nucl Med*. **54**, 1458-63

Shimada A., Charlton B., Taylor-Edwards C. & Fathman C.G. (1996) Beta-cell destruction may be a late consequence of the autoimmune process in nonobese diabetic mice. *Diabetes* **45**, 1063-1067

Signore A., Barone R., Procaccini E., Annovazzi A., Chianelli M., Scopinaro F., Ronga G., Multari G., Looman W.J. & Pozzilli P. (1996) *In vivo* measurement of immunoglobulin accumulation in the pancreas of recent onset type 1 diabetic patients. *Clinical and Experimental Rheumatology* **14**, 41-45

Signore A., Chianelli M., Ferretti E., Toscano A., Britton K.E., Andreani D., Gale E.A. & Pozzilli P. (1994) New approach for *in vivo* detection of Insulitis in type 1 diabetes: activated lymphocyte targeting with 123I-labelled interleukin 2. *European journal of endocrinology* **13**1, 431-437

Signore A., Chianelli M., Toscano A., Monetini L., Ronga G., Nimmon C.C., Britton K.E., Pozzilli P. & Negri M. (1992) A radiopharmaceutical for imaging areas of lymphocytic infiltration: 123I-interleukin-2. Labelling procedure and animal studies. *Nucl Med Commun.* **13**, 713-722

Signore A., Picarelli A., Annovazzi A., Britton K.E., Grossman A.B., Bonanno E., Maras B., Barra D. & Pozzilli P. (2003) 123I-interleukin-2: biochemical characterization and *in vivo* use fot imaging autoimmune diseases. *Nuclear Medicine Communications* **24**, 305-316

Signore A., Pozzilli P., Gale E.A., Andreani D. & Beverley P.C. (1989) The natural history of lymphocyte subsets infiltrating the pancreas of NOD mice. *Diabetologia* **32**, 282-289

Signore A., Procaccini E., Toscano A.M., Ferretti E., Williams A.J.K., Beales P.E., Cugini P. & Pozzilli P. (1994) Histological study of pancreatic beta-cell loss in relation to the insulitis process in the non-obese diabetic mouse. *Histochemistry* **101**, 263-269

Skyler J.S. (2013) Primary and secondary prevention of Type 1 diabetes. *Diabet Med*. **30**, 161-9

Smith P.H. & Davis B.J. (1983) Morphological and functional aspects of pancreatic islet innervation. *J Auton Nerv Syst.* **9**, 53-66

Soares da Silva P., Vieira-Coelho M.A., Pinto do O P.C., Pestana M. & Bertorello A.M. (1995) Studies on the nature of the antagonistic actions of dopamine and 5-hydroxytryptamine in renal tissues *Hypertens Res*. 18 Suppl 1:S47-51

Sokoloff L., Reivich M., Kennedy C., Des R., Patlak C.S., Pettigrew K.D., Sakurada O. & Shinohara M. (1977) The [14C]deoxyglucose method for the measurement of local cerebral glucose utilization: theory, procedure, and normal values in the conscious and anesthetized albino rat. *J Neurochem.* **28**, 897-916.

Sorensen J.S., Vaziri-Sani F., Maziarz M., Kristensen K., Ellerman A., Breslow N., Lernmark Å., Pociot F., Brorsson C., Birkebaek N.H. (2012) Islet autoantibodies and residual beta cell function in type 1 diabetes children followed for 3-6 years. *Diabetes Res Clin Pract*. **96**, 204-10

Souza F., Simpson N., Raffo A., Saxena C., Maffei A., Hardy M., Kilbourn M., Goland R., Leibel R., Mann J., Van Heertum R. & Harris P.E. (2006) Longitudinal noninvasive PET-based B cell mass estimates in a spontaneous diabetes rat model. *J Clin Invest.* **116**, 1506–1513

Srinivas M., Morel P., Ernst L., Laidlaw D. & Ahrens E. (2007) Fluorine-19 MRI for Visualization and Quantification of Cell Migration in a Diabetes Model. *MRM* **58**, 725-734

Stanescu D.E., Lord K. & Lipman T.H. (2012) The Epidemiology of Type 1 Diabetes in Children. *Endocrinol Metab Clin N Am*. **41**, 679–694

Stoeger A., Mur e., Penz-Schneeweiss D., Moncayo R., Decristoforo C., Riccabona G. & Fridrich L. (1994) Technetium 99m human immunoglobulin scintigraphy in psoriatic arthropathy: first results. *Eur J Nucl Med.* **21**, 342-344

Strandell E., Eizirik D.L. & Sandler S. (1990) Reversal of beta-cell suppression in vitro in pancreatic islets isolated from nonobese diabetic mice during the phase preceding insulin-dependent diabetes mellitus. *J Clin Invest*. **85**, 1944-50

Sweet I., Cook D., Lernmark A., Greenbaum C., Wallen A., Marcum E., Stekhova S. & Krohn K. (2004) Systematic screening of potential *b*-cell imaging agents. *Biochemical and Biophysical Research Communications* **314**, 976–983

Syrota A., Dop-Ngassa M., Cerf M. & Paraf A. (1981) 11C-L-methionine for evaluation of pancreatic exocrine function. *Gut* **22**, 907-915

Taborsky G.J. (2011) Islets Have a Lot of Nerve! Or Do They? *Cell Metabolism* **14**, 5-6

Thayer T.C. (2010) Use of Nonobese Diabetic Mice to Understand Human Type 1 Diabetes. *Endocrinol Metab Clin N Am.* **39**, 541–561

Thorens B. (1996) Glucose transporters in the regulation of intestinal, renal, and liver glucose fluxes. *Am J Physiol Gastrointest Liver Physio.l* **270**, 541-53

Timmers H.J.L.M., Hadi M., Carrasquillo J.A., Chen C.C., Martiniova L., Whatley M., Ling A., Eisenhofer G., Adams K.T. & Pacak K. (2007) The effects of carbidopa on uptake of 6-18F-Fluoro-L-DOPA in PET of pheochromocytoma and extraadrenal abdominal paraganglioma. *J Nucl Med*. **48**, 1599-1606.

Todd J.A., Bell J.I. & McDevitt H.O.(1987)HLA-DQ beta gene contributes to susceptibility and resistance to insulin-dependent diabetes mellitus. *Nature* **329,** 599–604

Trus M.D. (1981) Regulation of Glucose Metabolism in Pancreatic Islets. *Diabetes* **30**, 911-922

Turvey S.E., Swart E., Denis M.C., Mahmood U., Benoist C., Weissleder R. & Mathis D. (2005) Noninvasive imaging of pancreatic inflammation and its reversal in type 1 diabetes. *The Journal of Clinical Investigation* **115**, 2454-61

Ushiki T. & Watanabe S. (1997) Distribution and ultrastructure of the autonomic nerves in the mouse pancreas. *Microsc Res Tech.* **37**, 399-406

Ustione A., Piston D.W. & Harris P.E. (2013) Minireview: Dopaminergic Regulation of Insulin Secretion from the Pancreatic Islet. *Mol Endocrinol.* **27**, 1198-1207

Van Berkel A., Rao J.U., Kusters B., Demir T., Visser E., Mensenkamp A.R., van der Laak J.A., Oosterwijk E., Lenders J.W., Sweep F.C., Wevers R.A., Hermus A.R., Langenhuijsen J.F., Kunst D.P., Pacak K., Gotthardt M. & Timmers H.J. (2014) Correlation Between In Vivo 18F-FDG PET and Immunohistochemical Markers of Glucose Uptake and Metabolism in Pheochromocytoma and Paraganglioma. *J Nucl Med*. Jun 12 Epub ahead of print

Van Cauter E., Mestrez F., Sturis J. & Polonsky K.S. (1992) Estimation of insulin secretion rates from C-peptide levels. Comparison of individual and standard kinetic parameters for C-peptide clearance. *Diabetes* **41**, 368-77.

Virtanen S.M., Rasanen L., Ylonen K., Aro A., Clayton D., Langholz B., Pitkäniemi J., Savilahti E., Lounamaa R., Tuomilehto J. & Åkerblom H.K. (1993) Early introduction of dairy products associated with increased risk of IDDM in Finnish children. The Childhood in Diabetes in Finland Study Group. *Diabetes* **42**, 1786–90

Wang P., Yoo B., Yang J., Zhang X., Ross A., Pantazopoulos P., Dai G. & Moore A. (2014) GLP-1R-targeting magnetic nanoparticles for pancreatic islet imaging. *Diabetes.* Epub ahead of print

Wang R.F., Loc'h C. & Maziere B. (1997) Determination of unchanged [18F]dopamine in human and non-human primate plasma during positron emission tomography studies: a new solid-phase extraction method comparable to radio-thin-layer chromatography analysis. *J Chromatogr B Biomed Sci Appl.* **693**, 265-270.

Weihe E, Eiden LE. (2000) Chemical neuroanatomy of the vesicular amine transporters. *FASEB J.* **14**, 2435–2449

Weihe E, Schafer MK, Erickson JD, Eiden LE. (1994) Localization of vesicular monoamine transporter isoforms (VMAT1 and VMAT2) to endocrine cells and neurons in rat. *J Mol Neurosci.* **5**, 149–164.

Wierup N., Sundler F. & Heller R.S. (2014) The islet ghrelin cell. *J Mol Endocrinol*. **52**, R35-49

Williams A.J.K., Chau W., Callaway M.P. & Dayan C.M. (2007) Magnetic resonance imaging: a reliable method for measuring pancreatic volume in Type 1 diabetes *Diabetic Medicine* **24**, 35–40

Wilson J.E. (2003) Isozymes of mammalian hexokinase: structure, subcellular localization and metabolic function. *J Exp Biol.* **206**, 2049-2057

Woods S.C. & Porte D.Jr. (1974) Neural control of the endocrine pancreas. *Physiol Rev.* **54**, 596–619

Wu Z. & Kandeel F. (2010) Radionuclide probes for molecular imaging of pancreatic beta-cells. *Advanced Drug Delivery Reviews* **62**, 1125–1138

Yip L., Su L., Sheng D., Chang P., Atkinson M., Czesak M., Albert P.R., Collier A.R., Turley S.J., Fathman C.G. & Creusot R.J. (2009) Deaf1 isoforms control the expression of genes encoding peripheral tissue antigens in the pancreatic lymph nodes during type 1 diabetes. *Nat Immunol.* **10**, 1026–1033

Ylinen L., Teros T., Liukas A., Arvilommi P., Sainio-Pöllänen S., Veräjänkorva E., Pöllänen P. & Simell O. (2000) The role of lipid antigen presentation, cytokine balance, and major histocompatibility complex in a novel murine model of adoptive transfer of insulitis. *Pancreas* **20**, 197-205

Zhao C., Wilson M.C., Schuit F., Halestrap A.P. & Rutter G.A. (2001) Expression and distribution of lactate/monocarboxylate transporter isoforms in pancreatic islets and the exocrine pancreas. *Diabetes* **50**, 361–366

Ziegler A.G., Rewers M., Simell O., Simell T., Lempainen J., Steck A., Winkler C., Ilonen J., Veijola R., Knip M., Bonifacio E. & Eisenbarth G.S. (2013) Seroconversion to multiple islet autoantibodies and risk of progression to diabetes in children. *JAMA* **309**, 2473-2479